UNIVERSITY OF CALIFORNIA
SANTA CRUZ

STATISTICAL MODELS AND PERFORMANCE EVALUATION OF MOBILE AD HOC NETWORKS

A dissertation submitted in partial satisfaction of the
requirements for the degree of

DOCTOR OF PHILOSOPHY

in

ELECTRICAL ENGINEERING

by

Xianren Wu

March 2008

The Dissertation of Xianren Wu
is approved:

Professor Hamid R. Sadjadpour, Chair

Professor J. J. Garcia-Luna-Aceves

Professor Ravi Narasimhan

Dean Lisa C. Sloan
Vice Provost and Dean of Graduate Studies

Table of Contents

List of Figures

List of Tables

Abstract

Statistical Models and Performance Evaluation of Mobile Ad Hoc Networks

by

Xianren Wu

We consider the fundamental questions on how nodal mobility affects the behavior and performance of protocol stacks of wireless mobile ad hoc networks (MANETs). Being self-organized and infrastructureless autonomous networks, MANETs have spurred intensive interest both in academic and in industrial fields. A comprehensive understanding on the essentials of mobility is indispensable to the design and optimization of protocol stacks, tailored to the unique dynamic environments in MANETs.

In the thesis, we attempt to investigate all aspects of mobility effects on the network behavior. First, at the link level, we look at the point-to-point link behavior and propose a new two-state Markov model, which accurately captures the essential mobility characteristics and provides the most accurate modeling on link lifetime.

Second, we extend the analysis of link behavior to path dynamics, which represents the characteristics of a serial of links. Modeling and evaluation of path dynamics enable us to answer more fundamental questions, as cross-layer optimization on packet lengths and design guidance of caching timeout strategies in routing protocols. Summarizing all the results both in link-level and path-level analysis, a comprehensive analysis on performance, delay and storage trade-offs is further pursued both in unrestricted and in restricted networks.

Third, we characterize topology evolutions as a function of nodal mobility and develop a new model, which accurately reflects the characteristic of topology evolutions in MANETs. Exploiting the proposed model, we are capable of presenting the first analytical model, accurately evaluating the mobility effect on the overhead of proactive routing protocols.

Employing all the analytical findings on mobility modeling, the first general, parameterized analytical framework is finally proposed for the performance evaluation of proactive and reactive routing protocols in MANETs. The model captures the functionality of the routing protocols together with the characterization of the performance of the medium access control protocol (MAC), reveals the interplay between the protocol functionality and network parameters, and provides new insight on the relative benefits of proactive and on-demand routing in MANETS.

To my wife, Lin Wu and my lovely daughter, Shuangying (Sherri) Wu,

my parents, Rongchun Wu and Dongxiang Xiao,

in gratitude for their love and support,

I owe them everything.

Acknowledgments

I am extremely lucky to have support, encouragement and inspiration from many people, without them this work would not have been possible.

My greatest gratitude goes to my advisor Professor Hamid R. Sadjadpour for his guidance and consistent support. His knowledgeable, wise and inspiring discussions have guided me throughout my whole Ph.D. career. It was such a pleasure to work with him for all these years. Facing so many obstacles, I am lucky that he has always been there to show me the right direction and influenced me as an active thinker.

I also owe special gratitude to Professor Jose Joaquin Garcia-Luna-Aceves, for guiding me millions of times when I was stuck, pointing out the right directions, serving on my PhD committee and reading my thesis.

I am also grateful to Professor Ravi Narasimhan for serving on my PhD committee and spending time reviewing this work and giving valuable suggestions and comments on my work.

My fellow students made my life at UC Santa Cruz cheerful and memorable. I wish to thank Walter Wang, Xin Wang, Hui Xu, Christopher Rouchy, Roger Tilly and Bahador Amiri for all the enjoyable discussions. Your friendship is my best fortune. I would specially thank my parents. They are always supportive and encouraging, silent yet powerful. I know I owe you all my life. Finally, I cannot say more about my love and appreciation to my wife, Lin Wu and my daughter Shuangying (Sherri) Wu. Your exceptional love makes everything worthwhile.

Chapter 1

Introduction

1.1 Overview of Wireless Networks

Two main classes of networks, infrastructure network and ad hoc network, have been developed for wireless networking. Classical paradigms for infrastructure networks are cellular networks and wireless LAN's. In such networks, the network operator deploys a network infrastructure within the coverage area to provide wireless connectivity to the vicinity. The infrastructure is known as base stations in cellular networks, access points in wireless LAN's, and are connected together to a backbone network by wire or high-speed wireless backbone links. All communications on the wireless medium occurs in one hop between the mobile nodes to the local base station/access point.

Ad hoc networks, on the other hand, preclude the use of a wired infrastructure. These networks are applicable to locations in which a prior deployment of network infrastructure is impossible. Current applications are mostly connected to military and

rescue operations for long range outdoor networks, or to indoor network setting such as a conference room with a collection of laptop computers. Nodes are connected together to form a network on the fly. They also have routing capability and may act as the source, destination or a forwarding node to relay packet for other nodes.

Nodes in ad hoc networks could be static or mobile, characterizing two main categories of wireless ad hoc networks, i.e., wireless static ad hoc networks and wireless mobile ad hoc networks (MANETs). In this thesis, we focus on research issues in mobile ad hoc networks. However, to start with an understanding of the limit and scalability of both networks, we will outline the key theoretical results on ad hoc networks in the following.

1.2 Theoretical Aspects of Wireless Ad Hoc Networks

1.2.1 Communication Models

Let X_i denote the location of a node i in the wireless network. The *Protocol Model* establishes that node i transmits successfully to node j if the following condition is satisfied [36]

$$|X_k - X_j| \geq (1 + \Delta)|X_i - X_j|, \tag{1.1}$$

so that transmit node X_k will not block X_i and X_j communication. In the *Physical Model* node i transmits successfully to node j if the signal to interference and noise ratio

($SINR$) at node j satisfies [36]

$$SNIR = \frac{\dfrac{P_i}{|X_i - X_j|^\alpha}}{N_0 + \sum_{k \neq i} \dfrac{P_k}{|X_k - X_j|^\alpha}} \geq \beta, \tag{1.2}$$

where P_i is the transmit power of node i, α is the path loss parameter, N_0 is the noise power, and β is the minimum value of $SINR$ necessary for successful reception. It is known that if $\alpha > 2$ and each node transmits at the same power, then the *Protocol* and *Physical* models become equivalent [28].

1.2.2 Capacity and Scalability of Wireless Static Ad Hoc Networks

Gupta and Kumar [36] analyzed the capacity of static wireless networks through scaling law analysis. The network model consisted of sphere of unit area containing n total fixed nodes with identical properties. Nodes were placed either arbitrarily or randomly in the area. Communication among nodes was obtained through a single wireless channel shared among all nodes, and therefore subject to interference. Packets were sent from source to destination in a multihop fashion following the path close to the straight line that links the source to its destination. Therefore, each node could function as source, relay and destination of packets. They showed that there exists a Voronoi tessellation $\mathcal{V}_n$ on the unit sphere surface satisfying the following properties:

- Every Voronoi cell V contains a disk of area $100 \log(n)/n$ and corresponding radius $\epsilon(n) = c\sqrt{\log(n)/n}$, for some positive constant c.
- Every Voronoi cell is contained within a circle of radius $2\epsilon(n)$.

Each Voronoi cell $V \in \mathcal{V}_n$ is simply a cell of the network, and the cells do not have a regular shape because the network is arbitrary or random. With this tessellation, each cell contains at least one node with high probability (whp)[1], for some positive constant c [54]. which meets the connectivity requirement [36]. Furthermore, by choosing the transmission range equal to $8\epsilon(n)$ for each node, it allows direct communication between a cell and its adjacent cells. Accordingly, two cells are interfering neighbors if there is a point in one cell that is within a distance $(2+\Delta)8\epsilon(n)$ of some point in the other cell, in which $\Delta > 0$ is a given constant modeling condition where a guard zone is required to prevent a neighboring node from transmitting on the same channel at the same time [36].

Gupta and Kumar showed that, by using both *protocol* and *physical* models, the node throughput of static wireless ad hoc networks scale as $\Theta\left(1/\sqrt{n}\right)$ for the arbitrary placement of nodes, and as $\Theta\left(1/\sqrt{n\log(n)}\right)$ for the random placement of nodes. In either case, the capacity of each node decreases as the number of total nodes n in the network increases.

1.2.3 Capacity and Scalability of Wireless Mobile Ad Hoc Networks

Grossglauser and Tse [33, 34] presented a one-hop forwarding scheme for MANETs that attains $\Theta(1)$ per source-destination throughput.

The scheme is based on *multiuser diversity* [47] where each source node transmits a packet to the nearest neighbor; that is, using the simple path propagation model,

[1] With high probability means with probability $\geq 1 - \frac{c}{n}$.

the source reserves its channel for a receiver that can best exploit it. This neighbor node functions as a relay and delivers the packet to the destination when this destination becomes the closest neighbor of the relay.

The network model consists of a normalized unit area disk containing n mobile nodes. They considered a time-slotted operation to simplify the analysis. The position of node i at time t is indicated by $X_i(t)$. The process $\{X_i(\cdot)\}$ is stationary and ergodic with stationary uniform distribution on the disk, which yields node trajectories that are independently and identically distributed (iid).

At each time step, a scheduler decides which nodes are senders, relays, or destinations, in such a manner that the source-destination association does not change with time. Each node can be a source for one session and a destination for another session. Packets are assumed to have header information for scheduling and identification purposes.

Suppose that a source i has data for a certain destination $d(i)$ at time t. Because nodes i and $d(i)$ can have direct communication only $1/n$ of the time on the average, a relay strategy is proposed to deliver data to $d(i)$ via relay nodes. They assume that each packet can be relayed at most once.

According to the *Physical Model*, at time t, node j is capable of receiving at a given rate of B $bits/sec$ from i if

$$SNIR = \frac{P_i(t)g_{ij}(t)}{N_0 + \frac{1}{M}\underbrace{\sum_{k\neq i} P_k(t)g_{kj}(t)}_{I}} = \frac{P_i(t)g_{ij}(t)}{N_0 + \frac{1}{M}I} \geq \beta, \tag{1.3}$$

where $P_i(t)$ is the transmitting power of node i, $g_{ij}(t)$ is the channel path gain from node i to j, M is the processing gain of the system, and I is the total interference at node j. The channel path gain is assumed to be a function of the distance only, so that [33], [36]

$$g_{ij}(t) = \frac{1}{|X_i(t) - X_j(t)|^\alpha} = \frac{1}{r_{ij}^\alpha(t)}, \tag{1.4}$$

where $r_{ij}(t)$ is the distance between i and j.

Therefore, according to the above communication scheme, each node sends data to its destination in a two phase process. Packet transmissions from sources to relays (or destinations) occur during *Phase 1*, and packet transmissions from relays (or sources) to destinations happen during *Phase 2*. Both phases occur concurrently, but *Phase 2* has absolute priority in all scheduled sender-receiver pairs.

Because node trajectories are iid and the system is in steady-state, the long-term throughput between any two nodes equals the probability that these two nodes are selected by the scheduler as a feasible sender-receiver pair. According to [33, 34] this probability is $\Theta(\frac{1}{n})$. Also, there is one direct route and $n-2$ one-hop routes passing through one relay node for a randomly chosen source-destination pair. Thus, the service rate is $\lambda_j = \Theta(\frac{1}{n})$ through each actual relay node, as well as the direct route. Accordingly, the total throughput per source-destination pair λ_T is

$$\lambda_T = \sum_{j=1, j\neq i}^{n} \lambda_j = \sum_{j=1, j\neq i}^{n} \Theta\left(\frac{1}{n}\right) = \Theta\left(\frac{n-1}{n}\right) \overset{n\to\infty}{\longrightarrow} \Theta(1). \tag{1.5}$$

Thus, this scheme attains $\Theta(1)$ per source-destination throughput when n tends to infinity. However, the delay experienced by packets under this strategy was

shown to be large and it can be even infinite for a fixed number of nodes (n) in the system, which has prompted more recent work presenting analysis of capacity and delay tradeoffs [63, 6, 56, 28, 74, 53].

1.3 Research Motivation and Contributions

Introduction of mobility into wireless ad hoc networks boosts the achievable rate and scalability of wireless ad hoc networks, envisioned from the possibility of $\Theta(1)$ scalability. Mobility brings unique opportunities, as well as creates significant challenges to understand the network behavior. The results from scaling law analysis, presenting the network performance as a function of network size [36, 33, 34], by all means provide a bright picture to understand the large-size or asymptotic behavior of the networks. Extensive researches have been devoted to study the throughput-delay tradeoff and delay-limited throughput in MANETs [6, 28, 56, 23, 26, 27]. Their results reveal that mobility do enable the opportunity for system designer to arrive at a balanced design between the throughput and delay requirement. Similar observations are also extended in the scenario of restricted mobility [50, 53], where nodes' movement is restricted within certain predetermined region. And the study in [39] further shows the possibility of tradeoff between the storage and the throughput in MANETs. However, to achieve all these great performance necessitates a great design of protocol stacks, tailored to the characteristics of MANETs.

Being the defining feature of mobile ad hoc networks, mobility poses tremen-

dous challenges to the design of effective protocols in MANETs, by introducing highly dynamic network topologies. Changes in network topology (or topology evolutions), either from nodes mobility or instability in wireless links, make mostly deployed routing protocols (e.g. OSPF [18], RIP [49]) not applicable, due to their inability to handle such highly dynamic network behaviors. The design of effective protocols in MANETs inevitably necessitates a prior fundamental understanding on the dynamic characteristics of topology evolutions, introduced from nodes mobility. Simulation-based studies have been used as a powerful tool to gain insight on performance variations upon specific choices of mobility and network parameters. However, it is difficult to draw conclusions involving multidimensional parameter spaces, simply because running several simulation experiments for many combinations of network-parameter values becomes impractical.

In the thesis, we are thus well motivated to develop statistical models which accurately characterize the performance of protocols as a function of node mobility and are also capable of analytically evaluating protocol performance upon various mobility and network configurations. The main contributions of this thesis are the following:

- We propose the most accurate analytical model of link and path behavior in MANETs, which accurately characterizes the behavior of links and paths as a function of node mobility. The importance of this model is twofold. First, it enables the investigation of many questions regarding fundamental tradeoffs in throughput, delay and storage requirements in MANETs, as well as the relationship between many crosslayer-design choices (e.g., information packet length) and network dynamics (e.g., how long links last in a MANET). Second, it enables the

development of new analytical models for channel access, clustering and routing schemes by allowing such models to use link lifetime expressions that are accurate with respect to simulations based on widely-used mobility models.

- We provide a comprehensive coverage of MANETs with restricted mobility, where each node moves within a constrained area. These networks play an important role in the real world, where nodes usually travel only a portion of the entire network. As published in the *information assurance framework* [2] from the National Security Agency, such networks represent the more realistic scenarios for tactical users, especially for the users deployed in the division and rear area. We strive in the thesis to provide the first thorough analysis of two-dimensional restricted mobility networks on link dynamics, optimal segmentation of information stream, throughput, delay, and storage tradeoffs.

- We propose the first analytical framework for the modeling of proactive routing overhead as a function of node mobility. The framework enables an analytical characterization of topology changes as a function of node mobility, which is crucial to understand the analytical connection between routing overhead and topology changes due to mobility.

- We develop the first general, parameterized framework for analyzing protocol performance in mobile ad-hoc networks. In the framework, the adverse effects of signaling overhead on data packets are captured and analyzed through a two-customer queuing model of the operation of nodes. The framework is a combina-

torial model that parameterizes and evaluates the performance of routing protocols using a joint characterization of the routing and channel access functionalities. The model enables insightful understandings of essential behavior of on-demand and proactive routing protocols, as well as close-to-simulation performance predictions when adapted to specific protocols.

1.4 Outline of Thesis

The outline of the rest of the thesis is as follows. In Chapter 2, we first review mobility models and routing protocols, that set up the foundation of the analytical performance modeling and evaluation of mobility and protocol performance in MANETs. A comprehensive literature survey is also provided to summarize all the important previous research works.

Chapter 3 presents an analytical framework and statistical models to accurately characterize the lifetime of a wireless link and multi-hop paths in MANET. It is shown that the lifetimes of links and paths can be computed through a two-state Markov model and the analytical solution follows closely the results obtained through discrete-event simulations. The models are then applied to study practical implications of link lifetime on routing protocols. First, the optimal packet lengths are computed as a function of mobility, and show that significant throughput improvements can be attained by adapting packet lengths to the mobility of nodes in a MANET. Second, we show how the caching strategy of on-demand routing protocols can benefit from

considering the link lifetimes in a MANET. Eventually, we summarize all the analytical results into a comprehensive performance analysis on throughput, delay and storage of networks with unrestricted mobility.

Chapter 4 extends the statistical link and path models to provide a comprehensive performance evaluation of MANETs with restricted mobility, where each node moves within a constrained area. In details, it attempts in the chapter to provide the first thorough analysis of two-dimensional restricted mobility networks on link dynamics, optimal segmentation of information stream, throughput, delay, and storage tradeoffs.

Chapter 5 presents a mathematical framework for quantifying the impact of node mobility on the overhead of proactive routing protocols in MANETs. The analytical framework models signaling overhead as a function of stability of topology, and characterizes the statistical distribution of topology evolutions. OLSR protocol, as a leading example of proactive routing for ad hoc networking, is further singled out for analysis within the proposed analytical framework.

Chapter 6 provides a mathematical framework for the performance evaluation of proactive and reactive routing protocols operating in MANETs. The model captures the functionality of the routing protocols together with the characterization of the performance of the medium access control (MAC) protocol. It reveals the interplay between the protocol functionality and network parameters, and provides new insight on the relative benefits of proactive and on-demand routing in MANETS. The analytical results are corroborated with results obtained using discrete-event simulations.

Finally, the thesis is concluded in Chapter 7, drawing future research directions.

Chapter 2

Background and Related Works

This chapter gives an overview of mobility models as well as routing protocols employed in ad hoc network studies, and presents a survey of important literature works. The chapter begins by introducing the widely adopted mobility models in MANETs in Section 2.1. In particular, the random waypoint mobility models and the random direction mobility model which are the most heavily used mobility model in simulations or analysis are discussed in Sections 2.1.1 and 2.1.2.

Section 2.2 is devoted to provide an overview of routing protocols in MANETs. Two representative routing protocols, optimized link-state routing protocol (OLSR) and ad-hoc on-demand distance vector routing protocol (AODV) are further presented in more details in Sections 2.2.1 and 2.2.2. Finally, the chapter is concluded with a comprehensive literature survey on link models in MANETs.

2.1 Mobility Models

The aim of user mobility models in MANETs is to enable communication protocol and system simulations in order to measure their performance. To accomplish this task and to allow to obtain statistical valuable results, the models have to fulfill certain properties. Typically they have to

- be repeatable and have adjustable parameters representing various mobility scenarios,
- be stationary,
- be uncorrelated.

Modeling real-world user behavior is a challenging issue and often a trade-off between complexity and accuracy. One approach is to observe the mobility patterns in real systems. However, in practice such traces are not very useful for simulation studies since they only reflect one specific scenario that cannot be generalized. Furthermore they hardly fulfill the criteria of stationarity since real world scenarios typically have time dependent variations, e. g., regular commuters streams. As a consequence, many analytical and simulation-based studies of wireless networks are based on synthetic models that provide random mobility patterns.

An overview on existing synthetic models can be found in [9, 14]. Synthetic random walk mobility models are simple to implement in simulation tools and can be characterized by a small number of parameters. Two frequently used examples are

the random waypoint mobility model (RWMM) and the random direction mobility model(RDMM).

2.1.1 Random Waypoint Mobility Model

The random waypoint mobility model (RWMM) is commonly adopted in the simulation of mobile ad hoc networks. In the random waypoint mobility model, each node is assigned an initial location in a given area and travels at a constant speed v to a destination randomly and uniformly chosen in this area. The speed v is selected uniformly in a range of (v_{min}, v_{max}), independent of the initial location and destination. After reaching the destination, the node may pause for a random amount of the time after which a new destination and a new speed are determined, irrespective of all previous destinations, speeds and pause times. In contrast to the random direction mobility model that results in uniform stationary node distribution, the stationary distributions of location and speed in the random waypoint model differ significantly from the uniform distribution. In particular, it has been observed that the stationary distribution of the location of a node is more concentrated near the center of the region where the node moves [10, 55]. Also, v_{min} needs to be strictly positive to ensure that the average speed over time does not go to zero.

2.1.2 Random Direction Mobility Model

The mobility model considered here is the same model used in [51, 42, 43], that is also known as random direction mobility model (RDMM) [35, 9]. RDMM is an

important mobility model for MANETs. It improves RWMM on the stationary uniform nodal distribution, and has been widely adopted [42, 43, 51, 9, 35]. In RDMM, the movement of nodes is independent and identically distributed (iid) and can be described by a continuous-time stochastic process. The continuous movement of nodes is divided into mobility epochs during which a node moves at constant velocity, i.e. fixed speed and direction. But the speed and direction varies from epoch to epoch. The time duration of epochs is denoted by a random variable τ, assumed to be exponentially distributed with parameter λ_m. Its complementary cumulative distribution function CCDF $F_m(\tau)$ can be written as [51]

$$F_m(\tau) = exp(-\lambda_m \tau) \tag{2.1}$$

The direction during each epoch is assumed to be uniformly distributed over $[0, 2\pi)$ and the speed of each epoch is uniformly distributed over $[v_{min}, v_{max}]$, where v_{min} and v_{max} specify the minimum and maximum speed of nodes respectively. Speed, direction and epoch time are mutually uncorrelated and independent over epochs. Furthermore, when a node hits a cell boundary, the direction of node is reflected back with respect to the normal edge of the cell boundary and the speed is kept unchanged.

The stationary node distributions of the location and direction have been shown to be uniform for arbitrary direction, speed and travel time distributions, irrespective of the boundaries being reflected or wrapped around [6]. The minimum speed v_{min} can be zero and it stands for the case where nodes can stop and rest for a while during movements.

2.2 Routing Protocols

Routing protocols are broadly classified as distance vector and link state routing. Distance vector routing is a decentralized routing algorithm. Each node that participates in routing exchanges its estimated least cost path to all other nodes in the network through its directly connected neighbors . Since no single node has a global view of the network in the distance vector, convergence is slow.

Link state routing is a global routing algorithm in which each node computes the shortest path to every other node in the network using global knowledge about the network. In link state routing protocols, each node broadcasts the link state to its directly connected neighbors, to be further flooded over the whole network. This flooding gives a global topology view to each node. Link state algorithms offer better reliability and solve count-to-infinity and looping issues associated with distance vector routing protocols. The widely-used Open Shortest Path First (OSPF [18]) routing protocol is a link state protocol.

Topology-based wireless routing protocols are also broadly classified as proactive and reactive. Proactive routing protocols use periodic broadcasts to establish routes and maintain them; examples are Optimized Link State Routing (OLSR) [16] and Topology Broadcast Based On Reverse-Path Forwarding (TBRPF) [7]. Since they exchange topology information enabling each node to maintain an up-to-date view of the network, proactive protocols are also called table-driven protocols. The topology exchange can happen periodically (e.g. as in OLSR and TBRPF) or on an event driven basis (e.g.

as in DSDV [64] and TORA [60]). Proactive protocols can effectively route packets immediately to any other node in the network and do not suffer from a high starting latency. However, the periodic topology exchange results in a larger overhead especially when node mobility is high.

Reactive (or on-demand) protocols create routes on demand by sending route request messages when a new route is needed. Reactive protocols trace the reply messages to construct optimum paths to the destination. Since route discovery is done only on an as-needed basis, the control overhead is smaller than it is in proactive protocols. However, these protocols suffer from high route discovery latency. Some well-known reactive protocols are Dynamic Source Routing (DSR) [45] and Ad-Hoc On-Demand Distance Vector Routing (AODV) [65].

2.2.1 Optimized Link State Routing Protocol (OLSR)

The proactive OLSR [16] adapts a classical link state protocol for mobile ad hoc routing. As a proactive routing protocol, it uses periodic messages to update topology information at each node. In a classical link state protocol, the link state packet includes the entire neighbor list along with the associated link cost metric, thus generating large control packet overheard. Furthermore, these packets are broadcast to the entire network which does not scale well to the low bandwidth requirements of wireless ad-hoc networks. OLSR optimizes the classical link state protocol by reducing the control packet overhead and creating efficient flooding mechanisms. OLSR tries to contain duplicate broadcasts and limit broadcast domain by using a Multi- Point Relay (MPR)

set. The concept behind using MPR is to choose nodes in a network that will effectively cover the entire network. These nodes, called MPR nodes, are defined as one-hop neighbors with which there is bi-directional connectivity, and they, in turn, cover all the two-hop neighbors of a given node.

Each node maintains two sets of nodes, a MPRset and a MPRselectorset. The MPRset consists of the set of MPR nodes which the current node has selected, and the MPRselector consists of a set of nodes that have selected the current node as a MPR node. These MPR nodes act as the forwarding stations when they receive data from or destined to the nodes in its MPRselectorset. Selecting MPR nodes as the forwarding stations reduces the link state information because only the link state connectivity of the MPR node needs to be included in the link state control packets since a MPR node effectively represents its selector nodes. This reduces the size of the link state packets, thereby reducing overhead for OLSR.

Initially a node starts off with an empty MPRset and MPRselectorset. All one-hop neighbor nodes are considered as MPR nodes. This set decreases in size over time as the HELLO messages are received, because over a period of time the node will learn all its two-hop and MPR neighbors. OLSR uses three important elements: a neighbor sensing element, an efficient message flooding element, and a topology dissemination element. OLSR employs a simple neighbor sensing scheme to detect the neighbor link status, but does not rely on link level acknowledgments to detect link status. The link status can have three possible states: unidirectional, bidirectional and MPR. OLSR sends out a HELLO message periodically with a list of neighbors from which it has

heard, along with the neighbor link status. A node receiving a HELLO message for the first time from a neighbor marks the link as unidirectional in the local neighbor table and includes the neighbor identifier (ID) in its next HELLO message. The neighbor receiving this HELLO message on finding its node ID determines the link is bidirectional. Then, for subsequent HELLO messages from this neighbor, the link is marked bidirectional. Each node employs a distributed approximation algorithm to compute its MPRset and marks the corresponding node links as MPR in its local neighbor table. A neighbor marked MPR means the neighbor link is bidirectional and also the neighbor is a MPR for the current node. HELLO messages are only broadcasted to neighbors and are not relayed further. Each node learns all of its two hop neighbors through the periodic HELLO message. In addition the HELLO messages broadcast the transmitting nodes MPRset.

From the HELLO messages, the nodes know if they have been selected as a MPR. If they have, they place the corresponding node in its MPRselectorset. To disseminate link state topology information in the network, each MPR node with a non-empty MPRselectorset periodically broadcasts a Topology Control (TC) message. The TC messages contain the MPR node ID and its MPRselectorset. Other MPR nodes receiving the broadcasts relay this information. Using the topology information obtained from TC messages, the nodes can compute the shortest path to every node in the network and form the routing table. An important point to note here is that the routes in OLSR always contain MPR nodes as the forwarding agents. Therefore, OLSR does not always construct a shortest path, but does guarantee a path to the

destination. According to the protocol specification [16], OLSR performs well in a highly dense network with sporadic node movement. This characteristic can be attributed to OLSR being a proactive protocol and having routes always available.

The advantage of OLSR is that it reduces control information and efficiently minimizes broadcast traffic bandwidth usage. Although OLSR provides a path from source to destination, it is not necessarily the shortest path, because every route involves forwarding through a MPR node. A further disadvantage is that OLSR also has routing delays and bandwidth overhead at the MPR nodes as they act as localized forwarding routers.

2.2.2 Ad-Hoc On-Demand Distance Vector Routing (AODV)

AODV [65] uses a route discovery process to dynamically build new routes on an as needed basis. AODV is a distributed algorithm using distance vector algorithms, such as the Bellman Ford algorithm. When a route to a destination is unknown, AODV creates a route request packet and broadcasts it to its neighbors. Route request messages contain the source ID, destination ID, source sequence numbers, destination sequence numbers, hop count and broadcast ID. The source sequence number and broadcast ID increment each time a new route request is generated. The destination sequence number is the source sequence number of the destination node as last recorded by the source node. Each intermediate node receiving a route request caches the previous hop for the particular node originating the request; this helps to create a return path for the reply packets.

AODV uses the destination sequence number to maintain freshness of routes. The destination node or any intermediate node can reply to a route request. If an intermediate node has previously learned the path to the destination node, it can reply with the next hop information only if it satisfies the following condition: the locally stored destination sequence number is higher or comparable to the destination sequence number in the route request packet. AODV relies heavily on the sequence numbers to avoid the count-to-infinity problem associated with distance vector protocols. The broadcast ID and source ID pair help in discarding any redundant requests that reach a node. The replying destination or intermediate node unicasts a route reply message to the specific source node that created the route request. Nodes receiving a route reply message store the source ID of the node forwarding the message as the next hop towards the destination in order to forward future traffic toward this destination. The hop count in each message is incremented by one at each forwarding node, which helps track the distance to the source or destination node depending on the type of the message. A node generating a route request or route reply sets the hop count to zero, which is incremented at each intermediate forwarding node. This incrementing helps the intermediate node to determine the number of hops to reach the source or destination using the current path. The source node receiving a number of route replies from different paths uses the hop count in the route reply messages to choose the one with a lower hop count metric as the shortest route to the destination. Once a route is formed, AODV uses the current route until the route expires or any topology changes occur. Each node also maintains a precursor list [10] of nodes that helps it identify the nodes it has to inform of

a broken link. The precursor list is created from the route request packets and includes a list of nodes that are likely to use the current node as the next hop. Each node monitors the status of each of its links, and when a link connectivity change occurs, the node creates a route error message and informs the members of the precursor list about the non-reachability of specific routes. AODV relies on medium access control (MAC) layer schemes or the use of beacon packets at periodic intervals to find the status of its directly connected neighbors. Topology changes or expiring timers associated with the route request, reply and beacon packets allow AODV to detect link failures.

AODV uses a progressive ring search technique to control the broadcast domain. Basically, it increases the time-to-live (TTL) value in each broadcast of the initial route request until it receives a route reply. AODV, however, only works on symmetric links although Nesargi and Prakash have proposed extensions for ADOV in environments with unidirectional links [58].

The advantage of AODV is that it creates routes only on demand, which greatly reduces the periodic control message overhead associated with proactive routing protocols. The disadvantage is that there is long route discovery delay when a new route is needed, because ADOV queues data packets while discovering new routes and the queued packets are sent out only when new routes are found. This situation causes throughput loss in high mobility scenarios, because the packets get dropped quickly due to unstable route selection.

2.3 Literature Survey of Models of Link Dynamics

Samar and Wicker [70, 69] were first to explore the problem of analytical evaluation of link dynamics and show that the analytical formulation can be incorporated into the protocol design and greatly improve the network performance. However, when evaluating the distribution of link lifetime, they only consider the scenario where both of the communicating nodes maintain their velocity during the whole communication session, i.e. speed and direction were kept unchanged. Graphically, the trajectory of nodes for this simplified scenario is a straight line crossing the circle of transmission range, where one node is treated as static and located at the center of the circle and the other node moves at relative velocity. Clearly, this simplification overlooks the possibilities that when communicating with each other, either of the two nodes may change their velocity and the resulting trajectory will be a polylines with several turning points inside the circle of transmission range. Therefore, the resulting distribution of link lifetime from the simplified analysis could be greatly deviated from the reality, especially when the ratio R/v between the radius R for the circle of communication range and the speed v becomes larger, i.e. meaning that link could last longer and nodes are more likely to change their velocity and direction during the communication session. Generally, the simplified analysis [70, 69] is more conservative and tends to underestimate the distribution of link lifetime.

In addition to the work presented in [69]-[31], several existing approaches identify temporal stable links through mobility-prediction and utilize this information to

design efficient routing protocols for MANETs. In [72], the location and velocity information provided from a Global Position System (GPS) are utilized to compute link expiration time (LET) to improve the performance of existing routing protocols, assuming that both of the nodes will maintain their velocity unchanged during the prediction interval.

In [51], a probabilistic link availability model is developed to quantify the probability of future link existence. When an active link between two nodes is available at time t, the probability of link availability at future time $t + t_0$ is quantified through this model and a dynamic clustering algorithm then uses this information to form a more temporal stable cluster. However, this model is not practical to quantify link lifetime because the link could be broken during the prediction time interval and resume active before time $t + t_0$. For this reason, [42, 43] improve the model by proposing algorithm trying to predict the probability that an active link between two nodes will be continuously available for a predicted period.

Besides mobility-prediction based approaches, a routing metric termed as *associativity* is developed for assessing link availability [73, 67]. In their model, each node sends out beacon signal periodically to indicate its presence. Upon receiving a beacon, neighbor nodes increase the value of their associativity with the beaconing node. The value of associativity varies over time and location as nodes move nearby and leave, thus reflecting the connection stability of association of a node with respect to another node. Some other methods [22, 1] use the information of received signal strength as metric to select links with relatively strong signal strength. Compared to the mobility-prediction

based approaches, a common weakness of these methods is that they only utilize the past information and hardly reflect possible changes in link status happening in the future, especially in a wireless mobile environment.

Chapter 3

Analytical Modeling of Link Dynamics: Unrestricted Networks

The idea behind the chapter is that, while the behavior of wireless links is critical to the performance of MAC and routing protocols operating in a MANET, no analytical model exists today that accurately characterizes the lifetime of wireless links, and the paths they form from sources to destinations, as a function of node mobility. As a result, the performance of MAC and routing protocols in MANETs have been analyzed through simulations, and analytical modeling of channel access and routing protocols for MANETs have not accounted for the temporal nature of MANET links and paths. For example, the few analytical models that have been developed for channel access protocols operating in multihop ad hoc networks have either assumed static topologies (e.g., [15]) or focused on the immediate neighborhood of a node, such that nodes remain neighbors for the duration of their exchanges (e.g., [77]). Similarly, most

studies of routing-protocol performance have relied exclusively on simulations, or had to use limited models of link availability (e.g., [52]) to address the dynamics of paths impacting routing protocols (e.g., [75]).

We introduce in the chapter the most accurate analytical model of link and path behavior in MANETs to date, and characterizes the behavior of links and paths as a function of node mobility. Our approach is based on a two-state Markovian model that reflects the movements of nodes inside the circle of transmission range and builds an analytical framework to accurately evaluate the distribution of link lifetime. The proposed model subsumes the model of Samar and Wicker [69, 70] as a special case, and provides a more accurate characterization of the statistics of link lifetime, accuracy of which have been validated through discrete simulations in Section 3.4 for both RDMM and RWMM mobility models.

The remaining of the chapter is organized as follows. Section 3.1 describes the network and mobility models used to characterize link and path behavior. Section 3.2 describes the proposed analytical framework and presents our results on link lifetime, and Section 3.3 extends these results to path dynamics. Sections 3.5 and 3.6 illustrate how our model can be applied to practical problems in MANETs. Section 3.5 applies our analytical framework to optimal segmentation (information packet length) of information streams. Our results reveal that packet lengths should be designed to be linearly proportional to the ratio R/v, and show that the optimal packet length for a given K-hop path should be designed to be $R/(vK)$. Section 3.6 discusses improving packet caching policies in on-demand routing protocols by taking advantage of the

characterization of link and path lifetimes. A comprehensive coverage of throughput, delay and storage requirement is then followed in section 3.7.

3.1 Network Model

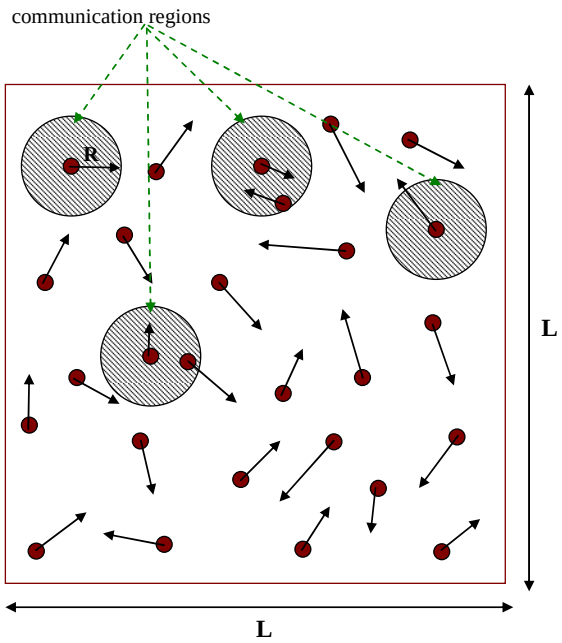

Figure 3.1: Network Model: Unrestricted Networks

Consistent with previous analytical models of MANETs [33, 34, 28], we consider a square network of size $L \times L$ in which n nodes are initially randomly deployed, as depicted in Fig. 3.1.. The movement of each node is unrestricted, i.e, the trajectories of nodes can be anywhere in the network. The model of node mobility falls into the general category of random trip mobility model [12], where nodes' movement can be described by a continuous-time stochastic process and the movement of nodes can be

divided into a chain of trips.

Communication between two nodes is allowed only when the distance between them is less than or equal to R and can be performed reliably. Communication zone of a given node consisting of the circle of radius R satisfies the *physical model (Eq. 1.2)* requirement with certain outage probability in the wireless fading environment.

A typical communication session between two nodes involves several control and data packet transmissions. Depending on the protocol, nodes may be required to transmit beacons to their neighbors to synchronize their clocks for a variety of reasons (e.g., power management, frequency hopping). Nodes can find out about each other's presence by means of such beacons, or by the reception of other types of signaling packets (e.g., HELLO messages). Once a transmitter knows about the existence of a receiver, it can send data packets, which are typically acknowledged one by one, and the MAC protocol attempts to reduce or avoid those cases in which more than one transmitter sends data packets around a given receiver, which typically causes the loss of all such packets at the receiver. To simplify our modeling of link lifetime, we assume that the proper mechanisms are in place for neighboring nodes to find each other, and that all transmissions of data packets are successful, as long as they do not last beyond the lifetime of the wireless link between transmitter and receiver. Relaxing this simplifying assumption is beyond the subject of this thesis, as it involves the modeling of explicit medium access control schemes (e.g., [15]).

3.2 Link Lifetime

A bidirectional link exists between two nodes if they are within communication range of each other. In this thesis, we do not consider unidirectional links, given that the vast majority of channel access and routing protocols use only bidirectional links for their operation. Hence, we will refer to bidirectional links simply as links throughout the rest of the thesis.

The wireless link between nodes m_a and m_b is broken when the distance between nodes m_a and m_b is greater than R. When a data packet starts at time t_1, the positions of node m_b could be anywhere inside the communication circle defined by the transmission range of m_a and is assumed as uniformly distributed[1].

Let B $(bits/s)$ be the transmission rate of a data packet, L_p be the length of the data packet, and $t_1 + T_L$ denotes the moment that node m_b is moving out of the communication circle. A data packet can be successfully transferred only if nodes m_a and m_b stay within their communication range during the whole communication session of the data packet, that is,

$$L_p/B \quad \leq \quad T_L \tag{3.1}$$

where T_L is the link lifetime (LLT) denoting the maximum possible data transfer duration. Statistically, T_L specifies the distribution of residence time that measures the duration of the time, for node m_b, starting from a random point inside the communica-

[1]In mobile ad hoc network, the traffic is generated randomly and nodes are moving randomly. When a node initiate traffic to other nodes, the target node could be anywhere in the network and the relays could also be anywhere in the communication range. Therefore, a uniform distribution assumption naturally fits into the scenario.

tion circle with equal probability, to continuously stay inside the communication circle before finally moving out of it. Furthermore, its complementary cumulative distribution function (CCDF) is denoted by $F_L(t)$

$$F_L(t) = P(T_L \geq t) \tag{3.2}$$

The link outage probability P_{L_p} associated with a particular packet length L_p can be evaluated as

$$P_{L_p} = P(T_L < \frac{L_p}{B}) = 1 - F_L(\frac{L_p}{B}) \tag{3.3}$$

3.2.1 Distribution of Relative Velocity

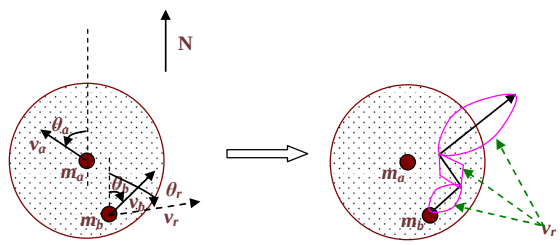

Figure 3.2: Graphical Illustration of Relative Velocity: Unrestricted Networks

Fig. 3.2 shows the transmission zone of a node (node m_a) which is a circle of radius R centered at the node. The figure shows another node (say node m_b) starting to communicate data with node m_a at time t_2. As shown in the left side of the figure, at time t_2, node m_a is moving at speed v_a with direction θ_a, while node m_b moves at speed v_b with direction θ_b.

Alternatively, if we consider node m_a as static, node m_b is moving at their

relative speed and *direction* v_r and θ_c, respectively. An example of resulting trajectories of node m_b moving at relative velocity is given in the right side of Fig. 3.2. With the assumption that both θ_a and θ_b are uniformly distributed within $[0, 2\pi)$, it can be concluded that the composite direction $\theta_c = \theta_b - \theta_a$ is also uniformly distributed within $[0, 2\pi)$. In this case, the relative speed v_r can be expressed as

$$v_r = \sqrt{v_a^2 + v_b^2 - 2v_a v_b \cos\theta_c} \tag{3.4}$$

Conditioning on v_a and v_b and noting the symmetric property of θ_c, the distribution of v_r can be computed as

$$p(v_r) = E_{\{v_a, v_b\}}(p(v_r|v_a, v_b)) \tag{3.5}$$

$$\begin{aligned} p(v_r|v_a, v_b) &= p(\theta_c)|\frac{d\theta_c}{dv_r}| \\ &= \frac{1}{\pi}|\frac{d}{dv_r}(arccos(\frac{v_a^2 + v_b^2 - v_r^2}{2v_a v_b}))| \\ &= \begin{cases} g(v_r, v_a, v_b), & |v_a - v_b| \leq v_r \leq v_a + v_b \\ 0, & otherwise \end{cases} \end{aligned} \tag{3.6}$$

where $g(x, y, z) = \frac{2}{\pi}\frac{x}{\sqrt{2(x^2y^2+x^2z^2+y^2z^2)-x^4-y^4-z^4}}$.

In particular, if both nodes move at the same speed $v = v_a = v_b$, we will have

$$p(v_r|v) = \begin{cases} \frac{2}{\pi}\frac{1}{\sqrt{4v^2-v_r^2}}, & v_r \in [0, 2v] \\ 0, & otherwise \end{cases} \tag{3.7}$$

3.2.2 Distribution of Link Lifetime

The essence of modeling link dynamics in MANETs consists of evaluating the distribution of LLT, because it reflects the link dynamics resulting from the motions of

nodes. LLT measures the duration of time for a node to continuously stay inside the communication range of another node. In our model, this range is a circle.

Clearly, different mobility models and parameters lead to different LLT distributions, and the main challenge in modeling LLT consists of making the problem tractable and relevant. We know that the relative movement of nodes consists of a sequence of mobility trips, derived from the chain of mobility trips of the two communicating nodes. Let A_s be the starting point of the current mobility trip and the end point of the current trip be denoted by A_d. We have that A_d may be anywhere in the cell, i.e., inside or out of the communication circle. In the case that A_d is located inside the communication circle, it serves as the starting point (i.e., a new A_s) for the next trip and the whole process is repeated. In the evaluation of LLT, this process is repeated until the final A_d is outside of the communication circle.

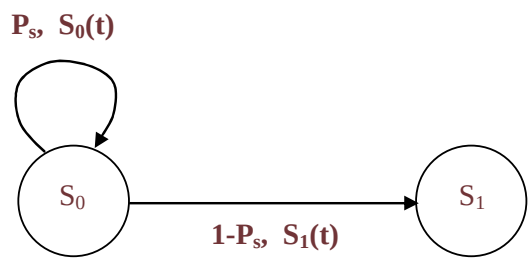

Figure 3.3: Two-state Markovian model for LLT evaluation

As illustrated in Fig. 3.3, the procedure for evaluating the LLT can be modeled as a two-state Markovian process. The residence state $\mathbf{S_0}$ represents the scenario where the end point A_d of the current trip is located inside the communication circle, while

the departing state $\mathbf{S_1}$ refers to the complementary scenario in which A_d is outside of communication circle. Compared to the model by Samar and Wicker [69, 70], in which only the last scenario (i.e., state $\mathbf{S_1}$) is considered, the two-state Markovian model reflects the motion of nodes more accurately, which leads to better results in evaluating link dynamics.

Let P_s be the *residence probability*, which denotes the probability that A_d is located inside the communication circle. The probability distribution function (PDF) $S_0(t)$ specifies the distribution of sojourn time of mobility epochs when a node stays in state $\mathbf{S_0}$. Correspondingly, the PDF $S_1(t)$ is used to measure the distribution of the departing time, when node moves out of communication circle and switches to state $\mathbf{S_1}$.

Before eventually moving out of the communication circle (i.e., being switched to the departing state $\mathbf{S_1}$), nodes may stay at the residence state $\mathbf{S_0}$ multiple times. Let N_i be the integer variable counting the number of times for a node to remain in state $\mathbf{S_0}$, and let $\{s_{0,0}, \ldots, s_{0,N_i-1}\}$ be the associated random variables that specify the duration of time of trips for each return.

Clearly, $\{s_{0,0}, \ldots, s_{0,N_i-1}\}$ are random variables of the same distribution but correlated. However, to make our problem more tractable, we assume that $\{s_{0,0}, \ldots, s_{0,N_i-1}\}$ are statistically i.i.d random variables of distribution $S_0(t)$. Our simplifying assumption makes the final result slightly deviated from the real situation when the residence probability becomes larger. However, as we will see later, our model still provides a good approximation, even with a large residence probability.

We define s_1 as the random variable measuring the departing time of distribu-

tion $S_1(t)$. The conditional link life time $T_L(N_i)$ and $P(N_i = K)$ can be evaluated as follows:

$$T_L(N_i) = \sum_{i=0}^{N_i-1} s_{0,i} + s_1, \tag{3.8}$$

$$P(N_i = K) = P_s^K. \tag{3.9}$$

The characteristic function $U_{T_L}(\theta)$ for the LLT T_L can then be evaluated as

$$\begin{aligned} U_{T_L}(\theta) &= E(e^{j\theta T_L}) \\ &= \sum_{k=0}^{\infty} E(e^{j\theta(\sum_{i=0}^{k-1} s_{0,i}+s_1)})P(N_i = k) \\ &= \sum_{k=0}^{\infty} U_1(\theta)U_0(\theta)^k P_s^k \\ &= \frac{U_1(\theta)}{1 - U_0(\theta)P_s}, \end{aligned} \tag{3.10}$$

where $U_0(\theta)$ and $U_1(\theta)$ are the characteristic functions of $S_0(t)$ and $S_1(t)$, respectively.

When the communication circle is small with respect to the network size and nodes' speed, A_d is mostly located outside of the communication circle. Consequently, we have $P_s \ll 1$. Given that $U_0(\theta)$ is the characteristic function of $S_0(t)$, it follows that $|U_0(\theta)| \leq 1$. Finally, it is clear that $U_0(\theta)P_s \ll 1$. Therefore, Eq. (3.10) can be approximated as

$$U_{T_L}(\theta) \approx U_1(\theta) \tag{3.11}$$

For clarity, we call Eq. (3.10) Exact LLT (ES-LLT), which is based on the two-state Markovian model. The approximation in Eq. (3.11) is called Approximated LLT (AS-LLT), and it reflects the scenario considered by Samar and Wicker [69, 70]. As we will see later, for the random direction mobility model (RDMM), the analytical expression of AS-LLT is the same as the expression in [69, 70], except for a normalization factor.

3.2.3 Practical Implications

It is clear that the two-phase Markov model is a general model that can be applied to networks with different mobility models by adapting its two building blocks $S_0(t)$ and $S_1(t)$ to the specific network and mobility models, including but not restricted to the random trip mobility model.

However, in some practical scenarios, the analytical formulations of $S_0(t)$ and $S_1(t)$ might not be available. Under such circumstances, one can collect a trace data to obtain $S_0(t)$ and $S_1(t)$ and still give an accurate estimate of the overall link lifetime. By doing so, it can greatly reduce the amount of empirical data necessary to accurately estimate link lifetime. Furthermore, one can also obtain analytical formulations by curve-fitting empirical data and incorporate these formulations to our Markov model for an analytical study of the mobility characteristics.

3.2.4 Link Lifetime in Random Direction Mobility Model

The RDMM is an important mobility model for MANETs. It improves RWMM model on the stationary uniform nodal distribution, and has been widely adopted [42, 43, 51, 9, 35]. However, the analysis on the characteristic of link lifetime of RDMM is quite limited. For the reason, we provide a deeper understanding of RDMM by providing an analytical expression for characterizing its link lifetime.

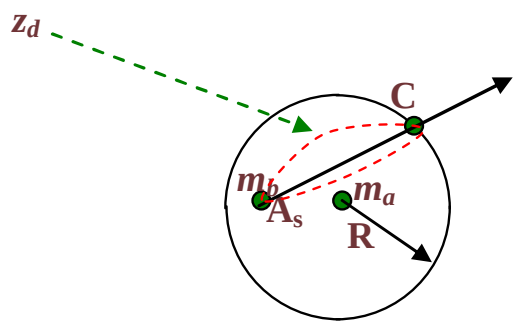

Figure 3.4: Graphical Illustration of z_d: Unrestricted Networks.

To evaluate the LLT T_L, we need to evaluate P_s, $S_0(t)$, and $S_1(t)$. Let z_d denote the least distance to be traveled by node to move out of the communication circle, starting from the position A_s and without changing the direction and speed v_r. A graphical illustration of z_d is presented in Fig. 3.4. The probability P_s can now be evaluated through z_d as

$$
\begin{aligned}
P_s &= E_{z_d}(P_s(z_d)) = \int_{z_d} P_s(z_d)p(z_d)dz_d && (3.12)\\
P_s(z_d) &= \int_{v_r} P(\tau \leq \frac{z_d}{v_r})p(v_r)dv_r \\
&= \int_{v_r} (1 - F_m(\frac{z_d}{v_r}))p(v_r)dv_r \\
&= \int_{v_r} (1 - exp(-2\lambda_m z_d/v_r))p(v_r)dv_r, && (3.13)
\end{aligned}
$$

where $P_s(z_d)$ is the conditional probability of P_s on z_d, and $p(z_d)$ is the PDF of z_d. The evaluation of z_d directly follows from [41]:

$$
p(z_d) = \begin{cases} \frac{2}{\pi R^2}\sqrt{R^2 - (\frac{z_d}{2})^2}, & \text{for } 0 \leq z_d \leq 2R \\ 0, & \text{elsewhere} \end{cases} \tag{3.14}
$$

$S_0(t)$ is the PDF of the time duration for nodes to return to state $\mathbf{S_0}$. Conditioning on z_d and assuming that the starting time is at time 0, $S(t)$ is the probability of node m_b changing its relative velocity at time t on condition that A_d is located inside the communication circle. Therefore,

$$
\begin{aligned}
S_0(t) = &\ E_{z_d}(S_0(t|z_d)) && (3.15)\\
S_0(t|z_d) = &\ \frac{1}{P_s}P(t = \tau, z_d \geq v_r\tau|z_d) = \frac{1}{P_s}P(\tau = t)P(v_r \leq \frac{z_d}{t}|z_d) \\
= &\ \frac{1}{P_s}2\lambda_m e^{-2\lambda_m t}\int_0^{\min\{V_m, \frac{z_d}{t}\}} p(v_r)dv_r, && (3.16)
\end{aligned}
$$

where $S_0(t|z_d)$is the conditional PDF on z_d and V_m is the maximum speed of v_r.

$S_1(t)$ can be evaluated in much the same way as we have done for $S_0(t)$. Conditioning on z_d and assuming that the starting time is at time 0, $S_1(t)$ is simply

the probability of the node m_b moving out of the communication circle at time t with relative velocity being kept constant. Similar to the previous case, we have

$$
\begin{aligned}
S_1(t) = & \quad E_{z_d}(S_1(t|z_d)) && (3.17)\\
S_1(t|z_d) = & \quad \frac{1}{1-P_s}P(t=\frac{z_d}{v_r}, z_d \leq v_r\tau|z_d) \\
= & \quad \frac{1}{1-P_s}P(\tau \geq t)p(v_r=\frac{z_d}{t})|\frac{d}{dt}(\frac{z_d}{t})| \\
= & \quad \frac{1}{1-P_s}exp(-2\lambda_m t)p_{v_r}(\frac{z_d}{t})\frac{z_d}{t^2}, && (3.18)
\end{aligned}
$$

where $S_1(t|z_d)$ is the conditional PDF on z_d using the Jacobian of the transformation.

Let us define v_{s_1} to be the conditional relative velocity associated with state $\mathbf{S_1}$ such that $p(v_{s_1}) = p(v_r|S_1)$ and it should be noted that the distribution of v_{s_1} can be greatly different from the distribution of $p(v_r)$. Accordingly, an alterative way to evaluate $S_1(t)$ is:

$$
\begin{aligned}
S_1(t) = & \quad E_{v_{s_1}}(S_1(t|v_{s_1})) && (3.19)\\
S_1(t|v_{s_1}) = & \quad \frac{1}{1-P_s}P(t=\frac{z_d}{v_{s_1}} \mid z_d \leq v_{s_1}\tau) \\
= & \quad \frac{1}{1-P_s}P(\tau \geq t)p(z_d = v_{s_1}t)\frac{d}{dt}(v_{s_1}t) \\
= & \quad \begin{cases} \frac{4e^{-2\lambda_m t}}{\pi(1-P_s)}\frac{v_{s_1}}{2R}\sqrt{1-(\frac{v_{s_1}t}{2R})^2}, & 0 \leq t \leq \frac{2R}{v_{s_1}} \\ 0, & \text{elsewhere} \end{cases}
\end{aligned}
$$

where $S_1(t|v_{s_1})$ is the conditional PDF of $S_1(t)$ on v_{s_1}. A detailed examination of Eq. (3.19) reveals that it shares the same core analytical expression of link lifetime

distribution of Eq. (15) in [70], with the only exception that a normalization factor $e^{-2\lambda_m t}/(1 - P_s)$ accounts for the probability of nodes leaving for state $\mathbf{S_1}$. It implies that AS-LLT formula, solely relying on $S_1(t)$, gives the same link lifetime distribution as in [70].

3.3 Path Lifetime in MANETs

We have examined the dynamics of link lifetime for a point-to-point link. However, for most cases in MANETs, a packet needs to be forwarded by several intermediate nodes before finally reaching the destination. The source node, intermediate nodes and destination node collectively form a multi-hop path for the packet. Clearly, path dynamics is also an essential metric for protocol design and optimization. Han et al. showed [37, 38] that path dynamics converge asymptotically to an exponential distribution, when links are assumed to be independent or of limited dependence. The result works well when a path involves a significant number of hops but not for paths with a small to moderate number of hops. In this section, we will extend the proposed analytical framework to evaluate path dynamics with small to moderate numbers of hops, assuming that each link along the path behaves independently of others. In reality, adjacent links have some correlation, which is difficult to model. Modeling dependent links requires a number of conditional probability distributions, and a solution may not be feasible. The independence assumption that we make greatly simplifies the analysis and still provides a good approximation.

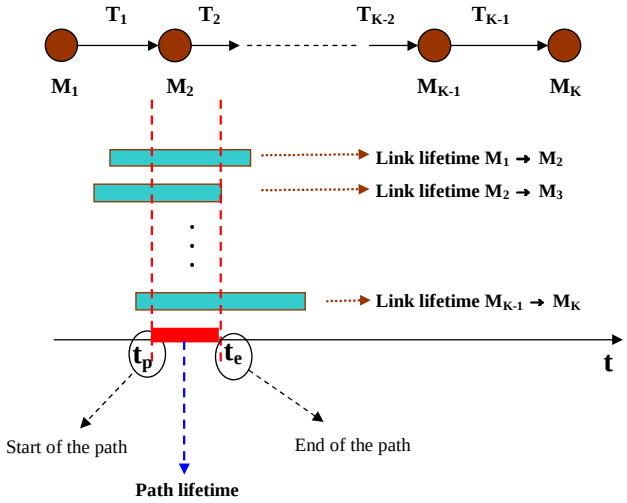

Figure 3.5: Path structure.

As illustrated in Fig. 3.5, a packet from source node M_1 needs to follow the ordered set of links $\{T_1 \rightarrow T_2 \rightarrow \ldots \rightarrow T_{K-1}\}$ to reach the destination node M_K. Successful delivery of the packet requires that none of these links on the path breaks during packet transmission. When any of the links breaks, the path no longer exists and the path discovery process needs to be reinitiated to find alternative paths. In other words, lifetime $T_P(K)$ of the $(K-1)$-hop path is the minimum lifetime of the links that form it, and can be written as

$$T_P(K) = \min\{T_1, \ldots, T_{K-1}\} \tag{3.20}$$

Because links are assumed to operate independently with i.i.d motion, their lifetime also follows the same statistical distribution as T_L. However, when the source node initiates a data transfer to the destination node, links may have been in existence for some time; therefore, as Figure 3.5 illustrates, the lifetime $T_i, i \in \{1, \ldots, K-1\}$ of the directional

link on the data path should be the *residual lifetime* of the link, i.e,

$$T_i = T_L(\epsilon_i), i \in \{1, \ldots, K-1\} \tag{3.21}$$

where $\epsilon_i \geq 0$ is a random variable representing the elapsed time of the link $M_i \rightarrow M_{i+1}$ before the data path started and clearly, $T_L = T_L(0)$.

From Section 3.2, we know that the evaluation of $T_L(\epsilon_i)$ depends on a set of three parameters, i.e., the spatial distribution of nodes at time ϵ_i, the distribution of speed $v_r(\epsilon_i)$ at time ϵ_i, and the residual change time distribution $\tau(\epsilon_i)$ at ϵ_i. At time 0 and ϵ_i, nodes are expected to follow the same stationary distribution and therefore resemble each other. Similarly, it can be expected that the speed distribution of v_r will be also the same. Therefore, we expect that the distribution of $\tau(\epsilon_i)$ and $\tau(0)$ will resemble each other. In particular, we know that the distribution of $\tau(0)$ for the RDMM model is exponentially distributed. Accordingly, because of the memoryless property of the exponential distribution, the distribution of $\tau(\epsilon_i)$ and $\tau(0)$ will exactly resemble each other. Finally, we conclude that the distribution of T_i will resemble the distribution of $T_L = T_L(0)$.

Summarizing the above discussion, the CCDF $F_P(K, t)$ of the lifetime for a $(K-1)$-hop path can be computed as

$$F_P(K, t) = F_L^{K-1}(t). \tag{3.22}$$

3.4 Model Validation

3.4.1 Simulation Setup

In the simulation, there are 100 nodes randomly placed in a $1000m \times 1000m$ square cell. Each node has the same transmit power and two profiles of radio transmission range are chosen for the simulation experiments. Both are within the coverage of IEEE 802.11 PHY layer and they are $\{200m, 100m\}$. After initial placement, nodes keep moving continuously according to the RDMM model. The mobility parameter λ_m is the same as the one in [31] ($\lambda_m = 4$), which means that nodes change their velocity at every $\frac{1}{4}$ hour in average. Furthermore, we assume that every node is moving at the same constant speed and only its direction is changed according to the RDMM model. The simulation with variable speeds can be obtained by averaging the results from every speed with respect to the distribution of speed v. However, it should be noted that the relative speeds between nodes are not constant and their statistics are derived in Section 3.2.1. Three different speeds are simulated $v \in \{1, 10, 20\}(m/s)$, which range from pedestrian speed to vehicle speed. Combining the power profile and velocity profile, six different scenarios are simulated $\{I : (200m, 1m/s); II : (100m, 1m/s); III : (200m, 10m/s); IV : (100m, 10m/s); V : (200m, 20m/s); VI : (100m, 20m/s)\}$.

Nodes are randomly activated for data transmission. The traffic of activated nodes is supplied from a constant bit rate (CBR) source with a packet rate of $0.5p/s$. Given that the choice of specific MAC layer and routing protocol may affect the results,

we assume perfect MAC and routing protocols, rendering zero delays or losses due to their functionalities. This enables the simulation to capture statistics solely due to mobility.

3.4.2 Accuracy of Models

Table 3.1: Residence Probability P_s: Unrestricted Networks.

Radius (m) (R)	**Speed** v (m/s)		
	$v = 1$	$v = 10$	$v = 20$
$R = 100$	$P_s = 0.194$	0.033	0.018
$R = 200$	$P_s = 0.3072$	0.058	0.033

Table 3.1 describes the residence probability P_s for all six scenarios. As shown in Eqs. (3.15) and (3.17), the characteristics of mobility are governed by the ratio between the radius R of the communication circle and the speed v, which we call the relative radius (ReR) $\frac{R}{v}$. Among the six different scenarios, there are five different ReR values $\{5, 10, 20, 100, 200\}$, given that IV and V scenario have the same ReR and exhibit similar results, as will be seen from simulations. As shown in Table 3.1, the residence probability increases with ReR, indicating that it is more likely for nodes with larger ReR to stay inside the communication circle.

Fig. 3.6 presents the results for link lifetime ES-LLT and AS-LLT predicted by our analytical model, as well as by the simulations. The results clearly confirm that the two-state Markovian model is a powerful tool to model link dynamics of the link lifetime distribution as a function of node mobility. It can be also observed that the ES-LLT formula, obtained from the Markovian model, shows a very good match with

simulations in all scenarios. On the other hand, the AS-LLT formula, which corresponds to the model by Samar and Wicker [69, 70] gives good approximations to the simulations only for small values of ReR ($\frac{R}{v}$), and greatly deviates from the simulations when ReR becomes large, i.e., larger residence probability P_s and larger possibility for nodes to stay inside communication circle.

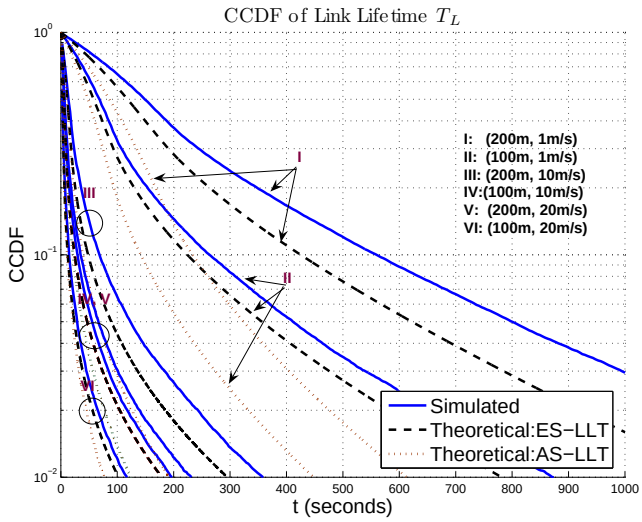

Figure 3.6: Link Lifetime T_L (RDMM): Simulated, ES-LLT(Markovian), and AS-LLT.

As stated in section 3.2.3, in some practical scenarios, the analytical formulations of $S_0(t)$ and $S_1(t)$ might need to be obtained from empirical data to characterize the overall link lifetime. Fig. 3.7 presents such a result, where trace data are generated from the RWMM. Because there is no analytical formulations of $S_0(t)$ and $S_1(t)$ for RWMM, the two-phase Markov model is applied by using empirical simulated data to estimate the link lifetime. The results clearly confirm the accuracy, effectiveness and generality of our Markov model to analyze more practical mobility models.

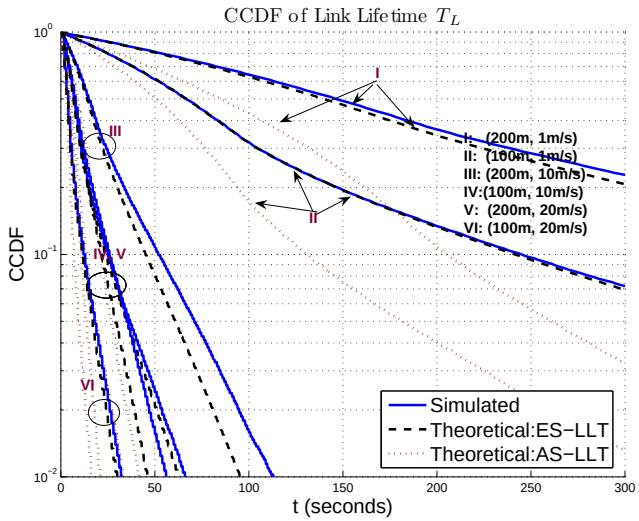

Figure 3.7: Link Lifetime T_L (RWMM): Simulated, ES-LLT(Markovian), and AS-LLT.

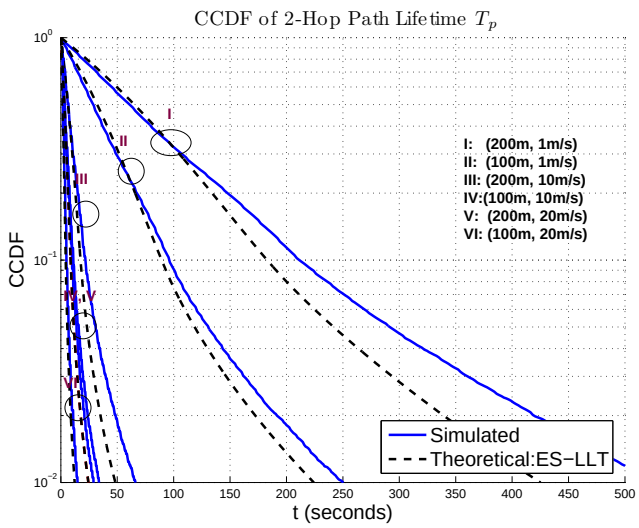

Figure 3.8: Simulation: 2-Hop Path Lifetime.

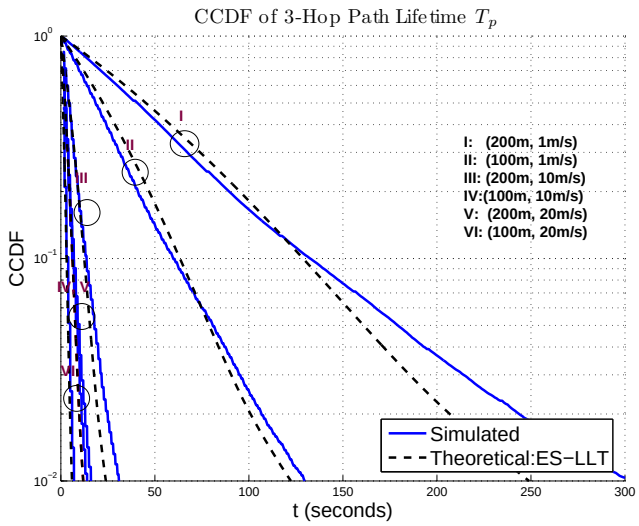

Figure 3.9: Simulation: 3-Hop Path Lifetime.

Figs. 3.8 and 3.9 present the results of path lifetime. It can be observed that path lifetime can be modeled accurately with the proposed Markovian model, and is only slightly affected by the independence assumption used to derive it.

In summary, the Markovian model (ES-LLT formula) is more accurate model than the AS-LLT formula [69, 70] for all ranges of ReR and shows good approximations to all simulations, in contrast to the AS-LLT formula that gives good approximation only when ReR is relatively small.

3.5 Packet-Length Optimization

3.5.1 Link Lifetime and Packet Length

Given that nodes move in a MANET, the data transfer can be temporarily broken if any link on the path to the destination is broken. An alternative path may not be available immediately, and significant delay can be incurred in repairing a route. Within the context of MANETs, it is important to use information packet lengths that maximize the end-to-end throughput. If a information data-packet length is too long, frequent link breaks can lead to significant packet dropout during the transfer. On the other hand, if data packet length is too short, the packet-header overhead and channel access overhead can reduce the effective throughput significantly. Hence, a judicious choice of information packet length as a function of link dynamics can be of great importance in maximizing throughput in MANETs. However, this problem has been overlooked in the past, because its solution requires knowledge of statistics of link lifetime. With the computed CCDF in Section 3.2, we are able to provide packetizing schemes optimized on various systematic constraints.

When the length of packets is constant, it is natural to ask what the optimal packet length would be. For every packet length L_p, we know that there is an associated link outage probability P_{L_p} specifying the probability of link breach during packet transfer. Every dropped packet during link outage is either lost or must be retransmitted and therefore reduces the effective throughput. The optimal packet length is chosen such that the total throughput is maximized.

One approach is to simply choose the maximum possible packet length L_0 that satisfies a pre-defined link outage probability requirement. We call this strategy link outage priority design (LOPD) and it can be described as

$$L_0 = max_{L_p} \; P_{L_p} \leq \omega_p \tag{3.23}$$

where ω_p is a constant specifying the link dropout probability requirement.

Alternatively, we can use a cost function $C(L_p, P_{L_p})$ that incorporates the negative effect from the packet retransmission into evaluating the effective throughput $ET(L_p)$ for a specific packet length L_p. The cost function $C(L_p, P_{L_p})$ could be a systematic constraint from upper layer, such as the negative effects from delay and packet retransmissions. Further optimizing the effective throughput $ET(L_p)$ gives the optimal packet length L_0. Consequently, we refer to this strategy link throughput priority design (LTPD).

In LTPD, when the packet length is L_p, we can describe the effective throughput $ET(L_p)$ function as

$$ET(L_p) = (1 - P_{L_p}) \cdot L_p - C(L_p, P_{L_p}) \cdot P_{L_p} \cdot L_p \tag{3.24}$$

The optimal packet length L_0 will be the one that maximizes the effective throughput

$$L_0 = max_{L_p} \; ET(L_p) \tag{3.25}$$

Normally, P_{L_p} is a monotonically decreasing function w.r.t. packet length. When the cost function is chosen to be a constant penalty value, i.e., $(C(L_p, P_{L_p}) = C)$

by taking the derivative with respect to L_p, the optimal packet length L_0 is the value satisfying

$$1 - (1 + C)P_{L_0} = (1 + C)L_0 \left. \frac{dP_{L_p}}{dL_p} \right|_{L_p = L_0} \tag{3.26}$$

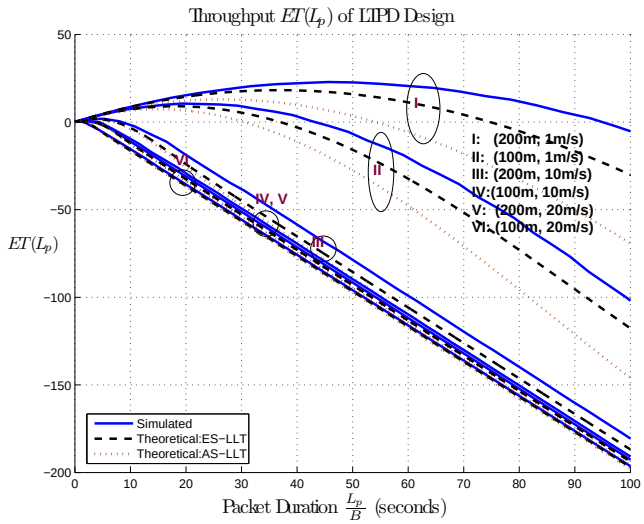

Figure 3.10: LTPD Design: Unrestricted Networks.

In Fig. 3.10, we exploit the application of the link lifetime distribution to the optimization of packet-length design using the same examples of the previous section. For illustration purposes, the cost function for our example of LTPD is chosen as a constant penalty value of 2 (i.e., $C(L_p, P_{L_p}) = 2$). However, it should be noted that the practical cost function can be much more complicated and determined by upper layers for a cross-layer optimization solution. The effective throughput $ET(L_p)$ is computed for every L_p and drawn for all three methods: Simulated, ES-LLT (Markovian model) and AS-LLT. As expected, ES-LLT approximates the simulation very well, while AS-

LLT tends to conservatively underestimate the effective throughput for larger ReR. In addition, all curves of the effective throughput (either Simulated, ES-LLT or AS-LLT formula) are convex functions with numerical solutions readily available.

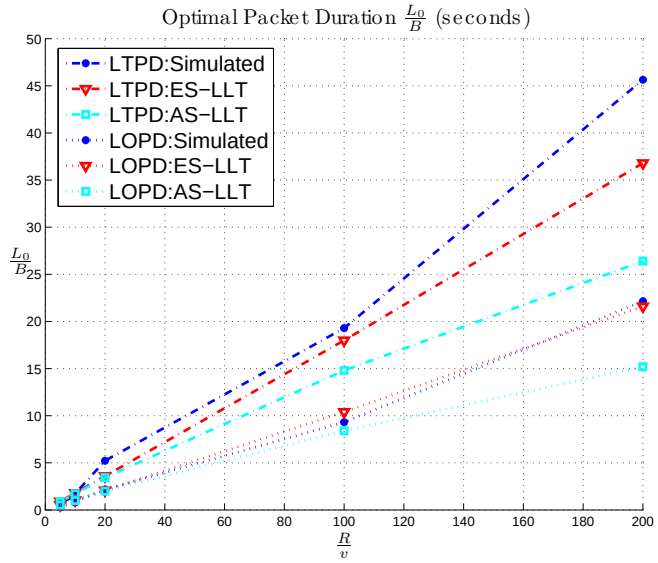

Figure 3.11: Optimal Packet Duration $\frac{L_0}{B}$: Unrestricted Networks.

The optimized solutions $\frac{L_0}{B}$ on packet design for all design methods are illustrated in Fig. 3.11. In the simulation, the link outage tolerance of LOPD is set to be $\omega_p = 0.1$, i.e., the maximum link outage probability should be less than 10%. Two key observations should be made: First, the ES-LLT (Markovian model) approaches the simulated optimal solution well for LTPD and LOPD, and signifies substantial improvement of throughput over the AS-LLT model ([69, 70]). Second, LTPD suggests a balanced design between longer packet and larger retransmission rate to offer higher throughput over LOPD. On the other hand, LOPD tends to be more conservative on throughput but renders fewer packet retransmissions.

Another important observation from Fig. 3.11 is that the optimal solutions, obtained from either the simulation or Markovian ES-LLT formula, exhibit linear proportion to the ReR value $\frac{R}{v}$. It suggests that mathematically, the optimal packet design should follow the rule[2]

$$\frac{L_0}{B} = \Theta(\frac{R}{v}) \tag{3.27}$$

3.5.2 Path Lifetime and Packet Length

We can also investigate the optimal packet length for a given path and the effect of hop count on the optimal packet length. Extending the optimal packet design example in Section 3.5 for a 2-hop path, the results we obtain are shown below.

In Fig. 3.12, we only present the results following LOPD, because the penalty of a path breakage is usually pretty high and a more practical design is to ensure that packet can get through the path with low outage probability. For example, in AODV [65], the source needs to flood the network to reinitiate a route to the destination, when an existing path breaks. Furthermore, similar to the case of link lifetime, the linear relationship between the optimal packet length and network parameters can also be observed. Although only the results for 2-hop and 3-hop paths are shown here, we have examined cases with different hop counts (various K) and they all exhibit similar behavior.

[2]We recall that $f(n) = \Theta(g(n)$ means there exist positive constants c_1, c_2 and M, such that $0 \leq c_1 g(n) \leq f(n) \leq c_2 g(n)\ \forall n > M$.

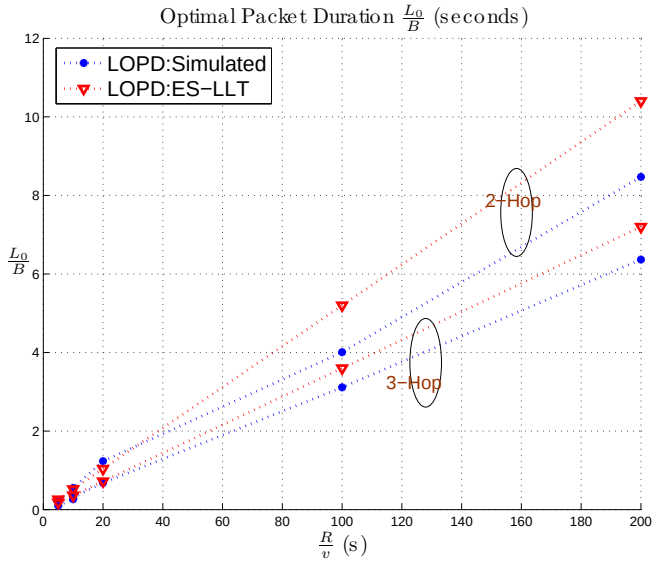

Figure 3.12: Optimal packet length for multi-hop paths: Unrestricted Networks.

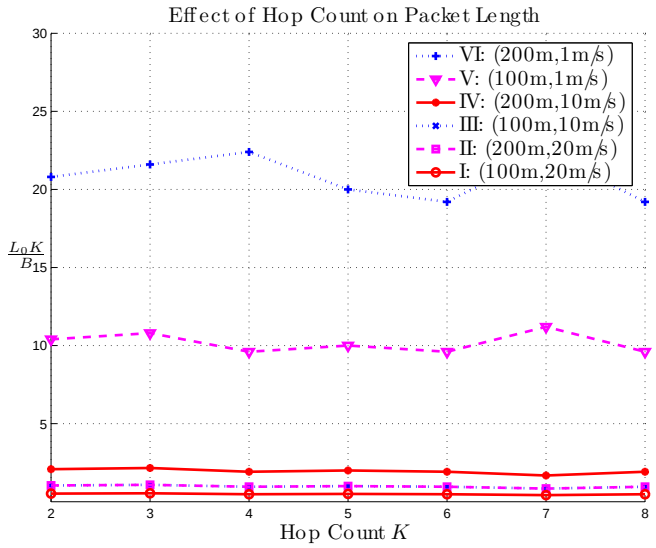

Figure 3.13: Effect of hop count on packet length: Unrestricted Networks.

Another aspect examined here is the effect of hop count on the choice of optimal packet length. In Fig. 3.13, for each K-hop path, the optimal packet length is chosen based on LOPD design criterion. We can see that the packet length should also be chosen such that[3]

$$\frac{L_0 K}{B} = \Theta(1). \tag{3.28}$$

Combining our observations from Figs. 3.12 and 3.13, we conclude that the packet length for a K-hop path should be designed as

$$\frac{L_0}{B} = \Theta(\frac{R}{vK}). \tag{3.29}$$

3.6 Cache Lifetime Optimization

From the previous analysis, we observe that the optimal packet length should be chosen based on the knowledge of hop distance between source and destination. Similarly, the route caching scheme of on-demand routing protocols should follow the same rule. However, without knowing the relationship represented in Eq.(3.29), it is difficult to determine the timeout value for different routes. As a result, on-demand protocols like DSR [45] use the same value for the parameter *RouteCacheTimeout* to set the timeout *for all* cached routes. However, based on Eq.(3.29), we know that the

[3]Equivalently, we can transfer K to the other side of this equation. It means that when the number of hops increases for a constant bandwidth B, the packet length should decrease.

cache timeout scheme for DSR and any on-demand routing protocol should be adapted to the hop count of the cached routes. An example of a mobility-adaptive cache timeout scheme for DSR derived based on the analytical guidance that we gain from our model is the following:

- A base parameter *RouteCacheTimeout* takes user input to set timeout value for a point to point link (one-hop path). Such value can be either chosen in ad hoc manner or determined from LTPD or LOPD design of section 3.5.

- The timeout value T_k of a route is determined based on the base parameter and the number (K) of links involved on the route. And it can be expressed as $T_k = RouteCacheTimeout/K$.

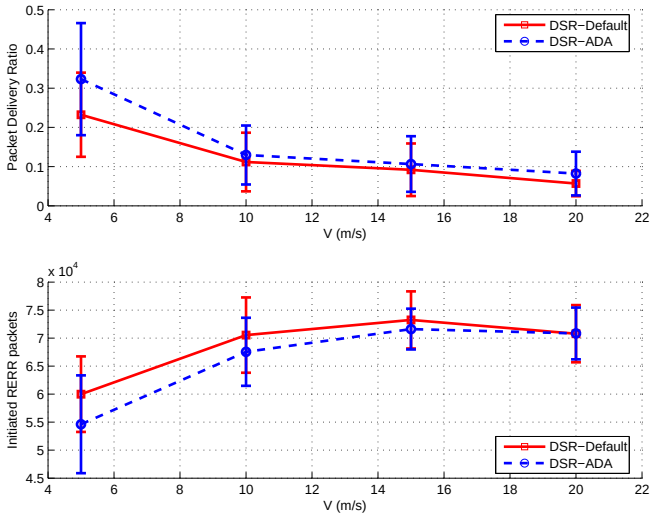

Figure 3.14: Illustrative Example of Cache Guideline.

Fig. 3.14 presents results of this illustrative hop-adaptive caching strategy for DSR. In the simulation, 50 nodes are randomly moving in a $1500m \times 500m$ area according

to the random waypoint model without pause. The minimum speed is zero and the maximum speed V varies. The source and destination pairs are randomly chosen. Ten pairs are simulated and traffics are supplied from CBR source at a rate $4p/s$. Each packet is of size 64 bytes and all simulations run for 900 seconds. Ten random seeds are simulated for each configuration. The implementation of DSR used for comparison is the default implementation in *Qualnet 3.9.5*.

Fig. 3.14 compares the default DSR (DSR-Default) and the hop-adaptive DSR (DSR-ADA). It can be observed that, by effectively timing out stale paths, DSR-ADA reduces the overhead incurred from route error (RERR) packets and improves the overall packet delivery ratio. This further confirms that our modeling framework can be used to improve existing routing protocols. However, it should be noted that the above DSR-ADA cache strategy is by no means a perfect solution to the caching problem in on-demand routing. It is meant simply as an example to illustrate the effectiveness of analytical results that are derived in the thesis.

3.7 Analysis of Throughput, Average Delay, and Storage

We consider the well-known two-hop forwarding scheme introduced by Grossglauser and Tse [33, 34] in the computation of the throughput of a MANET. Following a bottom-up approach and utilizing our analytical results on the optimal packet length in section 3.5, we rediscover exactly the same result on the throughput, showing the effectiveness of our models on the computation of throughput and capability to handling

more complex schemes. Furthermore, we give a comprehensive packet-level and bit-level analysis on the delay and storage requirement, in contrast to most studies where only the packet level analysis can be conducted.

3.7.1 Throughput

Because the two-hop forwarding scheme is such that packets are transferred only when nodes are close to each other, the packet length L_0 should be chosen according to the results from the analysis of link lifetime, i.e., $L_0 = \Theta(\frac{R \cdot B}{E(v)})$. Based on the mobility models in [31], we have one data packet transferred on average for every time duration of $I = \Theta(\frac{L^2}{E(v) \cdot R})$. Accordingly, the link throughput T_0 for one pair of nodes can be computed as

$$T_0 = \frac{L_0}{I} = \Theta(\frac{R^2 B}{L^2}) \tag{3.30}$$

Meanwhile, R should be chosen on the order of $\Theta(L/\sqrt{n})$, i.e., $\frac{R}{L} = \Theta(\frac{1}{\sqrt{n}})$[33, 34]. Therefore, the above equation is reduced to $T_0 = \Theta(B/n) = \Theta(1/n)$. For each source node, except for the direct path, we can have at most $n-2$ such 2-hop paths to help deliver its packet to destination. Therefore, the per source-destination throughput can be computed as

$$\Lambda(n) \leq T_0 \cdot (n-2) \Rightarrow \Lambda(n) = \Theta(1). \tag{3.31}$$

Thus far, we have obtained exactly the same results in [33, 34] on throughput, and the above analysis leads to the following conclusion on the throughput $\Lambda(n)$ of a MANET subjecting to the two-hop forwarding discipline.

Theorem 1 *For MANETs with unrestricted mobility, we have* $\Lambda(n) = \Theta(1)$ *for generic mobility models.*

3.7.2 Delay & Storage

To compute the delay and storage incurred in a MANET, we assume that every relay node maintains a separate queue for each S-D pair and the queue is served in a First-Come-First-Serve (FCFS) manner. Because all cells resemble each other and nodes have iid movements, it is clear that all such queues are similar.

Consider an S-D queue at relay node m_r, a packet arrives when node m_r and the previous relay node (or the source node) simultaneously come into the communication region; a packet departs when m_r meets another relay node (or the destination node) in the communication region. Both the inter-arrival time and the inter-departure time are of the same order as link interarrival time (LIT) from the mobility models in [31]. We also know from [31] that LIT can be characterized as exponentially distributed, each queue is then characterized of a Poisson arrival process with exponential service time, thus being an M/M/1-FCFS queue.

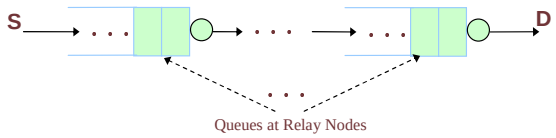

Figure 3.15: Tandem queue: Unrestricted Networks.

For each S-D pair, queues at relay nodes construct a M/M/1-FCFS feedforward

tandem network[4]as in Fig. 3.15. An important property of a M/M/1-FCFS feedforward tandem network is the *Jackson's theorem* (see [46], page 150), i.e., if the tandem network with exponential service time is driven by a Poisson arrival process, every queue in the tandem network behaves as if it were an independent M/M/1-FCFS queue and thus can be analyzed individually. Recall the following properties for a M/M/1-FCFS queue (see [46], chapter 3) in the following lemma.

Lemma 1 *Consider a discrete M/M/1-FCFS queue. Let* $1-\epsilon$ *be the* traffic intensity *and* λ *be the exponential* service rate *of the queue, the average delay is given by*

$$E(D) = \frac{1}{\lambda\epsilon} = \Theta(\frac{1}{\lambda}) \tag{3.32}$$

Furthermore, the mean and variance of the occupancy of the queue N_q *is*

$$E(N_q) = \frac{1-\epsilon}{\epsilon} = \Theta(1) \tag{3.33}$$

$$Var(N_q) = \frac{1-\epsilon}{\epsilon^2} = \Theta(1) \tag{3.34}$$

Recall that the service rate of each queue can be written as $\lambda = \Theta(\frac{E(v)R}{L^2})$ [31] and also that the delay for each S-D pair is the summation of delays occurred at relay nodes. Assuming that every relay node carries traffic for $\Theta(n)$ S-D pairs, we can now summarize the network performance in terms of average delay and storage in the following theorem.

[4]For delay to be finite, the arrival rate must be strictly less than the service rate but in this case, symmetric movements lead to a fully loaded tandem queue. To avoid this, we assume that if the available throughput is $\Lambda(n)$, each source generates traffic at a rate $(1-\epsilon)\Lambda(n)$, for some $\epsilon > 0$.

Theorem 2 *The average packet delay in MANETs with unrestricted mobility is given by*

$$D(n) \quad = \quad \Theta(\frac{L^2}{E(v)R}) \tag{3.35}$$

and the average information bit delay $D_b(n)$ is

$$D_b(n) = \frac{D(n)}{L_0} = \Theta(\frac{L^2}{R^2 B}) \tag{3.36}$$

Furthermore, the mean and variance of the packet occupancy (i.e., storage requirement) is given by

$$E(N_p) = Var(N_p) = \Theta(n) \tag{3.37}$$

and the corresponding bit storage requirement N_b is

$$E(N_b) = Var(N_b) = \Theta(n) \cdot \Theta(\frac{RB}{E(v)}) \tag{3.38}$$

Summarizing, we can make the following observations:

- Throughput of the network scales as $\Lambda(n) = \Theta(1)$ and packet-wise storage scales as $\Theta(n)$. Attaining optimal throughput comes with the price of increase in storage.

- Mobility can help alleviate packet delay but it does not help the bit-wise delay. It might be counter intuitive on a first glance. However, a detailed examination reveals that faster mobility brings more opportunities for nodes to deliver information packets but at the cost of reduced time for each communication. When information packets are optimally chosen, the negative effect from reduced communication time balances off the benefit from faster mobility. Eventually, the

only way to reduce the bit-wise delay is to increase the bandwidth and data rate for transmission, or use more transmission power to increase the communication range.

3.8 Conclusion

We have presented an analytical framework for the characterization of link and path lifetimes in MANETs with unrestricted mobility. Given the existence of prior attempts to incorporate link dynamics in the modeling of routing and clustering schemes [25, 75, 24], we believe that this new framework will find widespread use by researchers interested in the analytical modeling and optimization of MAC and routing protocols in MANETs. The advantage of our framework is that it accurately describes link and path dynamics as a function of node mobility.

We illustrated how our framework can be applied by using it to address the optimization of packet lengths and the design of route caching strategies as a function of link and path dynamics in MANETs. The optimized solutions obtained from the proposed analytical framework show a substantial improvement on network throughput and protocol performance. Furthermore, a performance analysis of throughput, delay and storage is also presented for MANETs using the two-hop forwarding scheme proposed by Grossglauser & Tse [33, 34] to give deeper insights to the understanding of system tradeoffs.

Chapter 4

Performance Evaluation of MANETs with Restricted Mobility: A Comprehensive Study

The earlier work in Chapter 3 contributes a two-state Markov model that better describes the mobility behaviors for communicating nodes. The proposed model shows improvement in characterizing the statistics of link lifetime, while subsumes the model of Samar and Wicker [69, 70] as a special case. By characterizing link lifetime, further study is pursued on the crosslayer optimization problem on segmentation of the information stream and to provide solutions to maximize the end-to-end throughput of wireless networks with unrestricted mobility.

Complementarily, another important contribution is to be made in the chapter by providing a comprehensive coverage of MANETs with restricted mobility, where

each node moves within a constrained area, by utilizing the proposed analytical model on link dynamics in Section 3.2. These networks play an important role in the real world, where nodes usually travel only a portion of the entire network. As published in the *information assurance framework* [2] from the National Security Agency, such networks represent the more realistic scenarios for tactical users, especially for the users deployed in the division and rear area. The only prior work that was aware is given by Groenevelt et al. [32]. It covers delay aspects of such networks, but only for the case of one-dimensional restricted mobility. For this reason, this chapter provides the first thorough analysis (to the best of our knowledge) of two-dimensional restricted mobility networks on link dynamics, optimal segmentation of information stream, throughput, delay, and storage tradeoffs.

The chapter is organized as follows. Section 4.1 describes system models including network and mobility models. Section 4.2 presents the analytical results on link lifetime, along with simulation for model validation. Section 4.3 uses the derived statistics of link lifetime in section 4.2 for the problem of optimal segmentation of information stream. The analytical treatment on characterizing distribution of link inter-arrival time is given in Section 4.4. Section 4.5 provides a thorough analysis of throughput, delay and storage capacity of a MANET with restricted mobility, followed by concluding remarks in section 4.6.

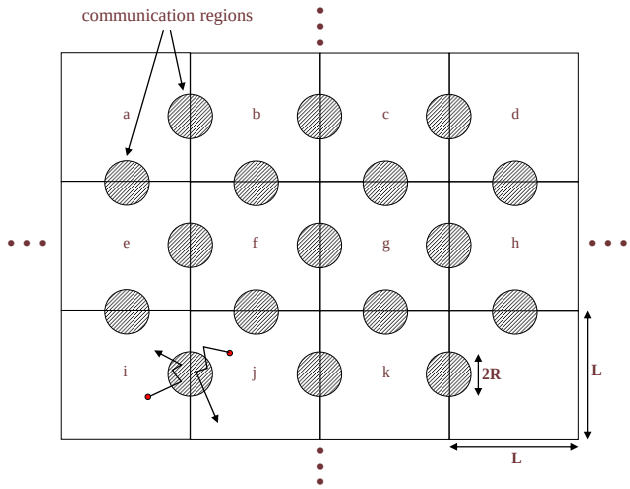

Figure 4.1: Network Model: Restricted Networks

4.1 Network Model

In many tactical applications [2], nodes of a MANET traverse only a small portion of the entire area covered by the network. We consider a square or rectangular area partitioned into squarelets similar to prior analytical models of MANETs and as depicted in Fig. 4.1. The entire network is divided into multiple squarelets, which we call *cells*, and each cell is of size $L \times L$.

Communication between nodes in neighboring cells is allowed around their cell boundaries and all nodes transmit with uniform power. According to the protocol model (Eq. 1.1 in Chapter 2), the allowable communication region should be deliberately designed to avoid excessive interference to nearby cells and to satisfy protocol model. Referring to the design in [53], a feasible solution is to choose circular regions centered at cell boundaries, as depicted in Fig. 4.1.

The movement of each node is restricted into the cell where it is initially located. Each source node randomly chooses its destination and in most cases, the source and destination nodes are not within the same cell. As a result, most data traffic need to travel across cells and links over neighboring cells are focal points for such networks. The analysis is focused on inter-cell links, since analysis of intra-cell links have been already covered in earlier work (Chapter 3).

4.2 Link Lifetime

Let B $(bits/s)$ be the transmission rate of a data packet, L_p be the length of the data packet, and $t_0 + T_a$ (or $t_0 + T_b$) denotes the moment a node m_a (or m_b) is moving out of communication range. A packet can be successfully transferred only if nodes m_a and m_b stay within communication range during the entire communication session, that is,

$$L_p/B \leq T_L \tag{4.1}$$

$$T_L = min(T_a, T_b). \tag{4.2}$$

T_L is the link lifetime (LLT) which dictates the maximum possible data transfer duration. Statistically, T_a and T_b specify the distribution of residence time that measures the duration of the time, for either nodes m_a or m_b, starting from a random location inside the communication region with equal probability and continuously stay inside the communication region before finally moving out of it.

Given that the motions of nodes are iid, the distribution of T_a and T_b is the

same. We call it the *single-node link lifetime* (S-LLT) distribution. Furthermore, its CCDF is denoted by $F_S(t)$, i.e., $F_S(t) = P(T_a \geq t) = P(T_b \geq t)$. Clearly, we can compute the link CCDF $F_L(t)$ as

$$F_L(t) = F_S^2(t). \tag{4.3}$$

And the link outage probability P_{L_p} associated with a particular packet length L_p can be evaluated as

$$P_{L_p} = P(T_L \leq \frac{L_p}{B}) = 1 - F_L(\frac{L_p}{B}). \tag{4.4}$$

4.2.1 Single-Node Link Lifetime (S-LLT)

From the above, it follows that the essence of modeling link dynamics in MANETs consists of evaluating the distribution of S-LLT, because it reflects the link dynamics resulting from the motions of nodes. S-LLT measures the duration of time for a node to continuously stay inside the communication range of another node. In our model, this range is a circle.

To evaluate the S-LLT T_S with the two-state Markov model in Section 3.2, we need to evaluate P_s, $S_0(t)$, and $S_1(t)$, which we do next. Let z_d denote the least distance to be traveled by node to move out of the communication circle, starting from the position A_s with the direction and speed v being kept unchanged. A graphical illustration of z_d is presented in Fig. 4.2. The probability P_s can now be evaluated through z_d as

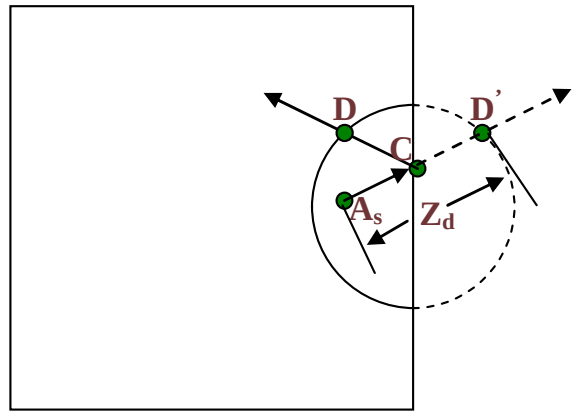

Figure 4.2: Graphical Illustration of z_d: Restricted Networks.

$$P_s = E_v(P_s(v)) \tag{4.5}$$

$$\begin{aligned} P_s(v) &= \int_{z_d} P(\tau \leq \frac{z_d}{v}) p(z_d) dz_d \\ &= \int_{z_d} (1 - F_m(\frac{z_d}{v})) p(z_d) dz_d \\ &= \int_{z_d} (1 - exp(-\lambda_m z_d / v)) p(z_d) dz_d \end{aligned} \tag{4.6}$$

where $P_s(v)$ is the conditional probability of P_s on v. $p(z_d)$ is PDF of z_d and from Section 4.2.2, we know that it can be calculated as

$$p(z_d) = \begin{cases} \frac{2}{\pi R^2} \sqrt{R^2 - (\frac{z_d}{2})^2}, & \text{for } 0 \leq z_d \leq 2R \\ 0, & \text{elsewhere} \end{cases} \tag{4.7}$$

where R specifies the radius of the communication circle.

$S_0(t)$ is the PDF of the time duration for nodes to return to the state S_0.

Conditioning on speed v and assuming that the starting time is at time 0, $S(t)$ is the probability of the node changing its velocity at time t on condition that A_d is located inside the communication circle. Hence,

$$
\begin{aligned}
S_0(t) = & \quad E_v(S_0(t|v)) \qquad (4.8) \\
S_0(t|v) = & \quad \frac{1}{P_s} P(t = \tau, z_d \geq v\tau | v) \\
= & \quad \frac{1}{P_s} \lambda_m e^{-\lambda_m t} \int_{vt}^{2R} p(z_d) dz_d \\
= & \quad \begin{cases} \frac{2\lambda_m e^{-\lambda_m t}}{P_s \pi R^2} \int_{vt}^{2R} \sqrt{R^2 - (\frac{x}{2})^2} dx, & 0 \leq t \leq \frac{2R}{v} \\ 0, & \text{elsewhere} \end{cases} \\
= & \quad \begin{cases} \frac{4\lambda_m e^{-\lambda_m t}}{\pi P_s} \left[\frac{\pi}{4} - \frac{vt}{4R} \{ \sqrt{1 - (\frac{vt}{2R})^2} + \sin^{-1}(\frac{vt}{2R}) \} \right] \\ 0, \qquad \text{elsewhere} \end{cases} \qquad (4.9)
\end{aligned}
$$

where $S_0(t|v)$ is the conditional PDF on v.

$S_1(t)$ can be evaluated in much the same way as we have done for $S_0(t)$. Conditioning on speed v and assuming that the starting time is at time 0, $S_1(t)$ is simply the probability of the node moving out of the communication circle at time t with velocity being kept constant. Hence,

$$
\begin{aligned}
S_1(t) &= E_v(S_1(t|v)) \qquad (4.10)\\
S_1(t|v) &= \frac{1}{1-P_s}P(t=\frac{z_d}{v},\ z_d \le v\tau|v)\\
&= \frac{1}{1-P_s}P(\tau \ge t)p(z_d = vt)(vt)'\\
&= \begin{cases} \frac{2e^{-\lambda_m t}}{(1-P_s)\pi R^2} v\sqrt{R^2-(\frac{vt}{2})^2}, & 0 \le t \le \frac{2R}{v}\\ 0, & \text{elsewhere}\end{cases}\\
&= \begin{cases} \frac{4e^{-\lambda_m t}}{\pi(1-P_s)}\frac{v}{2R}\sqrt{1-(\frac{vt}{2R})^2}, & 0 \le t \le \frac{2R}{v}\\ 0, & \text{elsewhere}\end{cases} \qquad (4.11)
\end{aligned}
$$

where $S_1(t|v)$ is the conditional PDF on v.

4.2.2 Distribution of z_d

From Section 4.2.1, we know that z_d denotes the least distance to be traveled by node to move out of the communication circle, if the direction and speed of node are kept unchanged. The current position of the node is randomly and uniformly distributed inside the communication circle. As illustrated in Fig. 4.2, there are two cases to be considered in calculating the z_d: 1) z_d is the distance along the direction of current velocity (i.e., line $A_s \to C$); 2) z_d is comprised of two parts, where the first part is the distance along current direction to hit the cell boundary and the other part is along the reflected direction starting from the reflecting point (i.e., lines $A_s \to C, C \to D$).

In the second case, we can consider as if the node travels across the boundary along the previous direction without being reflected back. Taking the above example,

it is equivalent to say that $A_s \rightarrow C, C \rightarrow D$ can be substituted by $A_s \rightarrow D^{'}$. In this way, z_d can be calculated as if it were moving in a complete circle.

We have thus successfully translated the problem of calculating z_d into a similar problem discussed by Hong and Rappaport [41] of calculating the distance traveled by a mobile user in its originated cell before finally being switched to adjacent cell for handoff. Following similar derivations as in [41], the distribution of z_d is given by

$$p(z_d) = \begin{cases} \frac{2}{\pi R^2}\sqrt{R^2 - (\frac{z_d}{2})^2}, & \text{for } 0 \leq z_d \leq 2R \\ 0, & \text{elsewhere} \end{cases} \tag{4.12}$$

where R is the radius of the communication circle.

4.2.3 Model Validations

In the simulation, there are a total of 100 nodes randomly placed for each $1000m \times 1000m$ square cell. Each node has the same transmit power and two profiles of the radio transmission range are chosen for simulation. Both are within the coverage of IEEE 802.11 PHY layer and they are $\{200m, 100m\}$. After initial placement, nodes keep moving continuously according to the RDMM model. The mobility parameter λ_m is chosen to be $\lambda_m = 4$ and three different speeds are simulated $v \in \{1, 10, 20\}(m/s)$, from pedestrian speed to normal vehicle speed. Combining the power profile and velocity profile, six different scenarios are simulated $\{I : (200m, 1m/s); II : (100m, 1m/s); III : (200m, 10m/s); IV : (100m, 10m/s);\ V : (200m, 20m/s); VI : (100m, 20m/s)\}$.

Nodes are randomly activated to randomly choose destination node for data

transmission. The traffic of activated nodes are supplied from a CBR source with a packet rate $0.5p/s$. Given that the choice of specific MAC layer and routing protocol may affect the results, we assume perfect MAC and routing, rendering zero delays or losses due to such functionality, enabling the simulation to capture statistics solely due to mobility.

Table 4.1: Residence Probability P_s: Restricted Networks.

	v (m/s)		
R (m)	1	10	20
100	0.09	0.01	0.005
200	0.17	0.02	0.01

Table 4.1 describes the residence probability P_s for all six scenarios. As shown in Table 4.1, the residence probability increases with the relative radius ReR $\frac{R}{v}$, indicating that it is more likely for nodes with larger ReR to stay inside the communication circle.

Fig. 4.3 presents the results of link lifetime with ES-LLT and AS-LLT formula of link lifetimes. The results clearly confirm that the two-state Markovian model is also a powerful tool to accurately model link dynamics of link lifetime distribution as a function of node mobility in restricted networks.

4.3 Segmentation Schemes and Their Optimization

In Fig. 4.4, we exploit the application of link lifetime distribution to the optimization of segmentation scheme, using the criterion derived in Section 3.5. For il-

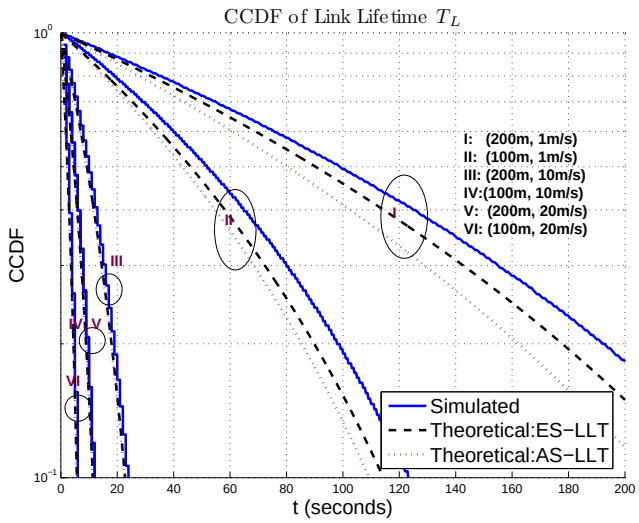

Figure 4.3: Link Lifetime T_L: Simulated, ES-LLT(Markovian), AS-LLT.

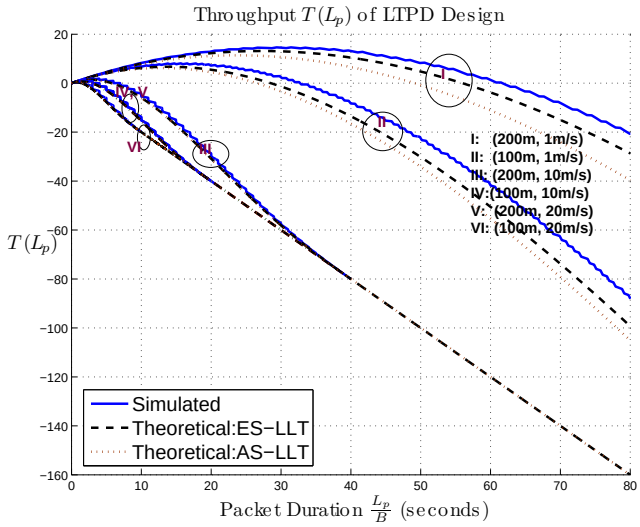

Figure 4.4: LTPD Design: Restricted Networks.

lustration purpose, the cost function for our example of LTPD design is chosen as a constant penalty value 2, (i.e., $C(L_p, P_{L_p}) = 2$).

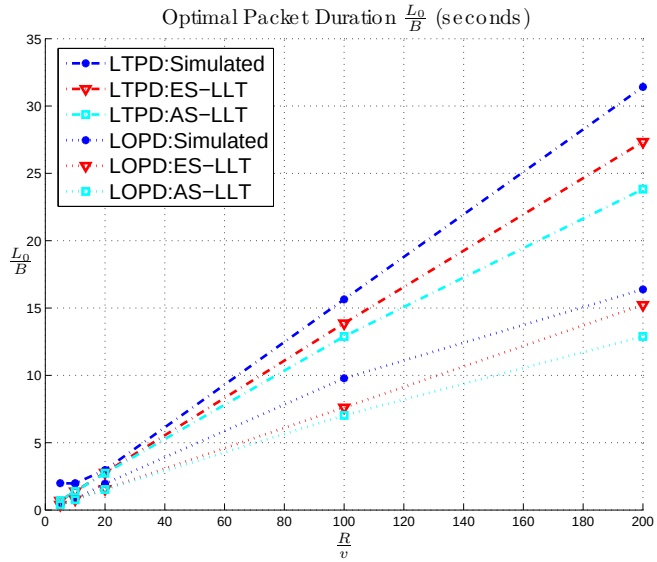

Figure 4.5: Optimal Packet Duration $\frac{L_0}{B}$.

The optimized solutions $\frac{L_0}{B}$ of both LOPD and LTPD protocols on information segmentation are illustrated in Fig. 4.5. In the simulation, the link outage tolerance of LOPD design is set to be $\omega_p = 0.1$, i.e., the maximum link outage probability should be less than 10%.

It is clear that the two key observations described in Section 3.5 are also corroborated from Figs. 4.4 and 4.5 in restricted networks. Another important observation from Fig. 4.5 is that the optimal packet (information block) length designs, obtained from either the simulation or Markovian ES-LLT formula, exhibit linear proportion to the ReR value $\frac{R}{v}$. It suggests that mathematically, the optimal information segmenta-

tion of restricted networks should also follow the rule[1]

$$\frac{L_0}{B} = \Theta(\frac{R}{v}). \tag{4.13}$$

4.4 Statistical Model of Link Interarrival Time (LIT)

In the section, exponential modeling of distribution of link interarrival time is proposed in Theorem 3 along with detailed mathematical proof.

Theorem 3 Let nodes A and B are moving independently of each other in two adjacent square cells of size $L \times L$. And their movement follow the RDMM model and are of average speed $E(v)$. Then LIT of such inter-cell links between nodes is approximately exponentially distributed with parameter λ_I, where λ_I and the mean time of I are given by

$$\lambda_I = \frac{\pi^2 \cdot E(v) \cdot R^3}{2L^4} \tag{4.14}$$

$$E(I) \approx \frac{2L^4}{\pi^2 \cdot E(v) \cdot R^3} \tag{4.15}$$

Proof The proof proceeds by modeling the meeting of two nodes in the communication region as a geometric variable with some probability p of success and then taking the limit to derive the exponential distribution. The probability p will depend on the speeds and the positions of the two nodes. The probability p is obtained through summarizing the three exclusive scenarios analyzed below.

We first consider the case where node B is inside the communication region within the time duration $[t, t + \Delta_t)$, while node A moves into the communication region

[1] Θ, Ω and O are the standard order bounds.

with some probability p_1. Because Δ_t is fairly small, we can assume that there is no change of directions within the duration Δ_t. The probability p_B that node B is located inside the communication region at time t can be obtained from the stationary distribution,

$$p_B = \int\int_{S_B} \zeta(x,y)dxdy \tag{4.16}$$

where $\zeta(x,y)$ stands for the stationary spatial nodes' distribution and S_B (or S_A) denotes the semicircle of the communication region in the cell B (or cell A). Meanwhile, we can also have similar definition of p_A. Because nodes are moving independently, the probability p_1 will be the product of p_B and p_{S_A}. p_{S_A} represents the probability of events that node A moves into the communication region within time frame $[t, t+\Delta_t)$. It can be noted that we have neglected the probability of node B moving out of the communication region within the time frame $[t, t+\Delta_t)$. In fact, the probability is on the same order of the third scenario and can be expressed as $o(\Delta_t)$.

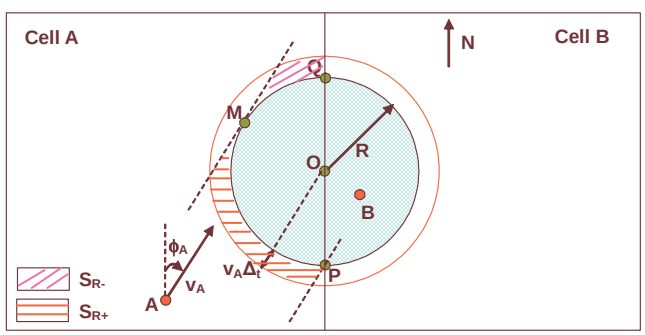

Figure 4.6: Illustration of the first scenario.

Clearly, the probability p_{S_A} varies with the initial location, speed v_A and direction ϕ_A of node A at time t. Without loss of generality, we can assume $\phi_A \in [0, \pi]$ in our analysis. Conditioning on v_A and ϕ_A, within time duration $[t, t + \Delta_t)$, node A can at most travel towards the center point O for a distance of $v_A \Delta_t$. It implies that node A should be located inside the ring area in *cell A* in Fig. 4.6 for it to move into the communication region within time duration $[t, t + \Delta_t)$.

To construct the ring area, we first draw two lines parallel to the direction ϕ_A. One line passes point P, while another line is a tangential line with respect to the circular communication region at point M. For every point on $arcA$, we can draw a line passing through the point (termed as *cross* point) and in the meanwhile being parallel to the direction ϕ_A. One outmost point (called *verge* point) on the verge of the ring area can then be determined by looking for the point lying on the line with a distance of $v_A \Delta_t$ from the *cross* point. The *verge* point should be inside *cell A* while outside the communication region. To ensure that node A can move into the contact region S_A within time duration $[t, t + \Delta_t)$ with velocity v_A and direction ϕ_A, the location of node A at time t should be within the shaded area S_{R+}, i.e., the intersection area formed by the ring and the two parallel lines along direction ϕ_A in Fig. 4.6.

Let $arcPM$ be the arc from point P to point M on the circumference. Conditioning on v_A and ϕ_A, the probability $p_{S_{R^+}}$ for node A moving into the communication can now be computed as

$$
\begin{aligned}
p_{S_{R+}|\{v_A,\phi_A\}} &= \int\int_{S_{R+}} \zeta(x,y)dxdy \\
&\approx v_A \cdot \Delta_t \cdot p_{arcPM} \qquad (4.17)
\end{aligned}
$$

where $p_{arcPM} = \int\int_{arcPM} \zeta(x,y)dxdy$. Consider the supplementary scenario where node A has the same location and speed at time t but moving at direction $\phi_A - \pi$. Obviously, node A should now be within the supplementary area S_{R-} in Fig. 4.6. Let $arcQM$ be the arc from point Q to M on the circumference. The complementary probability $p_{S_{R-}}$can now be obtained as

$$
\begin{aligned}
p_{S_{R-}|\{v_A,\phi_A\}} &= \int\int_{S_{R-}} \zeta(x,y)dxdy \\
&\approx v_A \cdot \Delta_t \cdot p_{arcQM} \qquad (4.18)
\end{aligned}
$$

where $p_{arcQM} = \int\int_{arcQM} \zeta(x,y)dxdy$.

Noting that $arcA = arcPM + arcQM$, where $arcA$ (or $arcB$) is the circumference of the communication circle inside *cell A* (or *cell B*). We will have $p_{arcA} = p_{arcPM} + p_{arcQM}$, and averaging over all possible v_A and ϕ_A's, the probability p_{S_A} is given by

$$
\begin{aligned}
p_{S_A} &= E_{v_A}\{\frac{1}{2\pi}\int_0^{\pi}(p_{S_{R+}|\{v_A,\phi_A\}} + p_{S_{R-}|\{v_A,\phi_A\}})d\phi_A\} \\
&= E_{v_A}\{\frac{1}{2\pi}v_A \cdot \Delta_t \cdot \int_0^{\pi}(p_{arcPM} + p_{arcQM})d\phi_A\} \\
&= E_{v_A}\{v_A \cdot \Delta_t \cdot p_{arcA} \cdot \frac{1}{2\pi}\int_0^{\pi} 1 \; d\phi_A\} \\
&= \frac{E(v_A)}{2} \cdot \Delta_t \cdot p_{arcA}. \qquad (4.19)
\end{aligned}
$$

The above leads to

$$
p_1 = p_{S_A} \cdot p_B = \frac{E(v_A)}{2} \cdot \Delta_t \cdot p_{arcA} \cdot p_B. \qquad (4.20)
$$

The next scenario for our proof consists of symmetric scenario where node A stays inside the communication region within the time duration $[t, t + \Delta_t)$, while node B is going to move into the communication region by some probability p_2. Following similar derivation and analysis, p_2 can be calculated as

$$
p_2 = \frac{E(v_B)}{2} \cdot \Delta_t \cdot p_{arcB} \cdot p_A. \qquad (4.21)
$$

The last scenario we need to consider for our proof is the case where both nodes A and B are located outside the communication region at time t but are going to move into the communication region within time duration $[t, t + \Delta_t)$. In contrast to the two prior scenarios in which one node is within the communication region while another one is located within the ring area at time t, in this case both nodes should be located within their respective ring area at time t.

It should be noted that the analytical procedure through geometric-variable analysis in the above scenarios can also be applied to analyze this scenario with minor

modifications expected. For the purpose of succinctness, we will not elaborate on the derivations and our analysis shows that the probability p_3 for this case can be summarized as

$$\begin{aligned} p_3 &= E\{v_A \cdot v_B \cdot \Delta_t^2 \cdot p_{arcA} \cdot p_{arcB} \\ &\quad \cdot (\frac{1}{2\pi})^2 \int_0^\pi \int_0^\pi 1 \;\; d\phi_A d\phi_B\} \\ &= \frac{E(v_A)E(v_B)}{4} \cdot \Delta_t^2 \cdot p_{arcA} \cdot p_{arcB} \\ &= o(\Delta_t). \end{aligned} \tag{4.22}$$

Summarizing all three scenarios, we obtain that the probability p is given by

$$\begin{aligned} p &= p_1 + p_2 + p_3 \\ &= \frac{1}{2} \cdot \Delta_t \cdot (E(v_A) \cdot p_{arcA} \cdot p_B \\ &\quad + E(v_B) \cdot p_{arcB} \cdot p_A) + o(\Delta_t). \end{aligned} \tag{4.23}$$

Taking the limit $\Delta_t \to 0$ gives an exponential distribution with parameter $\lambda_F \approx \frac{E(v_A) \cdot p_{arcA} \cdot p_B + E(v_B) \cdot p_{arcB} \cdot p_A}{2}$.

Till now, we have arrived at a proof of Theorem 3 on general mobility models. For RDMM model, it should be noted that the stationary spatial nodes' distribution is uniform, i.e., $\zeta(x, y) = 1/L^2$ [9, 6]. It in turn gives $p_{arcA} = p_{arcB} = \int\int_{arcA} \zeta(x, y) dxdy = \frac{\pi \cdot R}{L^2}$ and $p_A = p_B = \int\int_{S_A} \zeta(x, y) dxdy = \frac{\pi \cdot R^2}{2L^2}$. By substituting these equations into the above proof, Theorem 3 follows.

4.5 Analysis of Throughput, Average Delay and Storage

4.5.1 Throughput

We consider again the store-and-forward scheme in Section 4.3, where source node splits information stream to relay nodes in its neighbor cells, each relay stores information in the queue and delivers information from the queue only when it meets another relay nodes or the destination node in another cell. We also assume that every relay node maintains a separate queue for each source-destination pair and the queue is served in a First-Come-First-Serve (FCFS) manner. Because all cells resemble each other and nodes have iid movements, it is clear that all such queues are similar. Furthermore, we adopt a conservative scenario in which only one node per cell can act as the relay node of a specific route for delay analysis. In reality, every node can act as a relay, which leads to less delay but a much more complex network of queues.

For every cell, there should be at least one node inside the cell in order to maintain the connectivity of the network. Let $a(n) = \frac{L^2}{A_N}$ be the fractional cell size, where A_N is the overall size of the network. The connectivity requirement necessitates [28] that only when $a(n) \geq \frac{2log(n)}{n}$, each cell has at least one node *with high probability (whp)* , i.e., with probability $\geq 1 - \frac{1}{n}$. In this case, each cell will have $\Theta(na(n))$ nodes inside *whp* [28].

Recall that for inter-cell links, the size L_0 of a data packet should be chosen as $L_0 = \Theta(\frac{R \cdot B}{E(v)})$. With reference to Theorem 3, on average, every time duration of $E(I) = \Theta(\frac{L^4}{E(v) \cdot R^3})$ could have one data packet transferred. Accordingly, link throughput

T_0 for one such pair of nodes can be computed as

$$T_0 = \frac{L_0}{I} = \Theta(\frac{R^4 B}{L^4}) \tag{4.24}$$

Normally, R is chosen on the same order of L, i.e., $\frac{R}{L} = \Theta(1)$. The above equation will be reduced to $T_0 = \Theta(B) = c_0$, where c_0 is a constant. Furthermore, from the connectivity constraint, there is at least one such link available for each node.

Due to limited mobility and transmission range, each packet needs to travel via multiple relays from source to destination following the path close to the straight line linking source and destination. Let the straight line connecting source with destination in the snapshot of initial network deployment be denoted as S-D line. Clearly, a source transmits data to its destination by multiple relays along the adjacent cells lying on its S-D line.

Let K be the average number of source-destination (S-D) lines passing through every cell and each source generates traffic $\Lambda(n)$ $bits/s$. To ensure that all required traffic is carried and recall that on average there are $\Theta(na(n))$ nodes in every cell, we need that

$$K \cdot \Lambda(n) \leq T_0 \cdot \Theta(na(n)) \Rightarrow \Lambda(n) = O(\frac{na(n)}{K}) \tag{4.25}$$

For every cell, the following lemma gives the number K of S-D lines passing through it.

Lemma 2 *The number K of S-D lines passing through any cell is $\Theta(n\sqrt{a(n)})$,* whp.

The proof of this lemma follows the proof of Lemma 3 in [28], because the S-D lines are determined from the initial network deployment, which is a snapshot of MANET and can also be treated as one configuration of a static wireless network.

The above analysis leads to the following conclusion on the throughput $\Lambda(n)$.

Theorem 4 *For cell partitioned network with restricted mobility, we have* $\Lambda(n) = O(\sqrt{a(n)})$ *for generic mobility models. In particular, for a connected network* whp, $\Lambda(n) = O(\sqrt{\frac{log(n)}{n}})$.

4.5.2 Delay & Storage

Most packets need to travel across several cells before reaching their destinations and therefore, must be stored in the queue of relay nodes. Consider an S-D queue at relay node m_r, a packet arrives when node m_r and the previous relay node (or the source node) simultaneously come into the communication region; a packet departs when m_r meets another relay node (or the destination node) in the communication region. Both the inter-arrival time and the inter-departure time are of the same order as link interarrival time (LIT). Since LIT can be characterized as exponentially distributed, each queue is characterized by a Poisson arrival process with exponential service time, thus being a M/M/1-FCFS queue.

For each S-D pair, queues at relay nodes construct a M/M/1-FCFS feedforward tandem network. An important property of such a M/M/1-FCFS feedforward tandem network is the *Jackson's theorem* (see [46], page 150), i.e., if the tandem network with exponential service time is driven by a Poisson arrival process, every queue in the

tandem network behaves as if it were an independent M/M/1-FCFS queue and thus can be analyzed individually. Recall the following properties for a M/M/1-FCFS queue (see [46], chapter 3) in the following lemma.

Lemma 3 *Consider a discrete M/M/1-FCFS queue. Let* $1-\epsilon$ *be the* traffic intensity *and* λ *be the exponential* service rate *of the queue, the average delay is given by*

$$E(D) = \frac{1}{\lambda\epsilon} = \Theta(\frac{1}{\lambda}) \tag{4.26}$$

Furthermore, the mean and variance of the occupancy of the queue N_q *is,*

$$E(N_q) = \frac{1-\epsilon}{\epsilon} = \Theta(1) \tag{4.27}$$

$$Var(N_q) = \frac{1-\epsilon}{\epsilon^2} = \Theta(1) \tag{4.28}$$

Without loss of generality, we can assume that the overall size of network is of unit area to analyze the network. In this case, we will have $A_N = 1$ and $L = \sqrt{a(n)}$. The average distance between S-D pairs is given by $\Theta(1)$ and the average number of hops for each packet is $\Theta(1/\sqrt{a(n)})$. Recall that every relay node carries information for $\Theta(n\sqrt{a(n)})$ S-D pairs and the service rate of each queue from LIT is $\lambda = \Theta(\frac{E(v)}{\sqrt{a(n)}})$[2] *Jackson's theorem* indicates that the delay for each S-D pair is the summation of delays occurred at relay nodes.

We can summarize the network performance in terms of average delay and storage in the following theorem.

[2]It can be obtained by substituting $\frac{R}{L} = \Theta(1)$ and $L = \sqrt{a(n)}$ into Eq. (4.14).

Theorem 5 *The average packet delay in a cell-partitioned network with restricted mobility and RDMM mobility models is given by*

$$\begin{aligned} D(n) &= \overbrace{\Theta(\frac{1}{\sqrt{a(n)}})}^{\#\text{ of hops}} \cdot \overbrace{\Theta(\frac{\sqrt{a(n)}}{E(v)})}^{\text{delay at each hop}} \\ &= \Theta(\frac{1}{E(v)}) \end{aligned} \tag{4.29}$$

and the average information bit delay $D_b(n)$ is

$$D_b(n) = \frac{D(n)}{\Theta(\frac{RB}{E(v)})} = \Theta(\frac{1}{RB}) \tag{4.30}$$

Furthermore, the mean and variance of the packet occupancy (i.e., storage requirement) is given by

$$E(N_p) = Var(N_p) = \Theta(n\sqrt{a(n)}) \tag{4.31}$$

and the corresponding bit storage requirement N_b is

$$E(N_b) = Var(N_b) = \Theta(n\sqrt{a(n)}) \cdot \Theta(\frac{RB}{E(v)}) \tag{4.32}$$

Summarizing the analysis, several important observations can be drawn here.

- By optimally segmenting the information, throughput of the network scales as $\Lambda(n) = O(\sqrt{a(n)})$ and packet-wise storage scales as $\Theta(n\sqrt{a(n)})$. Choices made to improve throughput will come with the price at increase in storage.

- Mobility can help alleviate the packet delay but won't be helpful to the bit-wise delay. It might be counter intuitive at the first glance. The reason for this behavior of network is described in Chapter 3.

4.6 Conclusion

We have presented analytical results on the characterization of link lifetime, optimization of segmentation schemes and analytical modeling of link interarrival time for restricted networks. All these analytical findings are eventually summarized into the first comprehensive analysis on throughput, average delay, and storage requirements for MANETs with restricted mobility.

Chapter 5

Modeling of Topology Evolutions and Implication on Proactive Routing Overhead in MANETs

Mobility brings fundamental challenges to the design of protocol stacks for mobile ad hoc networks (MANETs). The mobility of nodes implies that the routing protocols of MANETs have to cope with frequent topology changes while attempting to produce correct routing tables. Proactive routing protocols, being the focus of the chapter , provide fast response to topology changes by continuously monitoring topology changes and disseminating the related information as needed over the network. However, the price they pay is the increase in signaling overhead as the topology changes increase, and this can further lead into smaller packet-delivery ratios and longer delays. In the worst case, "broadcast-storms" [59] can result, congesting the entire network. Hence, it

is essential to understand the intricate relations between routing overhead and topology changes for the design of routing protocols in MANETs.

Characterizing the impact of mobility on the performance of proactive routing protocols is a very complex problem. Consequently, the provision of such characterization has been limited to simulation-based approaches [13, 44, 5, 4, 17]. Few if any analytical studies have been pursued on this topic. Zhou et. al [81] gave an analytical view of routing overhead of reactive protocols, assuming static network (manhattan grid) with unreliable nodes and concludes the scalability of reactive protocols with localized traffic pattern. Topology changes resulting from node mobility was not considered in [81]. In [80], an information theoretic analysis is pursued to bound the memory requirement and overhead incurred by a hierarchical routing protocol for MANETs based on entropy rate of topology changes.

The previous work does provide a good understanding of the scalability properties of the signaling of routing schemes. However, to the best of our knowledge, there is no previous analytical work that establishes an analytical connection between routing overhead and topology changes due to mobility. Moreover, the past work has not even characterized topology changes as a function of node mobility, which is crucial to make the connection we seek.

In the chapter, we provide the first analytical framework for the modeling of proactive routing overhead as a function of node mobility. In doing so, we model topology changes explicitly as a function of node mobility. Section 5.1 summarizes the network model used in our analysis and formulates the problem to be solved. Sec-

tion 5.2 explains the general framework for the modeling of proactive routing overhead. Section 5.3 discusses properties of the topology of a MANET and factors that affect its stability. Section 5.4 explains our analytical model. Clearly, our results complement previous information theoretic analysis [80] by providing entropy rate and a model of topology changes.

Because of its practical importance, Section 5.5 applies our general framework to the analysis of the optimized link state routing protocol (OLSR) [16]. Our analysis of OLSR provides a better insight on its operation, and corroborates the effectiveness of our modeling framework. We compare our analytical results against *Qualnet* simulations based on scenarios assuming random node mobility. The results illustrate the accuracy of our analytical framework. Section 5.6 concludes this chapter.

5.1 System Model & Problem Statement

We consider a network operating in a square area, which is consistent with several prior analytical models [33, 34, 28]. The entire network is of size $L \times L$ and there are n nodes initially randomly deployed in such a "square network." Note that, although we consider a square network, our analysis can be extended to networks of any shape in a straightforward way.

Nodes are mobile and initially equally distributed over the network. The movement of each node is independent and unrestricted, i.e, the trajectories of nodes can lead to anywhere in the network. For node $i \in \{1, 2, \ldots, N\}$, let $\{T_i(t), t \geq 0\}$ be the

random process representing its trajectory and take values in D, where D denotes the domain across which the given node moves. To simplify our modeling task, we make the following assumption on the trajectory processes.

Assumption 1 [Stationarity] *Each of the trajectory processes ($T_i(t)$) is stationary, i.e., the spacial node distribution reaches its steady-state distribution irrespective of the initial location. The N trajectory processes are* jointly stationary*, i.e., the whole network eventually reaches the same steady state from any initial node placements, within which the statistical spatial nodes' distribution of the network remains the same over time.*

The above assumption is quite fundamental in the sense that it lays the foundation for the modeling of node movement. Most existing models, (e.g., random direction mobility models [42, 43, 51, 9, 35], random waypoint mobility models [55, 79] and random trip mobility model [11]) clearly satisfy our assumption. In other words, our assumption ensures that, on the long run, the network converges to its steady state and the stationary spatial nodes' distribution can be used in the performance analysis of the network.

The availability of communication links (e.g. from node i to node j) is governed by *physical model* described in Eq. 1.2. Eq. 1.2 simply states the physical requirement of the existence of a directional link from node i to node j at time t. Given that many routing algorithms require bi-directional links, we expect the SINR law to be satisfied for the reverse link, e.g., $j \rightarrow i$. We simply call a bi-directional link as a link in this chapter.

The topology (or connectivity graph) $\mathcal{G}(t)$ of the network at time t can be obtained by replacing the available wireless links with lines connecting the corresponding node pairs. We use the terms topology and connectivity graph interchangeably.

Given the above terminology and assumptions, in the chapter, we seek answers to the following questions:

- *Is there an analytical model to statistically characterize the distribution of topology changes in MANETs? If so, are we able to derive the associated parameters analytically?*

- *If there is such a model, are we able to apply the model to analyze the effect of mobility on the control overhead of proactive routing protocols? Or mathematically, could we find the function $\mathcal{F}$ that projects the control overhead $\mathcal{O}_d$ in MANETs given that we know the node mobility $\mathcal{V}$ and the control overhead $\mathcal{O}_s$ incurred by the protocol in a static topology?*

$$\mathcal{F} : \mathcal{O}_s \times \mathcal{V} \rightarrow \mathcal{O}_d \tag{5.1}$$

5.2 Proactive Routing Overhead in Dynamic Graphs

A routing protocol operates on the connectivity graph (topology) $\mathcal{G}$ of a MANET. Let $\vec{\mathcal{G}} = \{\mathcal{G}_i\}$ be the set of all possible connectivity graphs of the MANET. In steady-state, the connectivity graph $\mathcal{G}(t)$ travels across all such graphs with a stable distribution vector $\vec{p} = \{p_i\}$ derived from the stationary spatial nodes' distribution.

A change that occurs in the connectivity of the MANET induces the transition from a connectivity graph of the MANET to another connectivity graph. For simplicity, we refer to the transition from one connectivity graph to another as a *topology evolution*.

If we look at the connectivity graph from the standpoint of single node, a topology evolution can be triggered by changes in its immediate neighborhood or by updates received from its neighbors. If we observe the protocol behavior at a typical active node k, we can derive from $\vec{\mathcal{G}}$ the set of all possible local connectivity graphs $\vec{\mathcal{G}^k} = \{\mathcal{G}_i^k\}$ with the corresponding distribution vector $\vec{p^k} = \{p_i^k\}$.

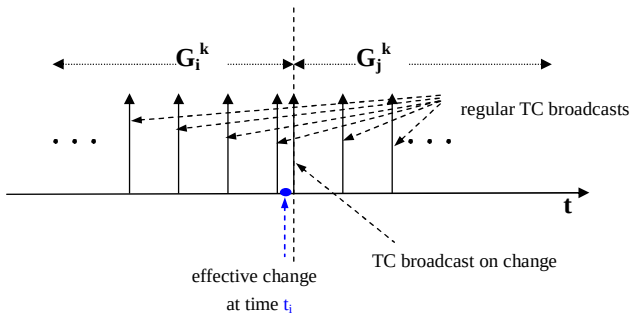

Figure 5.1: Protocol behaviors with local connectivity graphs.

As Fig. (5.1) illustrates, we assume that when there is no change in topology, nodes periodically broadcast topology control (TC) messages at regular interval T_c. For this case, the average TC messages per active node in static scenarios $\mathcal{O}_s$ is simply

$$P(\mathcal{O}_s) = P(\mathcal{G}_i^k) = 1/T_c, \forall i \tag{5.2}$$

If we assume that a topology change happens at time $t_i, KT_c < t_i \leq (K+1)T_c$, it induces the transition of the local connectivity graph from $\mathcal{G}_i^k$ to $\mathcal{G}_j^k$. The routing

protocol reacts to the change by advancing the TC message broadcast at some time $t_i^*, KT_c < t_i^* \leq (K+1)T_c$, rather than broadcasting at the next planned time $(K+1)T_c$. The subsequent TC message broadcast will perform regularly with graph $\mathcal{G}_j^k$. In this case, compared to the static scenario where no change occurs, the increase $\gamma_i(t)$ in generated TC message associated with $\mathcal{G}_i^k$ can be computed as follows:

$$\gamma_i(t_i) = \frac{(K+1)}{t_i^*} / \frac{K+1}{(K+1)T_c} = \frac{\lceil t_i^*/T_c \rceil}{t_i^*/T_c} \tag{5.3}$$

where $\lceil \cdot \rceil$ is the ceiling operator.

The average increase γ_i in generated TC messages in the graph $\mathcal{G}_i^k$ can be computed as

$$\gamma_i = E_{t_i}(\frac{\lceil t_i^*/T_c \rceil}{t_i^*/T_c}) \tag{5.4}$$

Statistically, γ_i measures the normalized transition cost for $\mathcal{G}_i^k$ and t_i^* is determined by the t_i that captures the stability of the local topology $\mathcal{G}_i^k$. Summing over all possible topologies, we can estimate the average number of generated TC messages per active node as

$$P = \sum_{\forall i} p_i^k P(\mathcal{G}_i^k) * \gamma_i \tag{5.5}$$

As we will see in Section 5.4, if we are only concerned with nodal mobility and given that nodes are moving randomly and independently of one another, we could assume that link changes arrive independently and $\{t_i\}$ are of identical statistical distributions, being a renewal process. We have then

$$P = \gamma \times \sum_{\forall i} p_i^k P(\mathcal{G}_i^k) \tag{5.6}$$

$$\gamma = E(\frac{\lceil \zeta^* / T_c \rceil}{\zeta^* / T_c}) \tag{5.7}$$

where ζ^* is decided on ζ and ζ is the observed stability of the local connectivity graph per active node. γ is the *penalty factor* that measures the cost in graph transitions for an active node and as we will see later, it is a function of nodal mobility and stability of the local connectivity graph. Furthermore, a closer look at Eq. (5.6) shows that the increased traffic overhead can be estimated from the average performance of static graphs, which is exactly the right term in the equation.

In a homogeneous network, every node in the network operates in a similar way. Therefore, we can expect similar results on the whole network. Hence, we propose a model that estimates the control traffic overhead from the knowledge of the mean overhead $\mathcal{O}_s$ that occurs in static scenarios. Mathematically, we can write it as the tentative answer for the question raised in Section 5.1 as

We could have a function $\mathcal{F}$ that projects the control overhead $P(\mathcal{O}_d)$ in MANETs with the knowledge of mobility $\mathcal{V}$ and control overhead $P(\mathcal{O}_s)$ of protocol at static scenarios. And the function can be written as,

$$\mathcal{F} : P(\mathcal{O}_d) = \gamma(\mathcal{V}) * P(\mathcal{O}_s) \tag{5.8}$$

However, we need to know the distribution of topology evolutions (t_i in Eq. (5.3)) for the computation of mobility effect on proactive routing overhead. To obtain such a

model, we will first discuss factors that affect the stability of topology and then propose analytical model for topology evolution.

5.3 Topology: Factors for Changes

5.3.1 Setup

Due to node mobility and the surrounding parallel transmissions, links between nodes are set up and broken dynamically. We introduce a $\{0, 1\}$-valued on-off process $f_{ij}(t), t \geq 0$ to model such link changes as $f_{ij}(t) = 1$ (or $f_{ij}(t) = 0$) if the unidirectional link from node i to node j, is available (or unavailable) at time $t \geq 0$. Clearly, we have $f_{ij}(t) = f_{ji}(t)$ because we only consider bi-directional links.

If we map every active (on) link to an edge in a graph with N vertices where each vertice stands for a node in V, we can obtain the time-varying graph (topology) $\mathcal{G}(t)$ with a time-varying set $E(t)$ of edges as

$$E(t) := \{\{i, j\} \in V \times V, i \neq j; f_{ij}(t) = 1\} \tag{5.9}$$

It should be noted that $\mathcal{G}(t)$ is the connectivity graph of the network, which is an *undirected* graph, given that we consider bi-directional links. Let E be the complete set of possible links in the graph, i.e.,

$$E := \{\{i, j\} \in V \times V, i \neq j\} \tag{5.10}$$

The complementary set $E^c(t)$ of $E(t)$ can be computed as

$$E^c(t) = E - E(t) \tag{5.11}$$

Each link change, such as new link formation or breakage of existing links, results in a change in the connectivity graph and could further result in a protocol event in the network to distribute such change. Let τ be the moment that the connectivity graph $\mathcal{G}(t)$ changes at time $t + \tau$ from its last change at time t. Clearly, τ is the random variable describing the duration of stability of the connectivity graph $\mathcal{G}(t)$. In general, there are two different scenarios responsible for changes of $\mathcal{G}(t)$. One is the creation or arrival of new link. Let τ_o be the random variable capturing the time duration of such new link arrivals or addition of new edges in $\mathcal{G}(t)$. Similarly, we have another random variable τ_f characterizing the breakage of existing links or deletions of edges in $\mathcal{G}(t)$. We will have

$$\tau = \min\{\tau_o, \tau_f\} \tag{5.12}$$

Our objective is first to identify the factors that affect the stability τ of the connectivity graph $\mathcal{G}(t)$ and then find the analytical model that characterizes the statistical distribution of τ.

5.3.2 Factors in Connectivity Graph

It is apparent from Eq. 1.2 that the availability of links depends on the wireless environment (captured in channel gain $g_{kl}(t)$) and also on the traffic and MAC schemes, which together decide the active set of transmitting nodes $A_s(t)$. If we do not explicitly model the shadowing effect and short-term channel variations such as channel fading between nodes, it is reasonable to assume that the channel gain can be computed

according to the exponential attenuation model, that is,

$$g = r^{-\alpha} \tag{5.13}$$

where r denotes the Euclidean distance between two communicating nodes and α is the exponential attenuation coefficient, normally ranging from 2 to 5 for various wireless environments.

By introducing a dynamic and sometimes intractable active set $A_s(t)$, the involvement of traffic and MAC schemes significantly complicates the problem with a dynamic varying interference term. We call such a term *environmental mobility*, which results from surrounding traffics and parallel transmissions.

When the MAC protocol schedules transmissions perfectly, multiple access interference is negligible compared to the noise and can be considered zero, i.e., no environmental mobility. In such case, the deciding factors for link availability lies in the transmission power and radio propagation loss and it can be expressed as

$$\frac{P_i(t)g_{ij}(t)}{N_0} \geq \beta \quad and \quad \frac{P_j(t)g_{ji}(t)}{N_0} \geq \beta \tag{5.14}$$

If all nodes transmit with a uniform power, given Eq. (5.13), the link between two nodes becomes available as soon as they are within communication range of each other, i.e., their Euclidean distance is smaller than the maximum radio coverage R for a transmitting node. Under these assumptions, the availability of links is purely a function of the relative distances between nodes, which in turn are determined by nodal mobility.

Thus far, we have identified two factors affecting the connectivity graph, *environmental mobility* and *nodal mobility*. However, the defining feature of MANETs is *nodal mobility*, which is a natural result from nodal movements. Accordingly, given that no analytical models exist for topology evolutions resulting from *nodal mobility* in MANETs, this is the focus of the model we describe next.

5.4 Modeling Nodal Mobility

Nodal motion changes the distances among nodes, and therefore results in the dynamic establishment and termination of links. Compared to the physical model in Eq. 1.2, links defined by Eq. (5.14) are longer and exist for the maximum possible duration of link availability if only the effects of mobility are considered. In practice, the offered traffic and the scheduling of packets provided by the MAC protocol renders a smaller utilization of links. Hence, the link utilization under a real MAC protocol is smaller than the one predicted by Eq. (5.14).

For each link in set $E(t)$, let $T^o_{ij}(t)$ denote the *residual* lifetime of the link after time t, i.e., $T^o_{ij}(t)$ is the amount of the time that elapses from time t until link is unavailable. Correspondingly, for each link in set $E^c(t)$, $T^f_{ij}(t)$ be the *residual* silence time of link after time t, i.e., $T^f_{ij}(t)$ is the amount of time elapsed from time t until a link is available. Due to the underlying stationarity implied from the joint stationarity of trajectory processes, it suffices to consider only the case $t = 0$ and we can simply

drop the time parameter t. Hence, $T_{ij}^o = T_{ij}^o(t)$. Clearly, we have

$$\tau_o = \min\{T_{ij}^o \text{ of link \{i,j\}} \ , \forall\{i,j\} \in E(t)\} \tag{5.15}$$

$$\tau_f = \min\{T_{ij}^f \text{ of link \{i,j\}} \ , \forall\{i,j\} \in E^c(t)\} \tag{5.16}$$

For each link $\{i,j\}$, the associated link availability process $f_{ij}(t)$, where $t \geq 0$, is simply an on-off process with successive up and down states with associated time durations, denoted by random variables $f_{ij}(k); k = 1, 2, \ldots$ and $f_{ji}(k); k = 1, 2, \ldots$, respectively. Such a processes can also be obtained from nodes' relative trajectories. When only nodal mobility is considered as the variable of interest, according to Eq. (5.14), a link between nodes i and j in V is available at time $t \geq 0$ if and only if their distance is smaller than R. As a result, the link availability is given by

$$f_{ij}(t) := 1[\|T_i(t) - T_j(t)\| \leq R]; t \geq 0, \tag{5.17}$$

where $\| \cdot \|$ denotes the Euclidean operator to compute the distance.

Let $Z(t) = \sum_{\forall\{i,j\}} f_{ij}(t)$ and it is clear that $Z(t)$ is a renewal process comprised from a total number of $|E|$ on-off link availability processes, where $| \cdot |$ is the cardinality operator. Clearly, τ describes the refreshing interval, τ_o specifies the interval between upward renewals and τ_f denotes the interval between downward renewals of the renewal process $Z(t)$. By applying the well-known results from renewal processes and independent on-off processes in equilibrium [40], we have the following theorem on τ.

Theorem 6 [Stability Model]

When sets $E(t)$ and $E^c(t)$ involve a sufficient number of links and all such links are assumed to be independent, the distribution of τ_o and τ_f can be approximated by the exponential distribution with parameter λ_o and λ_f. And the distribution of stability τ of the connectivity graph is also exponentially distributed with parameter $\lambda = \lambda_o + \lambda_f$. Therefore,

$$P(\tau_o \leq t) = 1 - e^{-\lambda_o t} \tag{5.18}$$

$$P(\tau_f \leq t) = 1 - e^{-\lambda_f t} \tag{5.19}$$

$$P(\tau \leq t) = 1 - e^{\lambda t} = 1 - e^{-(\lambda_o + \lambda_f)t} \tag{5.20}$$

The above result is also known as Palm's theorem [40]. It states that the distribution of a superposition of N_r i.i.d random variables converges to the exponential distribution as N_r approaches infinity. This result can be generalized to incorporate cases of independent but non-homogeneous motions, where some nodes may follow different mobility models from others.

The independence assumption for links, and the application of Palm's theorem, can be questioned in MANETs, because of the broadcast nature of their links. However, if the movement of nodes satisfies some *mixing conditions* known as *m-dependence* [37], the statement in Theorem (6) still holds. Such relaxed conditions introduce a form of asymptotic independence as the hop distance between links increases, while allowing dependence in neighborhoods. Specifically, *m-dependence* means that the correlation between links decreases as the hop-distance between links increases and links can be assumed to be independent when the hop distance between links is greater than a

given value m. Fortunately, most mobility models used to study MANETs fall in this category (e.g., the random waypoint mobility model, random direction mobility model and random trip mobility model) and our results can be applied to a wide-variety of scenarios.

5.4.1 Relations between λ_o and λ_f

We have observed that the new link formation process and link breakage process can be approximated by Poisson process with parameters λ_f and λ_o, respectively. For the new link formation process (or the link breakage process), λ_f (or λ_o) characterizes the average number of new link arrivals (or link breakages). Let us consider a time window T that is sufficiently large. The number of new link arrivals N_a and link breakages N_b within the time window can be approximated by

$$N_a = \lambda_f * T \tag{5.21}$$

$$N_b = \lambda_o * T \tag{5.22}$$

For a network with a finite number of nodes that is observed for an infinite length of time, the difference of the number of new link arrivals and link breakages can be denoted by

$$\lim_{T\to\infty}(N_a - N_b) = \lim_{T\to\infty} T * (\lambda_f - \lambda_o). \tag{5.23}$$

Clearly, the only choice is

$$\lambda_f = \lambda_o. \tag{5.24}$$

This indicates that, on the long run, the new link arrival process should be balanced off by the link breakage process. Otherwise, it contradicts the fact that the network only involves a finite number of nodes.

5.4.2 Analytical Evaluation of λ_f or λ_o

If we know the parameter for the link breakage or link creation process, we can infer the other one. The link breakage process is characterized by the distribution of residual link lifetime, a direct evaluation of which requires exact knowledge of the underlying mobility characteristics. However, we can make general statements on the underlying new link formation process, resorting to the exponential modeling with parameter λ_l of point-to-point link formation in [30].

For a particular connectivity graph $\mathcal{G}_i$ with associated sets E_i and E_i^c, there is a total number of $|E_i^c|$ potential point-to-point links that can be created. Because the time distribution of new link formation can be modeled as exponentially distributed with parameter λ_l, the stability for this particular connectivity graph can be measured with parameter

$$\lambda_f(\mathcal{G}_i) = |E_i^c| * \lambda_l \tag{5.25}$$

When a network is running in steady-state and inferring from the joint stationarity assumption of underlying trajectory processes, $\mathcal{G}(t)$ is a stationary and ergodic process that will experience all possible connectivity graphs with an associated proba-

bility vector derived from the steady-state nodes' distribution. By averaging all possible graphs, we can compute the parameter λ_f as

$$\lambda_f = E(|E_i^c|) * \lambda_l \tag{5.26}$$

where $E(\cdot)$ stands for expected value.

A general model of MANETs in steady-state exists and is known as a *random geometric graph* [62]. This model has been widely adopted in analytical works of MANETs and considered as an improvement over the model of *random graph* in static networks. Using the model of *random geometric graph*, we can compute λ_f as

$$\lambda_f = \bar{N_f} * \lambda_l \tag{5.27}$$

where $\bar{N_f}$ is the average number of potential link pairs and it can be computed as

$$\bar{N_f} = \frac{N * (N-1)}{2} * (1 - \frac{\pi R^2}{L^2}) \tag{5.28}$$

We thus arrive to the following theorem on the distribution of the stability τ of the connectivity graph.

Theorem 7 [Analytical Stability Model] *The distribution of stability τ of the connectivity graph in MANETs can be approximated as exponentially distributed with parameter λ and the parameter λ is given by*

$$\lambda = N * (N-1) * (1 - \frac{\pi R^2}{L^2}) * \underbrace{2E[V_*]R \int_0^L \int_0^L \pi^2(x,y)dxdy}_{\lambda_l} . \quad (5.29)$$

where $\pi(x, y)$ denotes the steady-state spatial nodes' distribution and $E[V_*]$ is the average relative velocity.

5.4.3 Model Validations

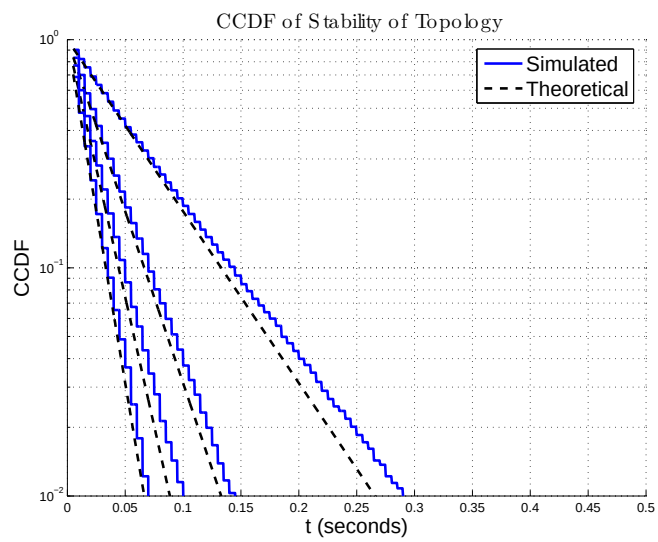

Figure 5.2: Distribution of Stability of Topologies: RWMM, $R = 250m$.

We validate our analytical model of the stability of topologies by comparing its results against simulations. In the scenario used for comparison, there are a total of 100 nodes randomly placed for each $1000m \times 1000m$ square cell. Each node has the same transmit power and the radio transmission range considered is

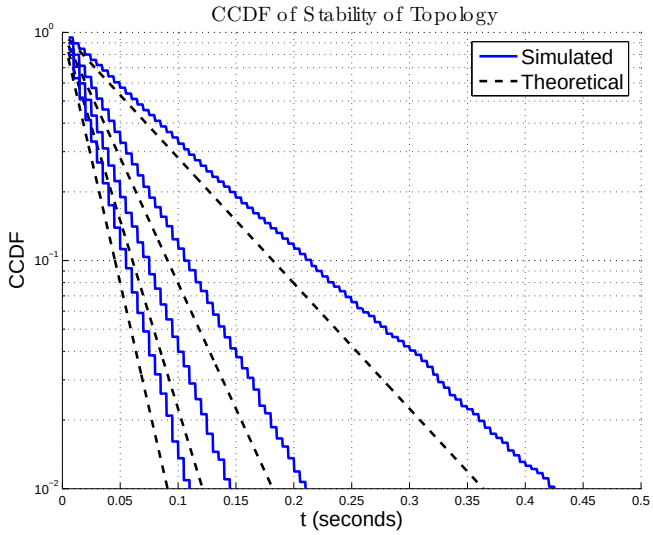

Figure 5.3: Distribution of Stability of Topologies: RDMM, $R = 250m$.

$250m$, that is the nominal coverage of IEEE 802.11 PHY layer. Four different speeds $\{5m/s, 10m/s, 15m/s, 20m/s\}$ are simulated for both the random waypoint mobility model (RWMM) and random direction mobility model (RDMM). Nodes are randomly activated to randomly choose destination node for data transmission. The traffic of activated nodes are supplied from a CBR source with a packet rate $0.5p/s$.

Figs. (5.2) and (5.3) present the results on complementary cumulative distribution function (CCDF) of the distribution of topology evolutions for RWMM and RDMM, respectively. It can be observed that for both cases, the exponential distribution model match pretty well with the simulation results and the analytical evaluation of the parameter also exhibits quite good approximation to the simulations.

5.5 Analyzing Control Traffic Overhead in OLSR

From the previous sections, we already know that the distribution of stability of the connectivity graph can be approximated as exponentially distributed with parameter λ given in Theorem 7. We apply our model to project the control traffic overhead of the OLSR protocol.

5.5.1 Parameterizing The MPR Selection Algorithm

As described in Section 2.2.1, by employing MPRs in OLSR, link changes need not result in a protocol event. However, the changes that happen at *critical links* (i.e., {MPR selector, MPR} pairs) surely trigger a protocol event. For the reason, we need to find a parameter that characterizes the performance of the MPR selection algorithm in OLSR, and further utilize it to derive the distribution of the connectivity graph. Before proceeding with choosing the appropriate performance metric, we need to first review the MPR selection algorithm. The MPR selection algorithm works as follows:

1. Select the node within the set of one-hop neighbor nodes as MPR node, if among the two-hop neighbor nodes, there are one or more than one nodes that are only covered by the node.

2. Choose a one-hop neighbor node as MPR node, if it covers the most of remaining two-hop neighbor nodes that are not covered by nodes in the MPR set. Repeat the step until all two-hop neighbor nodes are covered by the MPR set.

The MPR selection algorithm is a greedy algorithm and its performance varies depending on the graphs on which it operates. Its heuristic in nature, edge effects, and its graph-dependent performance significantly complicates the modeling problem and prevents an analytical modeling (if feasible) of the algorithm. For this reason, the parameter that we are looking for should reflect the statistical performance of the MPR algorithm and an evaluation of such parameter could be obtained by statistical evaluation with random geometric graph model.

A natural choice of the parameter should be the performance metric that answers the questions how much savings the MPR selection algorithm brings in reducing the duplicate flooding packet. Let's define $Neighbor\{i\}$ as the set of one-hop neighbor nodes and let $MPR\{i\}$ be the MPR set for node i. It is obvious that, $MPR\{i\} \subseteq Neighbor\{i\}$. Then the one-hop saving β_i from MPR selection can be evaluated as

$$\beta_i = \frac{|MPR\{i\}|}{|Neighbor\{i\}|} \tag{5.30}$$

Clearly, $0 < \beta_i \leq 1$. Eventually, we define a parameter β termed as *broadcast efficiency* to characterize the statistical performance of MPR selection algorithm. This parameter can be obtained through the statistical averaging over all possible nodes and graphs of the one-hop saving computed in Eq. (5.30).

$$\beta = E_{\mathcal{G},i}(\beta_i), 0 < \beta \leq 1 \tag{5.31}$$

The smaller β is, the more saving the MPR algorithm brings. β is also a statistical measure of the percentage of critical links ({MPR selector, MPR} pairs) out of total links in OLSR. From Section 5.4, we can infer that the distribution of link breakages of such links can also be approximated as exponentially distributed with parameter $\lambda_c = \beta * \lambda_o$[1].

5.5.2 Computation of Penalty Factor

The only remaining problem is to compute γ as a function of nodal mobility or the stability ζ of the local connectivity graph. First, we need to look at how ζ^* is determined from ζ, i.e., to understand how OLSR reacts to an effective change. Effective change means that the node detect a change in the set of MPR selectors, since OLSR operates on the sub-graph from critical links.

Fig. (5.4) illustrates how OLSR reacts to an effective change. Suppose that a change arrives at $KT_c < \zeta \leq (K+1)T_c$, then the next scheduled TC message is advanced to be broadcasted at time ζ^*, the choice of which depends on when the change actually happened. If $KT_c < \zeta \leq KT_c + \Delta$, then the TC message will be broadcasted at $\zeta^* = KT_c + \Delta$. For other cases $KT_c + \Delta < \zeta \leq (K+1)T_c$, TC message will be broadcasted immediately ($\zeta^* = \zeta$) when change is detected. The purpose of having Δ in OLSR is to avoid the case in which changes arrive too often and result in too much flooding from broadcasting TC messages. By aggregating such changes during Δ period

[1] It can be derived from the fact that parameters of exponential distribution of topology evolutions are linearly proportional to the number of links evaluated and β denotes the percentage of the number of MPR links out of total links.

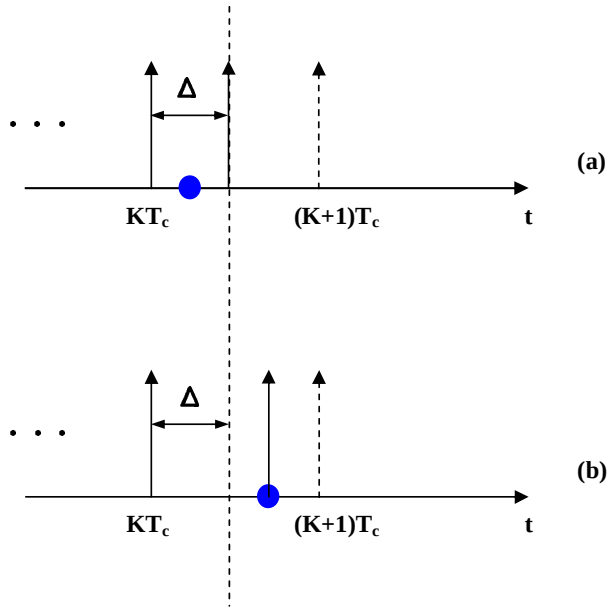

Figure 5.4: Graphical Illustration on Change Response

in one TC message, the protocol can limit the maximum TC message broadcast rate but still achieve satisfactory performance. Summarizing the above analysis, one has

$$\zeta^* = \begin{cases} KT_c + \Delta, & KT_c < \zeta \leq KT_c + \Delta \\ \zeta, & KT_c + \Delta < \zeta \leq (K+1)T_c \end{cases} \tag{5.32}$$

An effective change is the change that results in a change in the set of MPR selectors. Such changes depend on the stability of the local connectivity graph. Any changes in the local connectivity graph could lead to a re-computation of MPR set and further results in an effective change. We have the following itemized discussions on changes,

- A new link is detected in the local connectivity graph of node k. It will result in

a MPR set recomputation of neighbors within two hop distance of the new link. Such link may or may not lead to a change in MPR selectors of node k.

- A link breakage is detected in the local connectivity graph but not in the critical links of node k. For such cases, it still leads to a recomputation of MPR set but not necessarily affect the operation of node k.

- A link breakage in critical links of node k is detected and as a result, node k will detect a change in the set of MPR selectors. Such change is surely an effective change on node k and node k needs to react to the change by earlier TC message broadcast.

Due to the heuristic characteristic of MPR selection algorithm, an analysis of the first two scenarios could be significantly complicated (if feasible at all). Taking a conservative approach, we only consider the last scenario, where link breakage is detected in critical links. Because we know that the stability of overall critical links can be approximated by an exponential distribution with parameter λ_c, we can approximate the single-node stability ζ of critical links as also exponentially distributed with parameter $\lambda_s = N * \lambda_c$. Note that such approximation becomes closer as node density increases, i.e., nodes associated with more critical links.

We can then compute the penalty factor γ as a function mobility $\mathcal{V}$ as

$$\gamma(\mathcal{V}) = E(\frac{\lceil \zeta^*/T_c \rceil}{\zeta^*/T_c}) = f(\lambda_s) \tag{5.33}$$

where $f(\cdot)$ denotes mapping function and can be numerically computed after knowing the parameter λ_s of ζ (or ζ^*). It is also worthy of noting that the penalty factor is a

direct function of local connectivity graph and suggests that the stability of connectivity graph can greatly affect the protocol performance.

5.5.3 Simulations

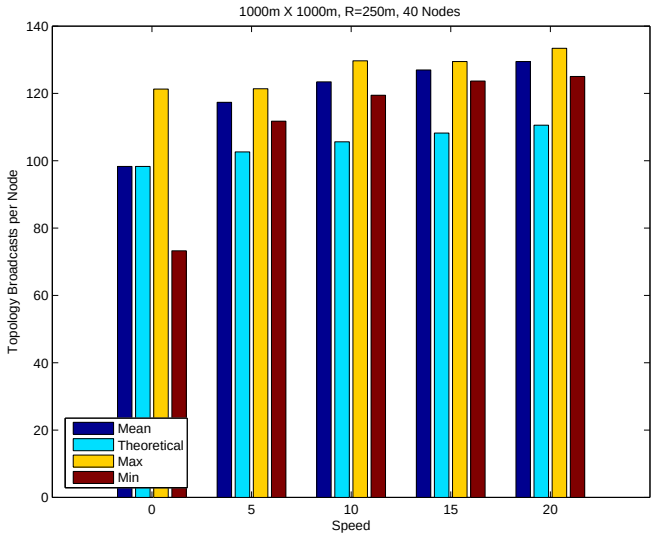

Figure 5.5: perfectMac: N40

In the simulation, the area of the network is a $1000m \times 1000m$ square cell. Each node has the same transmit power and the radio transmission range considered is $250m$. The number of nodes changes in the set $\{40, 60, 80, 100\}$ to simulate various node densities. The implementation of OLSR is the default implementation in *Qualnet 3.9.5*. Nodes are randomly activated to randomly choose destination node for data transmission. The traffic of activated nodes are supplied from a CBR source with a packet rate $0.5p/s$. And the movement follows the random waypoint model as the default setting in *Qualnet*. The maximum speeds considered are $\{0m/s, 5m/s, 10m/s, 15m/5, 20m/s\}$,

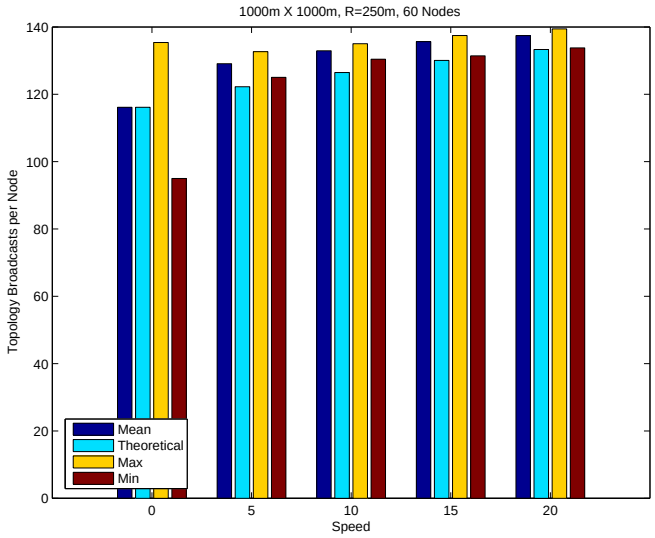

Figure 5.6: perfectMac: N60

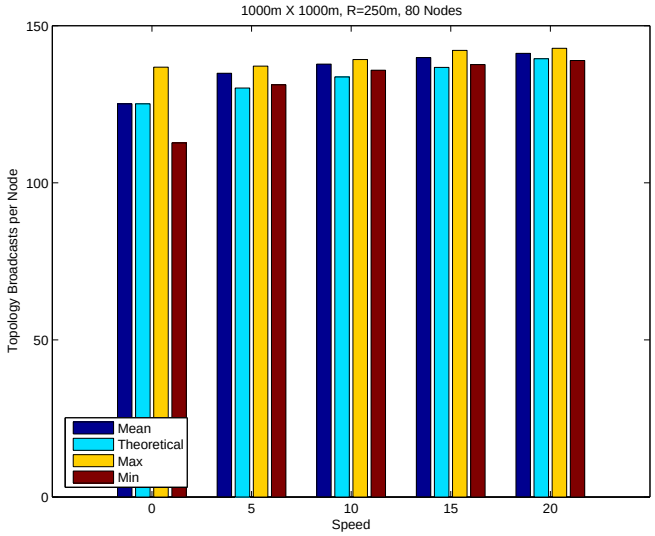

Figure 5.7: perfectMac: N80

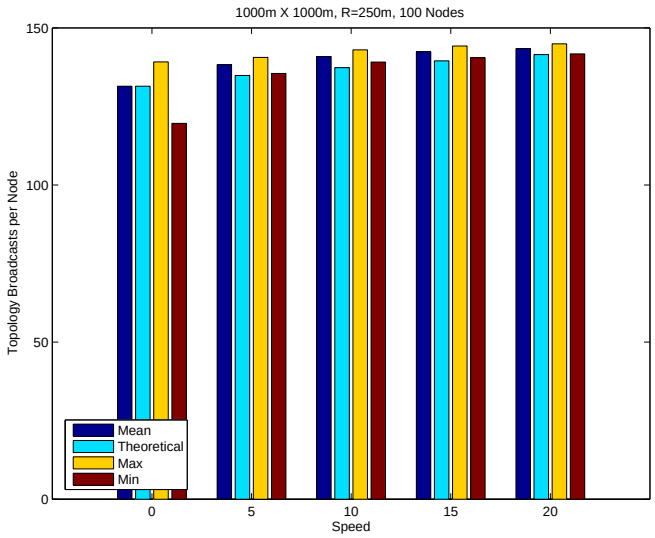

Figure 5.8: perfectMac: N100

ranging from static topologies, pedestrian speed to normal vehicle speed. The MAC layer is set as the 802.11 MAC. Overall, we simulate a total of 20 different network configurations. For each configuration, 50 simulations with random generated seeds are conducted to capture the statistical performance.

To study the effect of nodal mobility, we modified the *Qualnet* simulator to eliminate packet losses due to collisions in the channel. We call this case *perfect MAC*. Figs. (5.5) to (5.8) demonstrate the performance of the analytical model versus simulated performance when *nodal mobility* is the only performance factor. It can be observed that the analytical model provides a very good estimate compared to the simulations. Because we take a conservative approach in Section 5.5.2, the analytical model usually underestimates the overhead. As expected, the difference between the model and simulations decreases as node density increases, as critical links become more dominance

in the local connectivity graph or link changes at non-critical links brings less effect on the sub-graph from critical links.

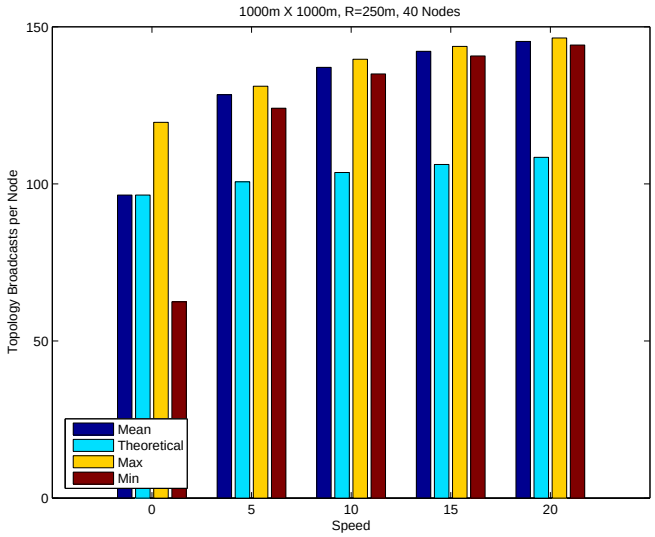

Figure 5.9: Real Mac: N40

To evaluate the model in practical scenarios, we used the original setting of *Qualnet* in interference computation. In this case, the real 802.11 MAC works under collisions and back-offs. The simulation results are then illustrated in Figs. (5.9) to (5.12). In general, the model still provides a good approximation; however, the difference between the model and simulations are more pronounced due to additional effect from *environmental mobility*. Overall, we believe that our model provides satisfactory performance in estimating the routing overhead and brings deeper insight on how mobility affect the routing overhead.

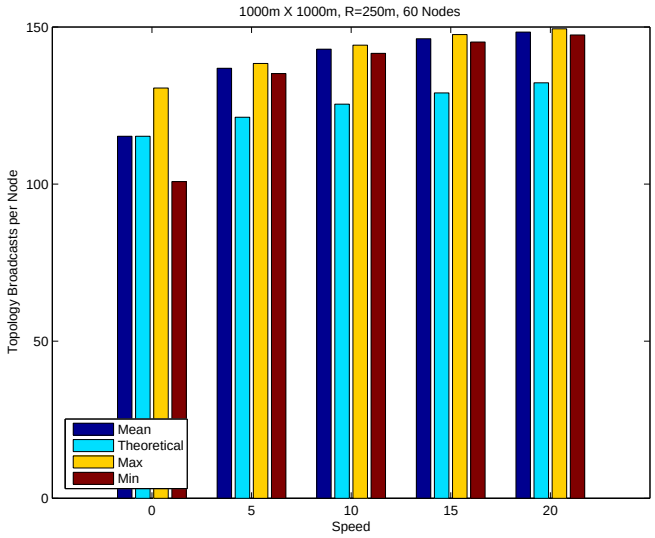

Figure 5.10: Real Mac: N60

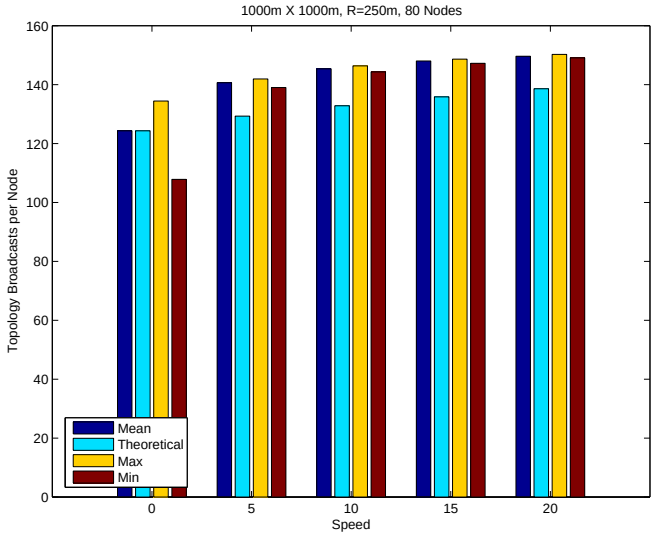

Figure 5.11: Real Mac: N80

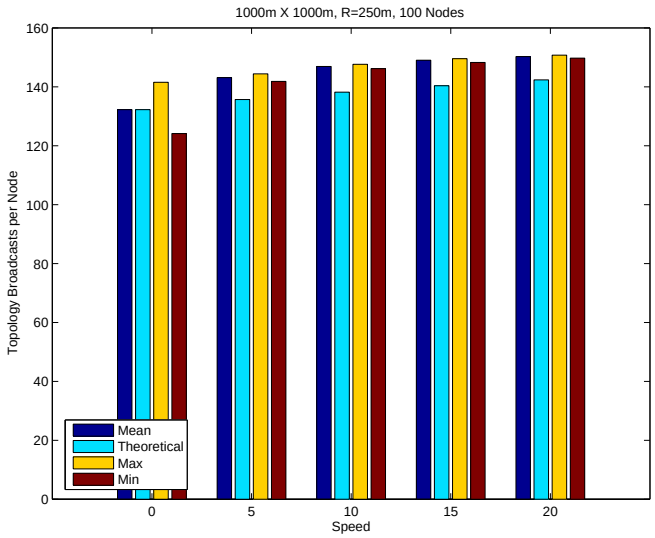

Figure 5.12: Real Mac: N100

5.6 Conclusion

We evaluated analytically the interdependence between routing overhead and the stability of the network topology by characterizing the statistical distribution of topology evolutions. The stability of topology can be modeled as exponentially distributed with a parameter computed from network configurations. Utilizing the proposed model, the routing overhead of OLSR was analyzed and the results showed that the proposed model gives good estimate of routing overhead and meanwhile provides good insight on how nodal mobility affects the routing overhead.

Chapter 6

Proactive or On-Demand Routing: A Unified Analytical Framework in MANETs

As reviewed in Section 2.2, the two main classes of routing protocols for MANETs are proactive and reactive (or on-demand). Proactive routing protocols provide fast response to topology changes by maintaining routing information for all network destinations and reacting to changes in the network. However, the price they pay is the signaling overhead incurred in maintaining routing information for those destinations for which large numbers of nodes have no interest. On the other hand, reactive routing protocols provide routing information on a need to have basis and, at least in theory, can reduce the signaling overhead incurred in maintaining routing tables compared to proactive approaches. However, on-demand routing may incur long setup times

in discovering the routes to destinations for which there is interest.

Given that proactive and reactive routing in MANETs have relative advantages and disadvantages, comparing the two is important. Significant work (e.g., [13, 20, 44, 48, 8, 3, 21]) has been conducted to evaluate and compare these protocols under network profiles of various mobility and traffic configurations. Such performance comparisons have been mostly conducted via discrete-event simulations. Simulation-based studies of routing schemes is indeed a powerful tool to gain insight on their performance for specific choices of network parameters. However, it is difficult to draw conclusions involving multidimensional parameter spaces, because running several simulation experiments for many combinations of network parameters is impractical.

Few if any analytical studies have been pursued on this topic, and has been mostly restricted to the analysis and comparison of routing control overhead [81, 76]. Zhou et al. [81] present an analytical view of routing overhead of reactive protocols, assuming a static Manhattan grid network and study the scalability of reactive protocols. Viennot et al. [76] proposed parametric models for proactive and reactive protocols to evaluate their individual routing control overheads. None of these works evaluates the effects of signaling overhead on unicast capacity at nodes, and neither of them reveals the underlying connection between protocol performance and network parameters.

Given that previous work does not establish an analytical connection between protocol performance (e.g. packet delivery ratio and delay) and network parameters (e.g. node density, mobility and traffic density), analytical models are needed to characterize and compare the performance of routing protocols as a function of the characteristics

of the physical layer, the operation of the underlying MAC protocol, and the mobility of nodes. This chapter proposes a general, parameterized framework for analyzing protocol performance in mobile ad-hoc networks. In our framework, the adverse effects of signaling overhead on data packets are captured and analyzed through a two-customer queuing model of the operation of nodes. The framework is a combinatorial model that parameterizes and evaluates the performance of routing protocols using a joint characterization of the routing and channel access functionalities in terms of packet delivery ratio and delay. This model focuses on the essential behavior of on-demand and proactive routing protocols, rather than on specific routing protocols. However, when tailored to specific protocol, the proposed model gives good approximations to simulated protocol performance with the *IEEE 802.11 MAC using the Distributed Coordination Function (DCF)*, further corroborating its effectiveness and correctness in dealing with protocol performance in more realistic scenarios.

Section 6.1 presents the mobility model, traffic model and simplified models of routing algorithms used in Section 6.2 to model the performance of proactive and on-demand routing in MANETs. Section 6.3 characterizes the performance of MAC protocols based on scheduling (TDMA) and contention (802.11 DCF). Section 6.4 compares our analytical results against extensive Qualnet simulations based on scenarios using various traffic loads, mobility and node density configurations. The results indicate that our analytical framework provides a good first-order approximation of the performance of MANET routing protocols, and that it can predict the impact of various network parameters analytically, which can then be followed by a simulation-based

Table 6.1: Summary of Parameters

N	Number of nodes
δ	Node density
V	Average nodes' speed
R	Radius of transmission circle
F	Number of parallel traffic flows in the network
K	Average hop-count per source-destination pair
λ_B	Mean broadcast flooding rate
T_L	Average link lifetime
C	Effective unicast capacity
ρ	Signaling efficiency
C_u	Unicast capacity per node

study focusing on concrete parameter values. Section 6.5 concludes this chapter.

6.1 Network Model

For convenience, we at first present a brief summary of parameters used throughout the chapter, as well as their short descriptions in Table 6.1. In the network, nodes are assumed to be mobile and to be equally distributed over the network initially. The movement of each node is independent and unrestricted, i.e, the trajectories of nodes can lead to anywhere in the network and the trajectory processes of nodes confirm to Assumption 1 in Chapter 5.

We consider a new traffic flow, which we also call a new session, as one that is associated by the arrival of a new application-level session request at a node i with some destination j, $j \neq i$ in the network. Traffic flows are randomly generated with uniformly distributed sources and destinations. In this work, we assume long-lived traffic flows in order to investigate protocol performance under steady state of node mobility and

traffic distributions. Short-lived traffic flows, reflecting transient behaviors, are beyond the scope of the chapter.

We assume that the network topology is well connected. More precisely, if an existing path for any traffic session is broken, then with high probability there is an alternative path available to support the continuing operation of the traffic flow. The alternative path is not necessarily disjoint with the former broken path.

We assume the following generic behavior of proactive and reactive routing protocols, which we believe capture the essential behavior of many designs and implementations of routing protocols. However, this analysis, and hence the generic protocols below, does not consider many protocol-specific techniques aimed at improving the efficiency with which protocols operate, such as multi-point relays, local repairs, and route caching mechanisms.

Proactive Routing Protocol Every node maintains a list of destinations and their routes by processing periodic topology broadcasts originated by each node in the network. When a packet arrives, the node checks its routing table and forwards the packet accordingly. Each node monitors its neighboring links and every change in connectivity with any neighbor results in a topology broadcast packet that is flooded over the entire network. In a well-connected network, the same topology broadcast packet could reach nodes multiple times and therefore enjoy a good packet reception probability. In this chapter, we assume that every node receives topology flooding packets reliably from other nodes.

Reactive Routing Protocol Nodes maintain their routing tables on a need-to-use basis. This implies that, when a new traffic session arrives, nodes have to set up the path between the source and destination before data packets can be forwarded. The path-setup process is called *route discovery*. Node i initiates this process upon the arrival of a "new traffic session" in order to discover a new path to a node j. To accomplish this, node i floods the whole network with route request (RREQ) packets searching for a route to destination j. Upon receiving the RREQ packet, node j sends out a route reply (RREP) packet along the reverse path to i. A *route maintenance* process is necessary to find alternative paths if existing paths are broken. A node i is informed that a link along an active path has broken, such that it can no longer reach the destination node j through that route. Upon reception of a notification of a route failure, node i can initiate a route discovery again to find a new route for the remaining packets destined to j.

6.2 Unified Framework for Quantifying Protocol Performance

In general, protocol performance should be the convolving result from protocol design philosophy and MAC performance at nodes. Bearing distinctive design philosophies, proactive and reactive protocols exhibit dramatic performance difference. Furthermore, signaling overhead changes significantly with different designs and in turn result in significant MAC performance variations. To evaluate the performance of a

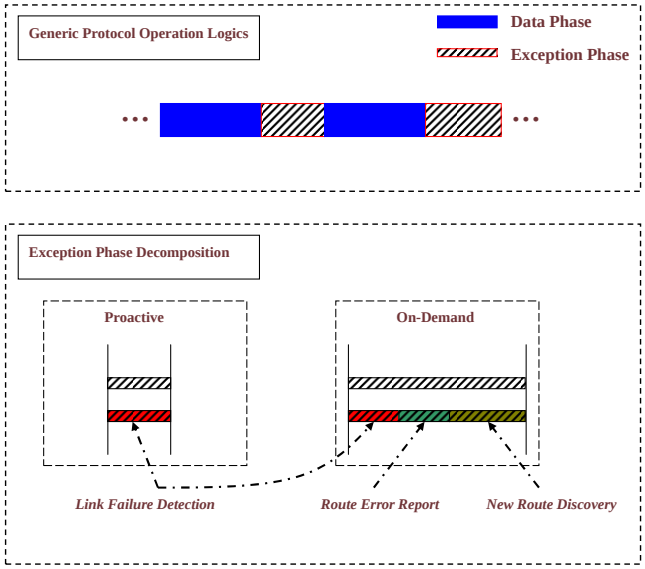

Figure 6.1: Generic Protocol Operation

protocol, we start with an analytical characterization of signaling overhead in terms of mean broadcast flooding rate λ_B. We then bring out a combinatorial model with two parameters: signaling efficiency ρ, capturing the generic effect from design philosophy; and unicast capacity C_u, measuring the MAC performance in handling unicast packets as well as reflecting the adverse effects from signaling overheads. These two parameters are then synthesized to produce the overall performance measure of protocol performance - effective unicast capacity C. Mathematically, the model can be written as,

$$C = \rho \times C_u \tag{6.1}$$

Nevertheless, Eq.(6.1) is a rather simple model for characterizing protocol performance, leaving out many nuances in protocol behaviors. However, this simple model captures

essential aspects of routing protocols, accounting for the complex interplay from protocol designs and MAC. Network parameters, such as node density, traffic, and mobility, are embedded in the model and their contributions will be analytically exploited, as we move on evaluating the model.

6.2.1 Mean Broadcast Flooding Rate λ_B: Characterization of Signaling Overhead

Clearly, a mean broadcast flooding rate λ_B that reflects routing overhead plays an essential role in determining protocol performance. Generating such flooding packets is directly connected with stability of topology. Knowledge of stability of topology can be applied to compute the mean broadcast flooding rate [78]. In our generic protocols, we assume that every topology change, mostly from nodes' mobility, triggers a broadcast flood event.

We know that a topology is comprised of the set of all active links participating in the protocol operation and it usually involves with significant number of active links. Let the set of all active links be denoted by $A_s(t)$ and $N_s(t) = |A_s(t)|$ be the number of links in the active set, where $|\cdot|$ is the cardinality operator and t is the time index. Note that the topology changes with time t and due to the ergodicity in the joint trajectory processes, its stationary distribution can be derived from the stationary spatial nodes' distribution with respect to the underlying mobility models[78].

When a network is running in steady-state and the process of topology change is ergodic, it will experience all possible topologies with an associated probability vector

derived from the steady-state nodes' distribution. By averaging all possible topologies, we can compute complementary cumulative distribution function (CCDF) $F(t)$ characterizing the stability of topology [78] as

$$F(t) \approx exp(-E(N_s(t)) * t/T_L). \tag{6.2}$$

It should be pointed out that only the breakage process of existing links are counted in the above analysis, while formation process of new links is not included. However, in proactive protocols such as the optimized link state routing (OLSR) protocol [16], both the formation and breakage process should be taken into account, because both of them could trigger protocol events. Luckily, in the long run, for a network with finite number of nodes, the formation and breakage process should be balanced off each other. Then the overall CCDF distribution accounting for both the formation and breakage process will be

$$F(t) \approx exp(2 \times -E(N_s(t)) * t/T_L) \tag{6.3}$$

It is also worthy to note that, for reactive protocols such as ad hoc on-demand distance vector (AODV) routing [65], only the breakage process will trigger the protocol event and the stability of topology should be evaluated by Eq.(6.2).

Summarizing the analysis, we can approximate the mean broadcast rate as

$$\lambda_B = \begin{cases} E(N_s(t))/T_L, & \text{reactive} \\ 2E(N_s(t))/T_L. & \text{proactive} \end{cases} \tag{6.4}$$

For reactive protocols, $E(N_s(t))$ can be approximated as,

$$E(N_s(t)) \approx K * F. \tag{6.5}$$

And for proactive protocols, $E(N_s(t))$ can be approximated as [78],

$$E(N_s(t)) \approx C_N^2 * (\pi R^2 * \delta). \tag{6.6}$$

6.2.2 Signaling Efficiency ρ: Reflections on Protocol Design Philosophy

We first parameterize the operation of a routing protocol focusing on a given traffic flow, say from node i to node j. Because we are interested in long-term behavior with steady traffic, the initial traffic and network setup cost are usually negligible.

As illustrated in Fig. 6.1, the operation of the traffic flow can be generally classified into two alternating phases: a data phase and an exception phase. During a data phase, an active path to a destination has been established and data packets are forwarded from node i to j along the active route. An exception phase is triggered when a link failure is detected in an active path and an alternative path needs to be discovered. Let T_a and T_e be the mean duration of a data phase and exception phase, respectively. And let *signaling efficiency* ρ be the ratio between the data phase and the overall time.

$$\rho = T_a/(T_a + T_e) \tag{6.7}$$

Both proactive and reactive protocols share similar data phases, because they are determined by the underlying joint trajectory processes for nodes. Therefore, one parameter T_a is used for both protocols. However, the time for exception phase is quite

different. As depicted in Fig. 6.1, further decomposition of an exception phase reveals that proactive and reactive protocols bear different behaviors. The exception phase T_e^p in proactive protocols involves only the time window W_l which is a protocol parameter for link failure detection, i.e,

$$T_e^p = W_l \tag{6.8}$$

For reactive protocols, the exception phase T_e^o involves four steps:

- Link failure detection, denoted by W_l.
- Link failure unicasted back to source, denoted by T_{lf}.
- RREQ broadcast flooding, denoted by T_{rreq}.
- RREP unicasted back to source, denoted by T_{rrep}.

From this decomposition, we have

$$T_e^o = W_l + T_{lf} + T_{rreq} + T_{rrep} \tag{6.9}$$

The signaling efficiency ρ^p (or ρ^r) of a generic proactive protocol (or reactive protocol) can then be evaluated as,

$$\rho^p = T_a/(T_a + W_l) \tag{6.10}$$

$$\rho^r = T_a/(T_a + W_l + T_{lf} + T_{rreq} + T_{rrep}) \tag{6.11}$$

For now, the routing signaling can be represented by a tuple of parameters called *signaling parameter tuple* (SPT) $\vec{\theta}_s = \{T_a, W_l, T_{lf}, T_{rreq}, T_{rrep}\}$.

6.2.3 Unicast Capacity C_u: Reflection on MAC performance

During a data phase, data packets are unicasted along the active path from a source to the destination. From a queuing perspective, nodes along the active path form a tandem network of queues. Given that every node takes two types of traffic (broadcast packets and unicast packets), each node can be modeled as a two-customer queue. To simplify the analysis, we make the following assumptions for the queuing model:

- The nominal packet length is L for both broadcast and unicast packets, while the model can be extended to incorporate various packet length distributions.
- The arrival process of broadcast (or unicast) traffic is Poisson with parameter λ_B (or λ_U). Such a Markovian-input assumption can be justified theoretically as the sum of a large number of independent random traffic flows from the neighboring nodes. Each node is now modeled as a M/G/1 FCFS queue.
- Every queue operates independently of any other. This is a strong hypothesis in our analysis, because the traffic among nodes may be heavily correlated, especially when data traffic between nodes originates from one same source rather than multiple independent streams. However, in practice, the model still gives a very satisfactory approximation, as observed from simulation results reported in [66].

Each node can now be represented by a tuple of parameters called *MAC parameter tuple* (MPT) $\vec{\theta}_m = \{\lambda_B, \lambda_U, \bar{S}_B, \bar{S}_U, \mathcal{V}_B, \mathcal{V}_U, P_e\}$, where $\{\bar{S}_B, \mathcal{V}_B\}$ (or $\{\bar{S}_U, \mathcal{V}_U\}$)

stand for the mean and variance of service time of broadcast packets (or unicast packets) respectively and P_e denotes the packet loss probability.

Knowing MPT, we can evaluate the unicast capacity C_u as,

$$C_u = E((1 - \lambda_B \bar{S}_B)\frac{1}{\bar{S}_U}) \tag{6.12}$$

Clearly, proactive (or reactive) protocols enjoy their individual unicast capacity C_u^p (or C_u^r), because they exhibit different MAC performance, mostly induced from different signaling overhead λ_B.

Eq. (6.12) implies a significant constraint on network scalability. Specifically, to ensure protocols operating at correct logics, nodes performing the task of delivering packets should be functional. Since nodes are modeled as M/G/1 queues, for queues to be stable and functional, we can infer the scalability constraint [46] as,

$$E(\lambda_B \bar{S}_B + \lambda_U \bar{S}_U) < 1. \tag{6.13}$$

The left side of the equation is a function of network size N.

6.2.4 Delay Aspect & Packet Delivery Ratio

From the two-customer M/G/1 model, we can compute the one-hop delay of broadcast packets D_B or unicast packets D_U as [46]

$$\begin{aligned} D_B &= \bar{S}_B + \frac{\lambda_B(\bar{S^2}_B + \mathcal{V}_B) + \lambda_U(\bar{S^2}_U + \mathcal{V}_U)}{2(1 - \lambda_B \bar{S}_B - \lambda_U \bar{S}_U)} \\ D_U &= \bar{S}_U + \frac{\lambda_B(\bar{S^2}_B + \mathcal{V}_B) + \lambda_U(\bar{S^2}_U + \mathcal{V}_U)}{2(1 - \lambda_B \bar{S}_B - \lambda_U \bar{S}_U)} \end{aligned} \tag{6.14}$$

Since nodes are randomly moving under an ergodic process, the active path could experience all possible source-destination distributions and on the long run, the mean end-to-end delay D_p can be computed as

$$D_p \approx K \times D_U + D_{buf} \tag{6.15}$$

$$D_{buf} \approx (1-\rho) * T_e/2 \tag{6.16}$$

where D_{buf} specifies the average delay for packets stored in buffer during the exception phase.

The end-to-end packet delivery ratio (PDR) P_d can be approximated as

$$P_d \approx (1-P_e)^K \tag{6.17}$$

6.2.5 Evaluation of Signaling Parameter Tuple

In SPT $\vec{\theta}_s$, T_a measures the average path lifetime and can be approximated as $T_a \approx T_L/K$. T_L usually takes the form as $T_L = \Theta(R/V)$ [78] and can be written as,

$$T_L = c1 * R/V \tag{6.18}$$

where $c1$ is a constant determined from the underlying mobility model. T_{lf} is the average time of RRER packets traveling back to the source. Since the path can break at any point in the middle and if assumed uniform distribution of such breakages, it is computed as

$$T_{lf} = K/2 * D_U. \tag{6.19}$$

T_{rreq} denotes the average time of broadcast packets from source to reach destinations and can be written as

$$T_{rreq} = K * D_B. \tag{6.20}$$

T_{rrep} denotes the average time of RREP packets delivered back to sources and is derived as

$$T_{rrep} = K * D_U. \tag{6.21}$$

6.3 MAC Parameter Tuple: Characterizing MAC Performance

The only remaining question consists of characterizing the performance of the MAC protocol, reflected in MAC parameter tuple $\vec{\theta}_m = \{\bar{S}_B, \bar{S}_U, \mathcal{V}_B, \mathcal{V}_U, p_e\}$, which we do next. Particularly, we consider three representative MAC schemes. One is the global time division multiple access (GTDMA [68]), which serves as a lower achievable bound. The second one is also a TDMA scheme, but the scheduler is locally optimal (LTDMA [57]). In practice, no such schedulers are used, because instant global topology information is required and the design of any such scheduler is known to be an NP-hard problem. However, such a scheme serves the purpose of an upper performance bound for scheduled MAC protocols. Finally, we consider the widely deployed contention-based MAC scheme, 802.11 DCF MAC, which we aim at characterizing more practical protocol analysis.

6.3.1 Global Time Division Multiple Access

In the GTDMA scheme, the channel access of nodes is organized as frames in time and each frame is further organized into N slots. In every frame, every node in the network is assigned a slot for transmission and the duration of slot should allow nodes to transmit the maximum transmission unit (MTU).

Let's Δ_g be the duration of a slot and the duration of a framework will be $\Delta_f = N\Delta_g$. In such fashion, every node will get one slot to sent out one packet (either broadcast packet or unicast packet) for every Δ_f time. During the scheduled access, there will be no collision in packet transmission and thus it is safe to assume that the packet loss probability will be zero, i.e,[1]

$$P_e = 0 \tag{6.22}$$

It is also clear that every node enjoys a deterministic service time of Δ_f. For such special case, M/G/1 model is thus reduced to a two-customer M/D/1 model. Correspondingly, one have

$$\mathcal{V}_B = \mathcal{V}_U = 0 \tag{6.23}$$

$$\bar{S}_B = \bar{S}_U = \Delta_f \tag{6.24}$$

6.3.2 Local Genie-TDMA

In contrast to GTDMA, LTDMA is a localized TDMA scheme where the transmission of nodes are scheduled locally. For node i, if it has $N_r - 1$ neighbors, the channel

[1]Note that we don't consider wireless environmental effects, e.g. fading, conforming to the well-known protocol model [36].

access is still grouped as frames but each frame has only N_r slots for all N_r nodes, who are within coverage of nodes i. However, the design of such a scheduling scheme for all nodes without collisions is sometimes impossible or an NP problem. We assume that there is always one such Genie-scheduler and the results obtained serve as an upper bound on performance.

For such a scheme, the packet loss probability is also zero

$$P_e = 0 \tag{6.25}$$

However, the service time now becomes,

$$\mathcal{V}_B = \mathcal{V}_U = \Delta_g^2 Var(N_r) \tag{6.26}$$

$$\bar{S}_B = \bar{S}_U = \Delta_g E(N_r) \tag{6.27}$$

where Δ_g denotes the time duration of a slot and $Var(\cdot)$ is the variance operator of a random variable. Clearly, N_r is a random variable characterizing the statistical distributions of the number of nodes in a communication circle. If distributions of nodes are uniform, N_r will be binomial distributed as

$$P(N_r = K) = C_N^K p^K (1-p)^{N-K} \tag{6.28}$$

$$p = \pi R^2 \times \delta / N, \tag{6.29}$$

where p is the probability of two nodes being within communication range of each other. Then, we have

$$E(N_r) = Np \tag{6.30}$$

$$Var(N_r) = Np(1-p) \tag{6.31}$$

6.3.3 Contention-based MAC

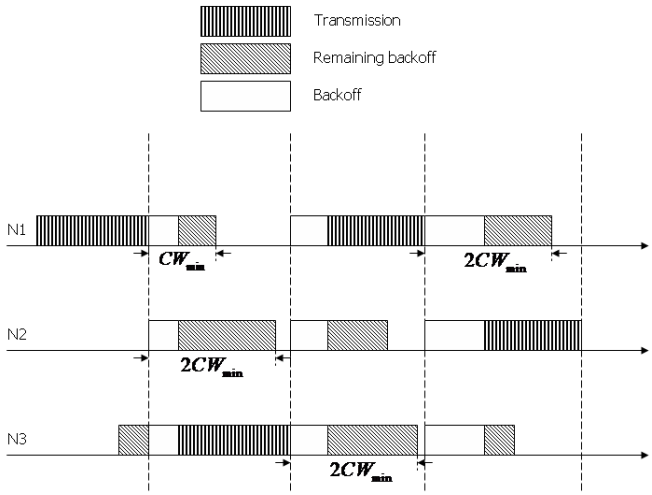

Figure 6.2: Graphical Illustration of CSMA/CA scheme.

We consider the well-known 802.11 DCF MAC, employing carrier sense multiple access with collision avoidance (CSMA/CA) technique. In such a scheme, broadcast packets and unicast packets are processed differently and will therefore have different service time.

For unicast packets, a rotating back-off mechanism is adopted to resolve contention. The whole procedure is illustrated in Fig. 6.2. For the first transmission of a packet, if the channel is sensed to be idle for an interval greater than Distributed Inter-Frame Space (DIFS), the node initializes a backoff timer. And the value of the backoff timer is uniformly selected within the initial contention window (CW) CW_{min}. The timer decrements when the channel is sensed to be idle, freezes when the channel becomes busy and restart when the channel becomes idle for a DIFS again. When

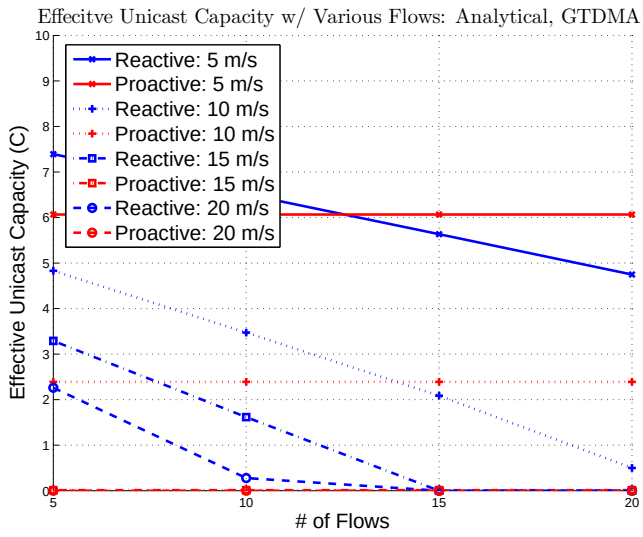

Figure 6.3: Effective Unicast Capacity, Various Flows: Analytical, GTDMA.

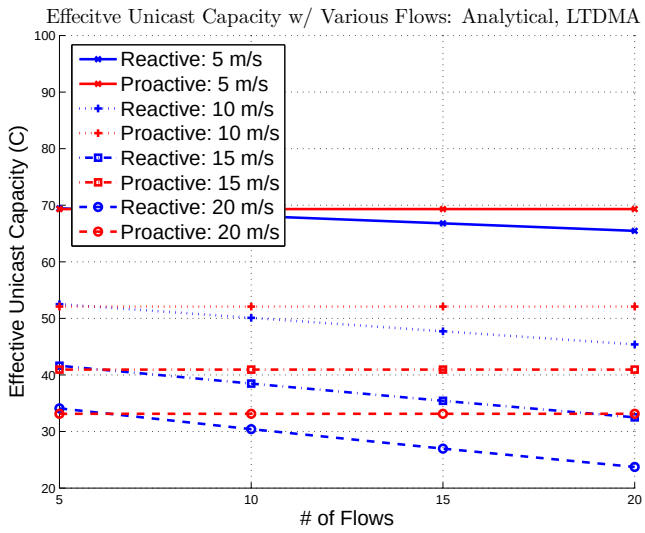

Figure 6.4: Effective Unicast Capacity, Various Flows: Analytical, LTDMA.

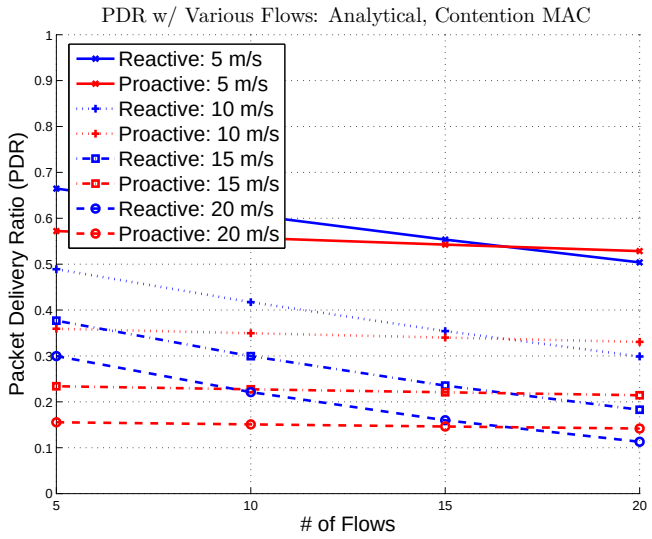

Figure 6.5: PDR, Various Flows: Analytical, Contention-based MAC.

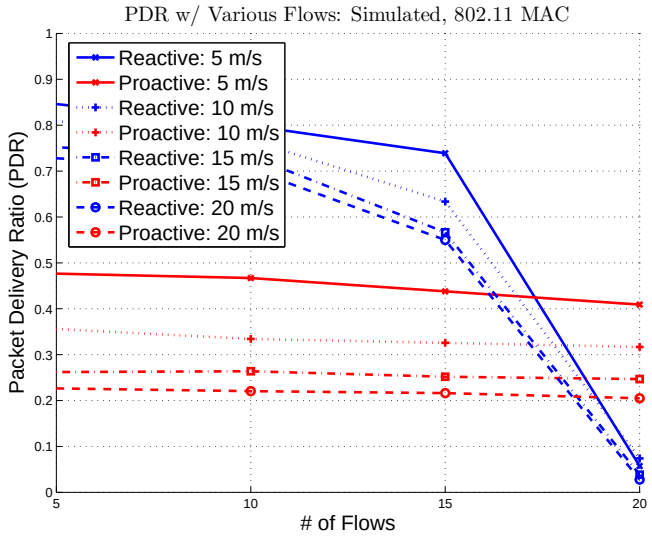

Figure 6.6: PDR, Various Flows: Simulated, 802.11 MAC.

the timer counts down to zero, packet is transmitted immediately and waits for an acknowledgment (ACK) confirmation. In case that an ACK is not received and the last transmission is declared a failure, the value of CW is doubled for retransmission, until it reaches the upper limit of CW_{max} specified by the protocol.

For broadcast packets, no retransmission are attempted and no ACK is needed. Each broadcast packet is transmitted only once. Therefore, broadcast packets only need to go through the first trial phase of unicast packet transmission, i.e., the phase with the initial contention window of CW_{min}.

To analyze the MAC performance of a node i, we first look at its probability generating function $C_i(z)$ of channel occupancy, as observed from node i. Channel occupancy of node i is used to characterize the distribution of channel utilizations from its neighboring nodes. $C_i(z)$ employs a generic representation form as $C_i(z) = \sum_n P(C_i = n)z^{n+1}$, where C_i is expressed in discretized slot duration, $P(C_i = n)$ denotes the probability of channel being sensed as busy for a continuous period of n slots and z is a dummy variable. Such discretized slot representation may introduce some small deviations. However, because the slot duration η is usually a very small value, such discretization effect could be neglected.

Clearly, the identity channel generating function $C_i(z) = p(C_i = 0)z = z$ would mean that $n = 0$ always, i.e., the channel is permanently sensed idle by node i. We assume that all packets sent to the channel are of the same length L. Therefore, there are only two kinds of channel status: idle because of no packet arrival and busy because of some arrival with packet length L. In this case, we can simplify the generating

function as $C_i(z) = (1 - p_a + p_a * z^L) * z$, where p_a is the probability of packet arrivals from neighboring nodes at the same time slot. Clearly, it also corresponds to the packet collision probability of node i, i.e., $P_e = p_a$.

The packets competing with node i consist of the sum of all traffic from neighboring nodes. The distribution of such arrival process can be approximated as Poisson, deduced from the superposition of random variables. Mathematically, the mean rate λ_i^c of competing traffic can be written as

$$\lambda_i^c = E(\sum_{\forall k \in \{\text{neighbors}\}} (\lambda_B^k + \lambda_U^k)) \tag{6.32}$$

Then, the packet loss probability will be the probability of collision traffic arriving within a duration of a slot and can be computed as,

$$\begin{aligned} P_e &= \lambda_i^c * \eta \\ &\approx (Np - 1)(\lambda_B + \lambda_U) * \eta \end{aligned} \tag{6.33}$$

where $\eta = 20\mu s$ in 802.11 DCF MAC.

We then look at the service aspect of M/G/1 model under such a MAC scheme. Let $\phi(z, L, \alpha, \gamma)$ be the probability generating function of service delay for each packet, where the collision probability is α and the back-off window value is γ. ϕ includes channel access time and the time needed to transmit the packet. The back-off counter value M is uniformly chosen within γ with the probability of $\frac{1}{\gamma}$.

Without collision, the total time to access the channel is the time needed for M decreases, that is, M times the busy time slot random variable C_i which can be expressed

by generating function $\sum_{i=1...\gamma} \frac{1}{\gamma} C_i(z)^i$. Once the channel is accessed the time needed to transmit the packet is fixed and equal to L. Therefore, it can be expressed by generating function z^L. Hence the service time when no collision occurs comes from adding the previous two quantities, or equivalently the corresponding generating function is equal to the product of the above generating functions, i.e.,

$$\frac{z^L}{\gamma} \sum_{i=1...\gamma} C_i(z)^i = \frac{C_i(z)^{\gamma+1} - C_i(z)}{C_i(z) - 1} \frac{z^L}{\gamma}. \tag{6.34}$$

Eq.(6.34) is exactly the probability generating function of service time for broadcast packets, where packet collisions are not concerned.

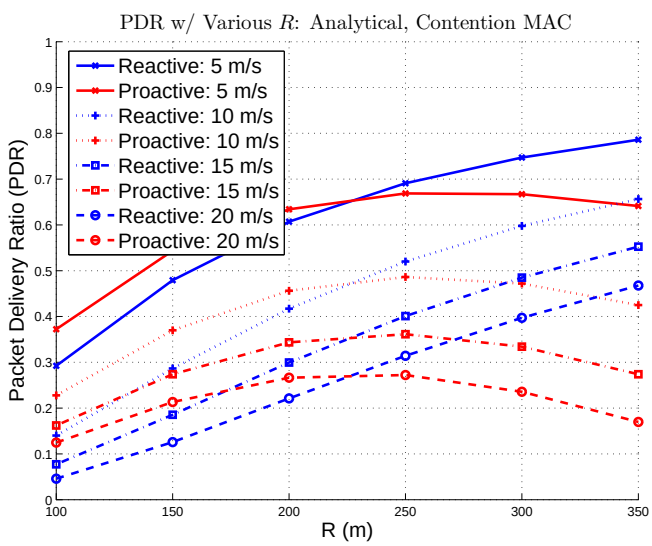

Figure 6.7: PDR, Various R: Analytical, Contention-based MAC.

In case there is collision, the nodes select a new back-off number in a doubled contention window $\{1...2\gamma\}$ and the procedure is repeated which results in an additional

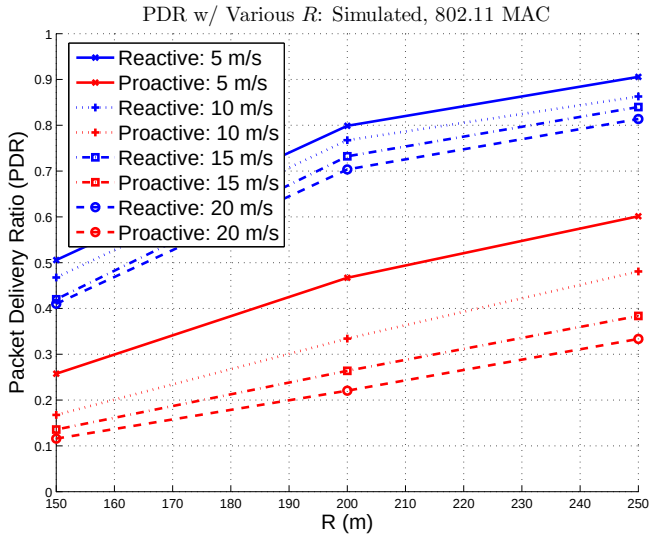

Figure 6.8: PDR, Various R: Simulated, 802.11 MAC.

service delay term. We obtain

$$\begin{aligned}\phi(z, L, \alpha, \gamma) &= \frac{C_i(z)^{\gamma+1} - C_i(z)}{C_i(z) - 1} \frac{z^L}{\gamma} \\ &\times \quad (1 - \alpha + \alpha\phi(z, L, \alpha, 2\gamma)). \end{aligned} \tag{6.35}$$

Computing the probability generating function of service time through Eq.(6.35) for unicast packets requires a recursive computation, until the contention window length reaches the maximum value CW_{max}.

Finally, we can summarize the probability generating function of service time for both broadcast packets $\phi_B(z)$ and unicast packets $\phi_U(z)$ as,

$$\phi_B(z) = \frac{C_i(z)^{CW_{min}+1} - C_i(z)}{C_i(z) - 1} \frac{z^L}{CW_{min}} \tag{6.36}$$

$$\phi_U(z) = \phi(z, L, E(P_e^i), CW_{min}) \tag{6.37}$$

The mean service time for broadcast packets and unicast packets can then be computed

as,

$$\bar{S}_B = (\frac{d}{dz}\ \phi_B(z))|_{z=1} \tag{6.38}$$

$$\mathcal{V}_B = (\frac{d}{dz}\ (z * \frac{d}{dz}\phi_B(z))\Big|_{z=1} \tag{6.39}$$

$$\bar{S}_U = (\frac{d}{dz}\ \phi_U(z))|_{z=1} \tag{6.40}$$

$$\mathcal{V}_U = (\frac{d}{dz}\ (z * \frac{d}{dz}\phi_U(z))\Big|_{z=1} \tag{6.41}$$

6.4 Simulations

In the simulation, we consider a total of 100 nodes initially distributed randomly over a square network of size $1000m \times 1000m$. Three different transmission ranges $R \in \{150, 200, 250\}m$ are covered, all within the coverage of WiFi devices. Four different speeds $V \in \{5, 10, 15, 20\}m/s$ are simulated, from lower mobility to higher mobility scenarios. Traffic, supplied from CBR source at rate $0.5p/s$, is randomly generated with uniformly distributed sources and destinations. Different traffic flows $F \in \{1, 5, 10, 15, 20\}$ flows are simulated, covering low flow and moderate flow configurations. In addition, simulation results are obtained for both reactive (AODV [65]) protocol and proactive (OLSR [16]) protocol using the default implementation in *Qualnet 3.9.5*. The MAC layer is chosen as the default implementation of 802.11 MAC in *Qualnet*. Overall, a total of 120 different {radius, mobility, flow, protocol} configurations are simulated. For each configuration, the simulation result is obtained from 10 random runs. Each simulation run is conducted at a randomly generated seed with a time duration of 30 minutes.

Figs. 6.3 and 6.4 present results of effective unicast capacity for scheduled TDMA MACs. The results clearly reflect the significant adverse effects from signaling overhead. The analytical results reveal that reactive protocols are more susceptible to traffic increase, while proactive protocols are robust to change in traffic. In general, proactive protocols are preferred in network profile of high traffic configuration, conforming the similar finding in [76] through control overhead analysis. The results also indicate that as mobility increases, performance of both protocols will be significantly affected. Eventually, at certain point, proactive protocols will completely cease to operate due to the increase in overhead, while reactive protocols could still operate but at very low traffic rate. Therefore, reactive protocols are favored in very high mobility scenarios.

We then explore the effectiveness of the proposed model in analyzing the general behaviors of routing protocols with more realistic 802.11 DCF MAC, in terms of packet delivery ratio (PDR), under various {mobility, traffic flow} configurations. Note that when evaluating proactive protocols, the proposed model has been adapted to incorporate the analysis of OLSR protocol [78], accounting for artifacts from MPR technique. However, since there is no such analysis for AODV protocol, the generic reactive protocol described in Section 6.1 is used. Figs. 6.5 and 6.6 show that

- When tailored to specific protocols, the proposed model provides satisfactory approximation to simulated performance, as observed from good match between Fig. 6.5 and 6.6 for proactive (OLSR) protocol.

- Without incorporating specific techniques of AODV protocol (e.g. local repair), the proposed model still captures the essential behaviors of reactive protocols with respect to mobility and traffic flows, while failing to provide good matches to simulated performance.

It should be noted that although Fig. 6.6 only presents a small set of simulations, other obtained simulation results are similar and thus not presented. In summary, the parameterized analytical framework provides key insights into the compounding and interacting effects of network parameters, deeper understanding on essential protocol behaviors and capability of approximating practical performance with incorporation of protocol-specific techniques.

Utilizing the proposed model, we are now capable of investigating the effect from various network parameters. For example, we would like to know how the increase in transmission radius R affects protocol performance. Fig. 6.7 from the model immediately brings out the answer. The increase in R results in two conflicting effects: improvements in *signaling efficiency*, resulting from the shorter source-destination distance; deteriorations in *unicast capacity* with more competing neighbor nodes. Furthermore, proactive protocols should expect worse performance due to the performance degradation of unicast capacity. These analytical result agrees well with our intuition. However, as presented in Fig. 6.8, our simulation being extensive but not comprehensive, still fails to capture such behavior. Clearly, our analytical model is essential not only to confirm and complement the simulations, but also to supply inherent clues to

how changes in network parameters translate into performance variations.

6.5 Conclusion

We presented an analytical framework to evaluate the behavior of generic reactive and proactive protocols. In the model, the operation of the routing protocol is synthesized with the analysis of the MAC protocol to produce a parametric characterization of protocol performance. Corroborated from extensive simulations, the effectiveness and correctness of the model enable in-depth understanding of routing protocol performance.

Chapter 7

Conclusion and Future Research

7.1 Conclusion

In this thesis, we exploited the problem of analytically characterizing distributions of nodes mobility and assessing its impact on protocol performance in wireless mobile ad hoc networks. The presentation of the thesis can be generally categorized into two parts, i.e., statistically modeling of nodes mobility and analytical protocol performance assessment. Clearly, results from the first part serve as the foundation of the work in the second part.

When developing statistical models of nodes mobility, we aimed to develop statistical models to understand all levels of mobility. Link-level mobility, that signifies the distribution of lifetime of point-to-point wireless link, was discussed in Chapter 3. Extension to path-level mobility, specifying the distribution of lifetime of end-to-end communication link, was also made in Chapter 3. Specifically, two-phase Markovian

model was proposed in Chapter 3, presenting the most accurate characterization of distribution of link lifetimes. The analytical model was further incorporated into solution of many practical problems, e.g., optimal segmentation of information stream and optimization on route-caching strategy, showing the possibility of significant performance improvement upon the use of analytical models. In other aspects, results of analytical models also contribute to comprehensive scaling-law analysis on throughput, delay and storage trade-offs for both unrestricted networks in Chapter 3 and (the first piece of work) restricted networks in Chapter 4. Topology or graph-level mobility was investigated in Chapter 5, where asymptotic law is applied to approximate the distribution of topology as exponentially distributed. Parameters of such model can be analytically computed upon network configurations, revealing how nodes mobility translate into topology dynamics.

With all the handy works in mobility modeling, we moved on to evaluate impacts of nodes mobility on protocol performance. In Chapter 5, proactive routing overhead was discussed in detail with an analytical model, making the critical connection between topology dynamics and protocol signaling overhead and first revealing the relationship analytically. Chapter 6 presents the first analytical framework that effectively evaluates the generic behaviors of reactive and proactive protocols, where parameterized characterization of protocol performance was accomplished by a joint characterization of routing logics and MAC functionalities.

In short, we provided in-depth understanding of impacts of mobility on protocol performance and revealed the connections analytically. Many of the works presented

in the thesis are the first attempt and do accomplish the objective of characterizing essential behaviors of mobility and protocol performance, while by no means being comprehensive and perfect.

7.2 Future Research

Many of the works in the thesis were first attempts in the field and much of the work could be expected, not only mobility models but also performance models linking the mobility and protocol performance. Not to elaborate, we only name a few in the following.

In reality, due to environmental variations, wireless links are also volatile and subject to significant variations. The characterizations of lifetime of link-level, path-level and graph-level mobility will be dramatically different from the corresponding models in the thesis, where the pure impact from nodes mobility was considered. Clearly, a critical and interesting line of investigation would be to develop models to characterize both impacts as well as better performance models to understand or even predict protocol performance upon various mobility, environment and network configurations.

When developing mobility models, we observed that analytical works also contribute general guidances and techniques on improving the design of protocol stacks, exemplified by the optimization of route-caching strategy. Therefore, another interesting line of investigation would be incorporating and implementing such analytical techniques in all stacks to improve protocol performance. Applications could be (clearly, not lim-

ited to) design of schemes to setup paths with longer lifetime and adaptive optimization of periodic neighbor-sensing rate and adaptive route-caching schemes.

Bibliography

[1] S. Agarwal, A. Ahuja, J. P. Singh, and R. Shorey. Route-lifetime assessment based routing (rabr) protocol for mobile ad hoc networks. In *ICC 2000*, volume 3, pages 1697–1701, New Orleans, 2000.

[2] National Security Agency. *Assurance Technical Framework*, chapter 9. 3.1 edition, 2002.

[3] A. Al-Maashri and M. Ould-Khaoua. Performance analysis of manet routing protocols in the presence of self-similar traffic. *31st IEEE Conference on Local Computer Networks*, 0:801–807, January 2006.

[4] F. Bai, G. Bhaskara, and A. Helmy. Building the blocks of protocol design and analysis: challenges and lessons learned from case studies on mobile ad hoc routing and micro-mobility protocols. *ACM SIGCOMM Computer Communication Review*, 34(3):57–70, July 2004.

[5] F. Bai, N. Sadagopan, and A. Helmy. Important: a framework to systematically analyze the impact of mobility on performance of routing protocols for adhoc networks. In *Proceedings of IEEE Infocom*, San Francisco, 2003.

[6] N. Bansal and Z. Liu. Capacity, delay and mobility in wireless ad-hoc networks. In *Proceedings of IEEE Infocom*, 2003.

[7] B. Bellur and R.G. Ogier. A reliable, efficient topology broadcast protocol for dynamic networks. In *Proceedings of IEEE Infocom*, pages 178–186, March 1999.

[8] F. Bertocchi, P. Bergamo, G. Mazzini, and M. Zorzi. Performance comparison of routing protocols for ad hoc networks. In *IEEE GLOBECOM*, volume 2, pages 1033–1037, San Fransisco, California, USA, December 2003.

[9] C. Bettstetter. Mobility modeling in wireless network: categorization, smooth movement and border effects. *ACM Mobile Computing and Communication Review*, 5:55–67, January 2001.

[10] C. Bettstetter and C. Wagner. The spatial node distribution of the random waypoint mobility model. In *Proceedings of First German Workshop Mobile Ad-Hoc Networks (WMAN)*, pages 41–58, 2002.

[11] J.-Y. Le Boudec and M. Vojnovic. Perfect simulation and stationarity of a class of mobility models. In *Proceedings of IEEE Infocom*, Miami, 2005.

[12] J.-Y. Le Boudec and M. Vojnovic. The random trip model: stability, stationary regime, and perfect simulation. *IEEE/ACM Transactions on Networking*, 14(6):1153–1166, December 2006.

[13] J. Broch, D. A. Maltz, D. B. Johnson, Y. Hu, and J. Jetcheva. A performance

comparison of multi-hop wireless ad hoc network routing protocols. In *Mobicom'98*, pages 85–97, Dallas, 1998.

[14] T. Camp, J. Boleng, and V. Davies. A survey of mobility models for ad hoc network research. *Wireless Communication and Mobile Computing*, 2:483–502, 2002.

[15] M. Carvalho and J.J. Garcia-Luna-Aceves. A scalable model for channel access protocols in multihop ad hoc networks. In *Proc. ACM Mobicom 2004*, Philadelphia, Pennsylvania, September 2004.

[16] T. Clausen and P. Jacquet. *Optimized Link State Routing Protocol (OLSR)*. IETF RFC 3626, 2003.

[17] T. H. Clausen, G. Hansen, L. Christensen, and G. Behrmann. The optimized link state routing protocol, evaluation through experiments and simulation. In *IEEE Symposium on Wireless Personal Mobile Communications*, 2001.

[18] R. Coltun, D. Ferguson, J. Moy, and A. Lindem. Ospf for ipv6. Internet Draft, draft-ietf-ospf-ospfv3-update-18.txt, IETF Network Working Group, 2007.

[19] R. L. Cruz and A. V. Santhanam. Hierarchical link scheduling and power control in multihop wireless networks. In *Proceedings of 40th Annual Allerton Conference on Communications, Control and Computing*, October 2002.

[20] S. Das, R. Castaneda, J. Yan, and R. Sengupta. Comparative performance evaluation of routing protocols for mobile. In *The 7th International Conference on*

Computer Communications and Networks (IC3N), pages 153–161, Lafayette, Lousiana, USA, October 1998.

[21] S. R. Das, C. E. Perkins, E. M. Royer, and M. K. Marina. Performance comparison of two on-demand routing protocols for ad hoc networks. *IEEE Personal Communications Magazine special issue on Ad hoc Networking*, 8(1):16–28, February 2001.

[22] R. Dube, C. Rania, and K.-Y. Wang. Signal stability based adaptive routing (ssa) for ad hoc networks. *IEEE Personal Communications*, 4(1):36–45, February 1997.

[23] R. S. Blum E. Perevalov. Delay-limited throughput of ad-hoc networks. *IEEE Transactions on Communications*, 52(11):1957–1968, November 2004.

[24] D. Turgut et al. Longevity of routes in mobile ad hoc networks. In *VTC' 01*, Greece, May 2001.

[25] N. Sadagopan et al. Paths: Analysis of path duration statistics and their impact on reactive manet routing protocols. In *ACM MobiHoc 03*, Annapolis, MD, June 2003.

[26] A. E. Gammal, B. Prabhaker J. Mammen, and D. Shah. Optimal throughput-delay scaling in wireless networks - part i: The fluid model. *IEEE Transactions on Information Theory*, 14(6):2568–2592, 2006.

[27] A. E. Gammal, B. Prabhaker J. Mammen, and D. Shah. Optimal throughput-delay scaling in wireless networks - part ii: The constant-size packets. *[Online]. Available: http://www.stanford. edu/ mammen/papers/it-TDpkt.pdf*, 2006.

[28] A. E. Gammal, J. Mammen, B. Prabhaker, and D. Shah. Throughput-delay trade-off in wireless networks. In *Proceedings of IEEE Infocom*, volume 1, pages 464–475, 2004.

[29] A. J. Goldsmith and S. B. Wicker. Mdesign challenges for energy-constrained ad hoc wireless network. *IEEE Transactions on Wireless Communicationsw*, 9:8–27, August 2002.

[30] R. Groenevelt. *Stochastic Models in Mobile Ad Hoc Networks*. PhD thesis, INRIA, Sophia Antipolis, France, 2005.

[31] R. Groenevelt, G. Koole, and P. Nain. Message delay in mobile ad hoc networks. In *Performance*, Juan-les-Pins, October 2005.

[32] R. B. Groenevelt, E. Altman, and P. Nain. Relaying in mobile ad hoc networks: The brownian motion mobility model. *Springer Journal of Wireless Networks (WINET)*, 12:561–571, October 2006.

[33] M. Grossglauser and D. Tse. Mobility increases the capacity of ad-hoc wireless network. In *Proc. of Twentieth Annual Joint Conference of the IEEE Computer and Communications Societies*, volume 3, pages 1360–1369, April 2001.

[34] M. Grossglauser and D. Tse. Mobility increases the capacity of adhoc wireless networks. *IEEE/ACM Transactions on Networking*, 10(4):477–486, August 2002.

[35] R. Guerin. Channel occupancy time distribution in a cellular ratio system. *IEEE Trans. on Vehicular Technology*, VT-35(3):89–99, August 1987.

[36] P. Gupta and P. R. Kumar. The capacity of wireless networks. *IEEE Trans. on Information Theory*, 46(2):388–404, March 2000.

[37] Y. Han and R. J. La. Path selection in mobile ad-hoc networks and distribution of path duration. In *Proceedings of IEEE Infocom*, Barcelona, April 2006.

[38] Y. Han, R. J. La, A. M. Makowski, and S. Lee. Distribution of path durations in mobile ad-hoc networks: Palm's theorem to the rescue. *Computer Networks*, 50(12):1887–1900, August 2006.

[39] J. D. Herdtner and E. K. P. Chong. Throughput-storage tradeoff in ad-hoc networks. In *Proceedings of IEEE Infocom*, 2005.

[40] D. P. Heyman and M. J. Sobel. *Stochastic Models in Operations Research*, volume I. McGraw-Hill, New York, 1982.

[41] D. Hong and S. S. Rappaport. Traffic model and performance analysis for cellular mobile radio telephone systems with prioritized and non prioritized handoff procedures. *IEEE Transactions on Vehicular Technology*, 35(3):77–92, August 1986.

[42] S. Jiang, D. He, and J. Rao. A prediction-based link availability estimation for mobile ad hoc networks. In *Proceedings of IEEE Infocom*, pages 1745–1752, April 2001.

[43] S. Jiang, D. He, and J. Rao. A prediction-based link availability estimation for routing metrics in manets. *IEEE/ACM Transactions on Networking*, 13(6):1302–1312, December 2005.

[44] P. Johansson, T. Larsson, N. Hedman, B. Mielczarek, and M. Degermark. Scenario-based performance analysis of routing protocols for mobile ad-hoc networks. In *Mobicom'99*, pages 195–206, Washington, August 1999.

[45] D. Johnson, Y. Hu, and D. Maltz. The dynamic source routing protocol for mobile ad hoc networks (dsr). Internet Draft, draft-ietf-manet-dsr-10.txt, IETF MANET Working Group, 2004.

[46] L. Kleinrock. *Queuing Systems, Volume 1: Theory.* John Wiley & Sons, Inc, 1975.

[47] R. Knopp and P. A. Humblet. Information capacity and power control in single-cell multiuser communications. In *Proc. of IEEE ICC*, June 1995.

[48] S. J. Lee, M. Gerla, and C. K. Toh. A simulation study of table-driven and on-demand routing protocols for mobile ad hoc networks. *Network, IEEE*, 13(4):48–54, 1999.

[49] G. Malkin. Rip version 2. Internet Standard, RFC2453, IETF Network Working Group, 1998.

[50] J. Mammen and D. Shah. Throughput and delay in random wireless networks with restricted mobility. *IEEE Transactions on Information Theory*, 53(3):1108–1116, 2007.

[51] A. B. McDonald and T. F. Znati. A mobility-based framework for adaptive clustering in wireless ad hoc networks. *IEEE Journal on Selected Areas in Communications*, 17(8):1466–1487, August 1999.

[52] A.B. McDonald and T. Znati. A path availability model for wireless ad-hoc networks. In *Proceedings WCNC'99 IEEE Wireless and Networking Conference*, New Orleans, September 1999.

[53] R. M. Moraes, H. R. Sadjadpour, and J.J. Garcia-Luna-Aceves. Mobility-capacity-delay trade-off in wireless ad-hoc networks. *Elsevier*, July 2005.

[54] R. Motwani and P. Raghavan. *Randomized Algorithms*. Cambridge University Press, 1995.

[55] W. Navidi and T. Camp. Stationary distributions for the random waypoint mobility model. *IEEE Trans. on Mobile Computing*, 3(1):99–108, January 2004.

[56] M. J. Neely and E. Modiano. Capacity and delay tradeoffs for ad-hoc mobile networks. *IEEE Trans. on Information Theory*, June 2005.

[57] R. Nelson and L. Kleinrock. Spatial TDMA: A Collision-Free Multihop Channel Access Protocol. *IEEE Transactions on Communications [legacy, pre-1988]*, 33(9):934–944, 1985.

[58] S. Nesargi and R. Prakash. A tunneling approach to routing with unidirectional links in mobile ad-hoc networks. In *Proceedings of the IEEE International Conference on Computer Communications and Networks (ICCCN)*, pages 522–527, 2000.

[59] S.-Y Ni, Y.-C Tseng, Y.-S Chen, and J.-P Sheu. The broadcast storm problem in a mobile ad hoc network. In *ACM Mobicom 1999*, pages 151–162, New York, 1999.

[60] V. Park and S. Corson. Temporally-ordered routing algorithm (tora) version 1. Internet Draft, draft-ietf-manet-tora-spec-04.txt , IETF MANET Working Group, 2001.

[61] V. D. Park and M. S. Corson. A highly adaptive distributed routing algorithm for mobile wireless networks. In *Proceedings of IEEE Infocom*, volume 3, pages 1405–1413. IEEE, April 1997.

[62] M. Penrose. *Random Geometric Graphs*. Oxford University Press, 2003.

[63] E. Perevalov and R. Blum. Delay limited capacity of ad hoc networks: asymptotically optimal transmission and relaying strategy. In *Proceedings of IEEE Infocom*, San Francisco, March 2003.

[64] C. Perkins and P. Bhagwat. Highly dynamic destination-sequenced distance-vector routing (DSDV) for mobile computers. In *ACM SIGCOMM'94 Conference on Communications Architectures, Protocols and Applications*, pages 234–244, 1994.

[65] C. E. Perkins and E. M. Royer. Ad hoc on-demand distance vector routing. In *Proc. of the 2nd IEEE Workshop on Mobile Computing Systems and Applications*, pages 90–100, New Orleans, February 1999.

[66] G. Rodolakis. *Analytical Models and Performance Evaluation in Massive Mobile Ad Hoc Networks - Chapter 2.2*. PhD thesis, Ecole Polytechnique, 2006.

[67] E. M. Royer and C. K. Toh. A review of current routing protocols for ad hoc mobile wireless networks. *IEEE Personal Communications*, 6(2):46–55, April 1999.

[68] I. Rubin. Access-control disciplines for multi-access communication channels: Reservation and TDMA schemes. *IEEE Transactions on Information Theory*, 25(5):516–536, 1979.

[69] P. Samar and S. B. Wicker. On the behavior of communication links of a node in a multi-hop mobile environment. In *ACM MobiHoc 04*, pages 148–156, 2004.

[70] P. Samar and S. B. Wicker. Link dynamics and protocol design in a multi-hop mobile environment. *IEEE Transactions on Mobile Computing*, 5(9):1156–1172, 2006.

[71] G. Shmarma and R. Mazumdar. Scaling laws for capacity and delay in wireless ad hoc networks with random mobility. In *ICC'04*, pages 3869–3873, 2004.

[72] W. Su, S-J. Lee, and M. Gerla. Mobility prediction and routing in ad hoc wireless networks. *International Journal of Network Management*, 11(1):3–30, January 2001.

[73] C. K. Toh. Associativity-based routing for ad hoc mobile networks. *Wireless Personal Communications: An International Journal*, 4(2):103–139, March 1997.

[74] S. Toumpis and A. J. Goldsmith. Large wireless networks under fading, mobility, and delay constraints. In *Proceedings of IEEE Infocom*, Hong Kong, March 2004.

[75] A. Tsirigos and Z.J. Haas. Analysis of multipath routing - part i: The effect on the packet delivery ratio. *IEEE Transactions on Wireless Communications*, 3(1):138–146, January 2004.

[76] L. Viennot, P. Jacquet, and T. H. Clausen. Analyzing control traffic overhead versus mobility and data traffic activity in mobile ad-hoc network protocols. *ACM/Springer Wireless Networks*, 4(10):447–455, July 2004.

[77] L. Wu and P. Varshney. Performance analysis of csma and btma protocols in multihop networks (i). single channel case. *Info. Sciences, Elsevier*, 120, 1999.

[78] X. Wu, H. R. Sadjadpour, and J. J. Garcia-Luna-Aceves. Link lifetime as a function of node mobility in manets with restricted mobility: Modeling and applications. In *WiOpt 2007*, April 2007.

[79] J. Yoon, M. Liu, and B. Noble. Sound mobility models. In *ACM Mobicom 2003*, San Diego, 2003.

[80] N. Zhou and A.A. Abouzeid. Routing in ad hoc networks: A theoretical framework with practical implications. In *Proceedings of IEEE Infocom*, pages 1240–1251, Miami, 2005.

[81] N. Zhou, H. Wu, and A. A. Abouzeid. Reactive routing overhead in networks with unreliable nodes. In *Mobicom'03*, San Diego, September 2003.